# DEVELOPMENT OF NOVEL ANALYTICAL METHODS FOR SELENIUM, GOLD, SILVER AND INDIUM DETERMINATION USING VOLATILE COMPOUND GENERATION, ATOM TRAPPING AND ATOMIC ABSORPTION SPECTROMETRY

A THESIS SUBMITTED TO
THE GRADUATE SCHOOL OF NATURAL AND APPLIED SCIENCES
OF
MIDDLE EAST TECHNICAL UNIVERSITY

BY

YASİN ARSLAN

IN PARTIAL FULFILLMENT OF THE REQUIREMENTS
FOR
THE DEGREE OF DOCTOR OF PHILOSOPHY
IN
CHEMISTRY

MAY 2011

Approval of the thesis:

**DEVELOPMENT OF NOVEL ANALYTICAL METHODS FOR SELENIUM, GOLD, SILVER AND INDIUM DETERMINATION USING VOLATILE COMPOUND GENERATION, ATOM TRAPPING AND ATOMIC ABSORPTION SPECTROMETRY**

Submitted by **YASİN ARSLAN** in partial fulfillment of the requirements for the degree of **Doctor of Philosophy in Chemistry Department, Middle East Technical University** by,

Prof. Dr. Canan Özgen _____
Dean, Graduate School of **Natural and Applied Sciences**

Prof. Dr. İlker Özkan _____
Head of Department, **Chemistry**

Prof. Dr. O. Yavuz Ataman
Supervisor, **Chemistry Dept., METU** _____

**Examining Committee Members:**

Prof. Dr. E. Hale Göktürk
Chemistry Dept., METU _____

Prof. Dr. O. Yavuz Ataman
Chemistry Dept., METU _____

Prof. Dr. Ahmet E. Eroğlu
Chemistry Dept., İYTE _____

Prof. Dr. Mürvet Volkan
Chemistry Dept., METU _____

Assoc. Prof. Dr. Jiří Dědina
Academy of Sciences of the Czech Republic _____

Date: May 16, 2011

**I hereby declare that all information in this document has been obtained and presented in accordance with academic rules and ethical conduct. I also declare that, as required by these rules and conduct, I have fully cited and referenced all material and results that are not original to this work.**

Name, Last name: YASİN ARSLAN

Signature :

## ABSTRACT

DEVELOPMENT OF NOVEL ANALYTICAL METHODS FOR SELENIUM, GOLD, SILVER AND INDIUM DETERMINATION USING VOLATILE COMPOUND GENERATION, ATOM TRAPPING AND ATOMIC ABSORPTION SPECTROMETRY

ARSLAN, Yasin

Ph. D., Department of Chemistry

Supervisor: Prof. Dr. O. Yavuz ATAMAN

May 2011, 193 pages

A novel analytical technique was developed where gaseous hydrogen selenide formed by sodium tetrahydroborate reduction is transported to and trapped on a resistively heated gold-coated W-coil atom trap for *in situ* preconcentration. The atom trap is held at 165 ºC during the collection stage and is heated up to 675 ºC for revolatilization; analyte species formed are transported to an externally heated quartz T-tube where the atomization takes place and the transient signal is obtained. For gold, a high volume gas liquid separator (HVGLS) was designed to improve the detection limit of Au down to the ng $mL^{-1}$ levels. In this apparatus, analyte and reductant solutions are collected in a limited volume and volatile analyte species are formed. After separation of the volatile analyte species from liquid phase, the entire analyte vapor is sent to an atomizer. A W-coil trap was used to further decrease the detection limit. The enhancement factor for the characteristic concentration was

found to be 10.7 when compared to HG-AAS performance without W-coil trap by using peak height values. Furthermore, the generation of analytically useful volatile form of Au has been studied. The flow injection generation was performed in a dedicated generator consisting of a special mixing apparatus and gas-liquid separator design. The on-line atomization in the quartz tube multiatomizer for atomic absorption (AAS) detection has been employed as the convenient atomization/detection mean. $^{198}$Au, $^{199}$Au radioactive indicator of high specific activity together with AAS measurements was used to track quantitatively the transfer of analyte in the course of generation and transport to the atomizer. In-situ trapping in GF for AAS was explored as an alternative to the on-line atomization. Transmission electron microscopy measurements proved the presence of Au nanoparticles of diameter of approximately 10 nm and smaller transported from the generator by the flow of carrier Ar. For silver, three types of GLS which are U-shaped, cylindrical and high volume gas liquid separators (HVGLS) were used to compare the sensitivities of these GLSs during Ag determination. The DL (3s) values were found as 29 ng $mL^{-1}$, 0.4 ng $mL^{-1}$ and 0.05 ng $mL^{-1}$ for U-shaped GLS, cylindrical GLS with W-coil trap and HVGLS with W-coil trap, respectively. For indium, two types of GLS which are cylindrical and HVGLS with W-coil trap were used. The LOD and characteristic concentration were found as 148 and 317 ng $mL^{-1}$ with cylindrical shape GLS. HVGLS with W-coil trap was used to improve sensitivity. In this case, LOD and characteristic concentration were found to be 0.46 and 0.98 ng $mL^{-1}$, respectively. Moreover, to increase the reactivity between indium and reductant solutions, $Ru(acac)_3$ catalyst was used. In this case, LOD and characteristic concentration were found to be 0.13 and 0.23 ng $mL^{-1}$, respectively. In the case of using this catalyst, sensitivity was enhanced around 1378 fold with respect to cylindrical GLS.

**Keywords:** Selenium, Gold, Silver, Indium, W-coil Trap, HVGLS, Multiatomizer, Volatile Compound Generation, AAS.

# ÖZ

UÇUCU BİLEŞİK OLUŞTURMA, ATOM TUZAKLAMA VE ATOMİK ABSORPSİYON SPEKTROMETRİ KULLANIMI İLE SELENYUM, ALTIN, GÜMÜŞ VE İNDİYUM TAYİNLERİ İÇİN YENİ ANALİTİK METODLARIN GELİŞTİRİLMESİ

ARSLAN, Yasin

Doktora, Kimya Bölümü

Tez Yöneticisi: Prof. Dr. O. Yavuz ATAMAN

Mayıs 2011, 193 sayfa

Uçucu haldeki selenyum hidrür bileşiğini oluşturmak için ve ayrıca oluşan bu türün altın kaplanmış W-sarmal tuzak üzerinde toplanmasını sağlamak amacıyla selenyum tayini için yeni bir teknik geliştirilmiştir. Bu durumda önce tuzak sıcaklığı 165$^{o}$C'da tutularak oluşan selenyum hidrür türlerinin tuzak üzerinde toplanması sağlanmış ve toplama aşamasından sonra tuzağın sıcaklığının 675$^{o}$C'a çıkartılması durumunda, W-sarmal tuzak üzerinde toplanan türlerin yüzeyden kalkarak atomlaştırıcıya ulaşması sağlanmıştır. Altın tayininde, ng mL$^{-1}$ düzeyinde gözlenebilme sınır değerlerine ulaşabilmek için yüksek hacimli gaz sıvı ayırıcı (YHGSA) tasarlanmıştır. Burada, analit ve indirgeyici çözeltiler belirli bir hacimde toplanır ve böylece uçucu analit türlerinin oluşması sağlanır. Uçucu analit türleri sıvı fazdan ayrıldıktan sonra atomlaştırıcıya taşınır. Ayrıca daha düşük gözlenebilme sınır değerlerine ulaşabilmek için tuzak olarak W-sarmal kullanılmış ve bu tuzak YHGSA'nın çıkışına bağlanmıştır. W-sarmalın tuzak olarak kullanılması durumunda pik yükseklikleri kullanılarak duyarlılıktaki artış 10.7 kat olarak bulunmuştur. Altın için başka bir

çalışmada ise, kesikli akış sistemi kullanılmıştır. Bu durumda atomik absorpsiyon spektrometre (AAS) cihazı tayin için kullanılırken çoklu atomlaştırıcı (multiatomizer) adı verilen bir aygıt ise atomlaştırıcı olarak kullanılmıştır. Buhar oluşturma verimini hesaplamak için $^{198}$Au, $^{199}$Au radioaktif madde kullanılmıştır. Ayrıca bu deneyde AAS cihazına alternatif olarak grafit fırın kullanılmıştır. Geçirmeli elektron mikroskopu kullanılarak oluşan uçucu türlerin 10 nm boyutlarında Au nanopartiküller ihtiva ettiği gözlenmiştir. Gümüş tayini için, U şeklinde GSA, silindiriksel GSA ve YHGSA kullanılmış ve bu üç ayrı GSA'nın duyarlılıkları karşılaştırılmıştır. Gözlenebilme sınır değerleri U şeklindeki GSA, W-sarmal tuzaklı silindiriksel GSA ve W-sarmal tuzaklı YHGSA için sırasıyla 29 ng $mL^{-1}$, 0.4 ng $mL^{-1}$ ve 0.05 ng $mL^{-1}$olarak bulunmuştur. İndiyum tayini için, silindiriksel GSA ve YHGSA ayrı ayrı kullanılmıştır. Silindiriksel GSA kullanıldığı zaman gözlenebilme sınır ve evrik duyarlılık değerleri sırasıyla 148 ve 317 ng $mL^{-1}$ olacak şekilde bulunmuştur. Duyarlılığı artırabilmek için YHGSA W-sarmal tuzak ile beraber kullanılmıştır. Bu durumda elde edilen gözlenebilme sınır ve evrik duyarlılık değerleri sırasıyla 0.46 ve 0.98 ng $mL^{-1}$'dir. Buna ek olarak indiyum ve indirgeyici çözeltilerin birbirleriyle olan reaksiyon hızını artırabilmek maksatıyla $Ru(acac)_3$ katalizörü, W-sarmal tuzaklı YHGSA sisteminde kullanılmıştır. Bu durumda elde edilen gözlenebilme sınır ve evrik duyarlılık değerleri sırasıyla 0.13 and 0.23 ng $mL^{-1}$ olarak bulunmuştur. Bu katalizörün kullanılması durumunda duyarlılığın silindiriksel GSA'ya göre yaklaşık 1378 kat arttığı görülmektedir.

**Anahtar Sözcükler:** Selenyum, Altın, Gümüş, İndiyum, W-sarmal Tuzak, YHGSA, Multiatomizer, Uçucu Bileşik Oluşturma, AAS.

To My wife, Serpil Arslan

No word can express my love to my princesss.....

## ACKNOWLEDGMENTS

I express my gratitude to my supervisor Prof. Dr. O. Yavuz Ataman for his guidance and helps during this work. I also would like to thank him for not only his support throughout my PhD but also treated me like a son.

I would like to thank Prof. Dr. Mürvet Volkan, Prof. Dr. Ahmet E. Eroğlu and Prof. Dr. E. Hale Göktürk for their helps, guidances and supports.

I am much indepted to Prof. Dr. Jiří Dědina for his help, guidance and support during my study in Prague, Czech Republic. During 6 months in Prague, he gave me continuous inspiration and encouraged me.

I wish to thank Dr. Thomas Matoušek, Stanislav Musil, Dr. Jan Kratzer, Dr. Vlasta Korunova, Dr. Miloslav Vobecký, Milan Svoboda, Diogo Pompeu de Moraes for their help, hospitality and friendship during my stay in Prague, the Institute of Analytical Chemistry of the Academy oof Sciences of the Czech Republic.

My deepest thanks are to my “wife and life” Serpil Arslan and all of my family members for loving me.

I would like to express my endless thanks to all my labmates, at first Dr. Sezgin Bakırdere and then Üftade Muşkara, Ahmet Yıldıran, Betül Arı, Şefika Özcan, Selin Bora, Pelin Özcan, Feriye Şenol, Emrah Yıldırım, Pınar Akay, İlknur Demirtaş, Melike Karakuş, Emine Kaya, Seval Ataman, Gamze Karaman, Meregül Maden, Njaw Njie for their supports and being a part of my life.

I am indepted to Dr. Erdal Kendüzler, Dr. İbrahim Kula, Dr. Fırat Aydın, Dr. Serap Titretir for their meaningful advices.

I would like to extend special thanks to Necati Koç for his technical support.

I offer sincere thanks to my friends, Yasin Kanbur, Halil Atak, Samed Atak, Okan Tarık Komesli for everything they have done for me.

I also wish to thank my colleagues in Chemistry Department of METU.

I would like to thank my PhD exam committee members for spending their valuable time.

This work was financially supported by ÖYP (Faculty Development Program) from the Middle East Technical University and university research fund BAP-08-11-DPT-2002 K120510 and TUBITAK 109T239 project.

I would like to extend my deepest thanks to Atatürk University for supporting me to complete my PhD in the Chemistry Department of METU.

## TABLE OF CONTENTS

## LIST OF TABLES

**TABLES**

## LIST OF FIGURES

**FIGURES**

## LIST OF ABBREVIATIONS

| | |
|---|---|
| **AAS** | Atomic Absorption Spectrometry |
| **AFS** | Atomic Fluorescence Spectrometry |
| **CF** | Continuous Flow |
| **$C_o$** | Characteristic Concentration |
| **DDTC** | Diethyldithiocarbamate |
| **EDL** | Electrodeless Discharge Lamp |
| **EDS** | Energy Dispersive X-ray Spectroscopy |
| **ETAAS** | Electrothermal Atomic Absorption Spectrometry |
| **ETV** | Electrothermal Vaporization |
| **FAAS** | Flame Atomic Absorption Spectrometry |
| **FAES** | Flame Atomic Emission Spectrometry |
| **FI** | Flow Injection |
| **FIGS** | Flame in Gas Shield |
| **GFAAS** | Graphite Furnace Atomic Absorption Spectrometry |
| **GLS** | Gas Liquid Separator |
| **HCL** | Hollow Cathode Lamp |
| **HG-AAS** | Hydride Generation Atomic Absorption Spectrometry |
| **HG-AFS** | Hydride Generation Atomic Fluorescence Spectrometry |
| **HPLC** | High Performance Liquid Spectrometry |
| **HVGLS** | High Volume Gas Liquid Separator |
| **ICP-MS** | Inductively Coupled Plasma Mass Spectrometry |
| **LOD** | Limit of Detection |
| **LOQ** | Limit of Quantitation |
| **MDF** | Miniature Diffusion Flame |
| **MMQTA** | Multiple Microflame Quartz T-tube Atomizer |

| | |
|---|---|
| **PEEK** | Polyether Ether Ketone |
| **PGMs** | Platinium Group Elements |
| **PP** | Peristaltic Pump |
| **PTFE** | Ploytetrafluoroethtlene |
| **QTA** | Quartz T-tube Atomizer |
| **RC** | Reaction Coil |
| **RF** | Radiofrequency |
| **RSD** | Relative Standart Deviation |
| **SC** | Stripping Coil |
| **SEM** | Scanning Electron Microscopy |
| **SQT** | Slotted Quartz Tube |
| **SQT-AT** | Slotted Quartz Tube Atom Trap |
| **SRM** | Standart Reference Material |
| **STEM** | Scanning Transmission Electron Microscopy |
| **TEM** | Transmission Electron Microscopy |
| **THB** | Tetrahydroborate |
| **VCG** | Volatile Compound Generation |

# CHAPTER 1

# INTRODUCTION

In last decades, scientists have figured out that some of the elements are very crucial for human body while some others are toxic even at very trace levels. Hence, novel techniques for the determination of variety of such elements in ultra trace levels became necessary. Preliminary studies of this type started with atomic absorption and emission spectrometry. To improve the sensitivity, several new techniques such as volatile compound generation and atom trapping methods on some surfaces have been developed. In this chapter, major techniques using atomic spectrometry and preliminary information on the analyte elements Se, Au, Ag and In together with the relevant literature survey for their determination will be presented.

## 1.1 Atomic Absorption Spectrometry (AAS)

Atomic absorption spectrometry is a technique for determining the concentration of a particular element in a sample. AAS is based on the absorption of electromagnetic radiation by neutral, ground state atoms produced by an atomizer [1]. AAS can be used to determine the concentration of over 70 different elements at ranged from mg $L^{-1}$ and ng $mL^{-1}$ levels [2]. Although AAS studies can be traced back to the nineteenth century, the modern form was largely developed during the 1950s by a team of Australian. They were led by Alan Walsh and workers at the CSIRO (Commonwealth

Science and Industry Research Organization) Division of Chemical Physics in Melbourne, Australia [3,4]. Initially, AAS was employed with a flame atomizer. In general, air/acetylene flames were used. Nitrous oxide/acetylene flames were also popular. The technique typically makes use of a flame to atomize the sample [5], but other atomizers such as a graphite furnace [6] have been also described in literature.

Hollow cathode lamp (HCL) is the most common radiation source in AAS. In addition, lasers, primarily diode lasers, due to their good properties, have been used [7]. A nebulizer is used to obtain fine droplets. It was reported that a typical nebulization efficiency, which is the ratio of the sample transfered to the flame to the amount of sample introduced to the nebulizer in a flame AAS (FAAS) system, varies from 1 to 10% [8]. Therefore, a high percentage of the sample is not efficiently transported to the atomizer.

Several analytical techniques have been used in literature to improve the sensitivity in atomic spectrometry. Fuwa and Vallee's tube or long-path absorption tube is given as an example. The length of the tube was almost a meter. In this system, a silica or vycor tube was used through which the light beam was passed; and directed to the upper end of a tubular flame [9]. Delves's micro sampling cup technique, which consisted of a spoon-like nickel cup where sample was mechanically pushed into the flame is another example to improve the sensitivity. In this system, a transient signal is produced by rapid atomization. As an example, 10 µL of untreated sample was used in order to determine lead in human blood [10].

### 1.2 Atomic Fluorescence Spectrometry (AFS)

AFS is another technique that has been used in literature for the determination of elements. AFS is based on the excitation of gaseous analyte atoms by radiation of

suitable wavelength and measurement of the resultant fluorescence radiation. Each atom has a characteristic fluorescence spectrum. The wavelength of the fluorescence line may be the same, greater, or smaller than the wavelength of the excitation line. There are three types of atomic fluorescence transitions, namely, resonance fluorescence, direct line fluorescence, and stepwise line fluorescence [11].

In order to obtain lower LODs, AFS can be coupled to a hydride generation system. In terms of LOD and linear range, it has advantages over AAS [12, 13]. Hydride generation atomic fluorescence spectrometry (HG-AFS) technique has been widely used as an analytical device in the literature to determine hydride forming elements [14]. Using direct transfer of generated hydrides to a miniature diffusion flame atomizer, LODs goes down to the pg $mL^{-1}$ [15-21]. This system has been used in many studies in the literature [22-26].

### 1.3 Inductively Coupled Plasma Optical Emission Spectrometry (ICP-OES)

The main handicap of the techniques which have been mentioned so far is the single analyte determination. They suffer from longer time consumption to complete the analysis in the case of multi-analyte determination. ICP-OES (Inductively Coupled Plasma Optical Emission Spectroscopy) and ICP-AES (Inductively Coupled Plasma Atomic Emission Spectroscopy) are the names used for the most popular technique using Ar plasma as a source. In this naming, the reference to atoms is misleading in a way because large fractions of the analyte species are ions in Ar plasma. In addition, the abbreviation as AES stands also for *"Auger Electron Spectroscopy"* which is a completely different method. Hence, it is better not to use ICP-AES for emission spectrometry in plasma. ICP-OES is the best abbreviation for this technique [27]. ICP-OES has the capability of measuring the many elements simultaneously. This technique can be used for the determination of approximately 70 elements in different

matrices [27]. Identification of the elements can be easily done by using the wavelengths of the elements, and the peak intensity is used in quantitative measurements. In general, a sample in liquid form is sent into plasma through nebulization where it is evaporated and dissociated into both free atoms and ions. Excited free atoms and ions lose their energy by collision with other particles or by radiative transition to lower energy levels. This radiation is called as *spontaneous emission of radiation* [11]. Samples are mostly analyzed in liquid form, occasionally in solid form, and quite rarely in gas form. ICP-OES is a very flexible technique because an existing analytical method can be easily adopted to another element [27]. No element-specific equipment such as hollow cathode lamps is necessary in the determinations. ICP-OES consists of an RF generator, pneumatic nebulizer, spray chamber, torch, wavelength selector, detector and a computer for data acquisition. There are two viewing modes namely radial or axial in it.

Advantages of this technique include

-No need for a different hollow cathode lamp for each element.

-Simultaneous multi-element detection.

-Flexibility of using several line in each analyte detections.

-High- speed analysis, relatively high sensitivity, and large linear dynamic range.

-Less sample volume consumption in the analysis than that used in flame AAS techniques for multi-element determinations.

-Determination of refractory elements such as Ti, Ta, Ru etc. due to high plasma temperatures.

Very high temperature in the plasma (6,000–10,000 K) destroys all samples completely. Therefore, in general, analytical results are not affected by the nature of the chemical bond of analytes of interest. Hence, interference caused by the matrix

can be reduced by the effect of high temperature in plasma. Researchers can control whether there is any spectral interference in the measurements by monitoring several line monitoring. Although each line of element has different sensitivity, spectral interference-free measurements are possible for most of the elements with different sensitivities by selecting interference-free lines.

Due to these and some other advantages, scientists have used this technique for several purposes, including (1) searching for new physical/chemical processes, (2) understanding the analytical processes, (3) development of the method, and (4) method validation [28]. In addition, this technique has not been used solely by scientists. Companies use this method for quality checks and governments for control and regulation.

There have been several attempts to improve the sensitivity in ICP-OES. Hydride generation-ICP-OES (HG-ICP-OES) is one of them. Detection limits for hydride forming elements in HG-ICP-OES method should be apparently lower than those obtained using conventional ICP-OES. The hydride generation method has the advantage of high sample introduction efficiency to the plasma; efficiency is close to 100% when compared with the conventional sample introduction system where pneumatic nebulisation is used with only 1–3% of the sample introduction to plasma. In addition, interference problems arising from matrix can be eliminated or minimized by using hydride generation. Analytes are separated from the matrix, usually eliminating spectral interferences completely, and non-spectral interferences in solution are limited to few exceptional cases. In this way, high accuracy and low detection limits are obtained [28]. Most of the hydride- or volatile-forming elements including Pb [29-31], Se [32,33], As [34-36], Sb [36], Ag, Au, Cd, Cu, Ni and Zn [37] have been determined by using HG-ICP-OES method.

## 1.4 Inductively Coupled Plasma Mass Spectrometry (ICP-MS)

The main deficiency of ICP-OES is that it is very difficult to obtain detection limits at ng $L^{-1}$ levels. ICP-MS offers extremely low detection limits in the sub-ppt level as well as quantitation at the high-ppm levels. Linear working range is wide. This capability makes the technique unique when compared with some other techniques such as GFAAS, FAAS, ICP-OES. It was commercialized in 1983 [38].

ICP-MS has several advantages for the determination of a large range of elements. These are;

-Multi element determination.
-Very low detection limits, as low as ng $L^{-1}$
-Monitoring of isotopic patterns.
-Wide linear dynamic range, 4-6 orders of magnitude.
-Low matrix interferences due to further dilution.
-High speed of analysis.
-Controlling of spectral interferences on each isotope by comparing natural and experimental isotopic abundance ratios

Weakest point or *"Achilles Heel"* of the ICP-MS system is the sample introduction. This is in common with ICP-OES. 1 to 2% of the sample can be introduced into plasma. Although there are some improvements in this field, design of the sample introduction system for ICP-MS has not changed dramatically since the ICP-MS was first introduced in 1983 [39].
A typical mass spectrometry consists of three basic components;

(i) an ion source that converts neutral structure into gas-phase ions

(ii) one or more mass analyzers that separate analytes according to their mass-to-charge ratio ($m/z$)

(iii) a detector that counts and stores the number of ions at each $m/z$ value

In ICP-MS instrument, sample is injected to the system in liquid form. In general, liquid samples are introduced to Ar plasma in small volumes. Liquid sample should be dispersed to eliminate instability or possibility to be extinguished. For this aim, a nebulizer is used in ICP-MS instrument to disperse the solution into a fine, gas-borne aerosol. In addition, spray chamber is used to remove larger droplets from the aerosol [40,41]. Conventional nebulizers operate at a flow rate of 1 mL $min^{-1}$ while micro-flow nebulizers are often used with the flow rates of 0.2-0.5 mL $min^{-1}$ to minimize the sample consumption. High efficiency "total consumption" nebulizers where the entire aerosol is injected into the plasma have recently been introduced [40,42,43]. Stable temperature and pressure stability, low washout time that is ideally less than two minutes are some of the requirements for a spray chamber. In addition, it should not suffer from significant memory effects [44]. Another function of the spray chamber is to remove solvent from the aerosol, improving ionization efficiency. In the case of a spray chamber that is cooled to 2 °C, sensitivity can be increased up to three times than conventional spray chamber at ambient temperature [40,45]. Matrix species like H and O also cause the formation of interfering polyatomic species [46]. Using the temperature controlling of spray chamber, these types of interferences can be easily eliminated or minimized.

HG has been also used as a sample introduction technique in ICP-MS. Lower detection limits and elimination of some spectral interference are some of the advantages of these combinations. Chang and Jiang used FI-VCG-ICP-MS system for the determination of some hydride forming elements such as As, Cd, and Hg in soybean oil and peanut samples [47]. Chung *et al.* studied the dietary exposure to Sb,

Pb and Hg of secondary school students in Hong Kong using HG-ICP-MS system [48]. Chandrasekaran *et al.* described a UV-assisted vapour generation-ICP-MS method for the determination of Se (IV) in natural water samples [49]. Volatile selenium species were formed by UV irradiation in the presence of low molecular weight organic acids and collected in a glass chamber before injection into the plasma [49]. Park and Do described a simple method for the determination of both inorganic and total mercury by isotope dilution CV-ICP-MS; Hg-199 enriched isotope was used in spiking studies [50]. A method to monitor both hydride and nonhydride-forming As species was described by Tsai and Sun in 10-mL microdialysate samples [51]. HPLC with a post-column UV/$TiO_2$ film reactor and HG-ICP-MS was used in separation and detection steps. LOD levels for As(III), MMA, DMA, and As(V) and AsB were found to be in the sub-mg $L^{-1}$ range for 10 mL sample volume [51].

ICP-MS can be combined with other instrument for the speciation and determination of different elements [52-58]. It is a good tool for speciation analysis. Not only the multiple element monitoring capacity but also the very low detection limits make ICP-MS very attractive for scientist to make speciation analysis. These types of the studies are very important for human health.

### 1.5 Sensitivity Improvement in Atomic Spectrometry

Simple and inexpensive ways of enhancing sensitivity will be described for laboratories equipped with only a flame AA spectrometer. Although there are many chemical preconcentration procedures to improve sensitivity of flame AAS, only some *atom trapping* techniques will be included here. One kind of atom trapping device is a slotted quartz tube (SQT) used for *in situ* preconcentration of analyte species followed by a rapid revolatilization cycle to obtain an enhanced signal. These devices provide limits of detection at a level of μg $L^{-1}$. Another kind of atom trapping

involves use of vapor generation technique and quartz or tungsten atom trapping surfaces. The analytical steps consist of the generation of volatile species, usually by hydride formation using $NaBH_4$, trapping these species at the surface of an atom trap held at an optimized temperature and finally re-volatilizing analyte species by rapid heating of the trap. These species are transported using a carrier gas to an externally heated quartz tube as commonly used in hydride generation AAS systems; a transient signal is formed and measured. These traps have limits of detection in the order of ppt.

### 1.5.1 Sensitivity Improvement in FAAS

#### 1.5.1.1 Slotted Quartz Tube (SQT)

The SQT was first introduced by Watling in 1977. He placed a heated slotted tube with two slots at at $120^o$ to each other on a conventional flame [59,60]. In this device, lower slot coincided with the laminar flame. On the other hand, another slot was on the tube at an angle of $120^0$ with respect to the lower slot. In principle, the angle between the slots may be $120^0$ or $180^0$. The sensitivities of the elements including Ag, As, Bi, Cd, Sb, Se, Sn and Pb were increased by two-to fivefold depending on the elements. Reduced flame speed, longer optical path and increased lifetime of free analyte atoms in flame are some of the reasons to improve the sensitivity [61]. In the preliminary studies of the SQT device, different kinds of flames such as air/acetylene, air/hydrogen and argon (entrained air)/hydrogen were used; however, the device was fairly popular when only air/acetylene was used [62]. In one of the studies with SQT, analyte hydrides were introduced the flame included the SQT. Using this approach, determination of Sn and Bi was carried out in copper based alloys [63,64]. While the detection limits were better than those could be obtained by flame AAS alone, determination of these analytes in such a heavy matrix was also a noteworthy

application. Because of these advantages, the use of a simple SQT with a flame atomizer has found popularity even in recent years [65].

#### 1.5.1.2 Water-Cooled U-tube Atom Trap

This technique was first introduced by Lau *et al*. [66]. They placed a water cooled U-tube atom trap with 4 mm o.d. and 3 mm i.d. on an air-acetylene flame. In principle, the function of U-tube technique is to trap atoms on cold quartz surface for preconcentration. A quartz U-tube was placed on the flame so that its lower side was in contact with the flame; the light beam was parallel to the upper side of the tube [62,66]. In order to allow an entrance and exit for water or air into the tube, its ends were bent to form a U-shape. In this technique, a sample solution is aspirated for a measured time interval; analyte atoms are collected on cold quartz surface. After the aspiration is stopped, water flow through the tube is replaced by air. Rapid heating of the quartz tube was achieved and the trapped analyte species were back into the flame and finally a transient absorption signal was obtained [62]. Passage of water through the quartz U-tube during the aspiration is used to supply a lower temperature on quartz surface with respect to flame, so that the analyte species are condensed on the relatively cooler surface of the quartz tube. The goal of the replacement of water with air after collection period of time is to cause a rapid heating and to release the analyte species condensed on the cool surface of tube into the beam of the hollow cathode lamp [62,66]. Sensitivity can be improved for volatile elements by 8-40 times using this type of atom trap [67]. U-tube is probably the first example of using the quartz surface as an atom trap. In addition, quartz surface was coated with aluminum or vanadium oxides for the determination of As, Cd, Pb, Se and Zn [68]. Coating with aluminum or vanadium oxides resulted in not only improvement in the reproducibility but also extending the life time of the quartz trap tube [68].

#### 1.5.1.3 Water-Cooled U-tube Atom Trap Combined with Slotted Quartz Tube

The idea of placing the U-tube trap in an SQT device is suggested by Roberts and Turner in order to combine the advantages of both techniques. Main disadvantage of this system is that the water vapor causing much noise in the signal [69]. To determine Ag, Cd, Cu, Fe, In, Pb, Tl and Zn in beer, Matusiewicz *et al.* prepared a combination of U-tube with a SQT around it. This device was named as integrated atom trap (IAT) [70]. A stainless steel trap surface was one of materials employed by some researchers instead of silica for the U-tube atom trap [71].

#### 1.5.1.4 Slotted Quartz Tube as an Atom Trap (SQT-AT)

Another way of releasing analyte species from the surface of silica was presented in 1993 [72]. In this work, instead of replacing water flow by air, it was suggested that the composition of the flame should be momentarily altered to effect fast re-atomization; the authors called this process as flame alteration [72]. The flame alteration approach was applied to SQT device by a Chinese group [73]. The same research group that used flame alteration for the first time, proposed another and simpler way of revolatilization that is called organic solvent aspiration/atomization [74]. This was used in these studies afterwards where the revolatilization mechanisms [75] and interferences [76] involved in SQT atom trap FAAS (SQT-AT-FAAS) were studied. In organic solvent aspiration technique, 10-50 µL of an organic solvent, most often isobutyl methyl ketone (IBMK), is introduced and nebulised into the flame; the momentary change in the flame fuel/oxidant ratio is believed to be the reason of reatomization from the quartz surface [74,75]. From these studies, SQT-AT-FAAS has evolved as an efficient alternative for the sensitivity enhancement with FAAS. The sensitivity improvements reported by using SQT-AT-FAAS is 100 fold or

higher. Developments in atom traps with particular emphasis on SQT have been recently reviewed by Ataman [77,78].

### 1.5.2 Volatile Compound Generation (VCG)

In atomic spectrometry, a sample can be introduced as in the liquid, solid or gaseous phase. Gaseous phase sample introduction techniques are usually based on volatile compound generation. A selective conversion of the analyte from the liquid sample to the gaseous phase is carried out via an appropriate chemical reaction resulting in a volatile compound of the analyte. Relative simplicity of the procedure and low cost of the apparatus are some of the reasons for the popularity of VCG. This technique which provides separation from the sample matrix offering considerable suppression of matrix effects. Furthermore, high efficiency of transport of gaseous analyte to the atomizer and simple analyte preconcentration result in exceptional detection limits. In principle, VCG techniques are widely utilized for trace element determination. Of the numerous approaches available (i.e., cold vapor, halination, ethylation, propylation, oxidation, hydridization, etc.), those based on the generation of volatile hydrides enjoy greatest popularity [79,80].

A resurgence of research interest in VCG, giving rise to an expansion of the scope of this technique to encompass an increasing number of analytes, as well as the alternative methodologies for their sampling, is under way. In the past decade, new approaches to VCG have arisen, such as photochemical vapor generation [81], UV alkylation [82]. In addition, new approaches to analyte pre-concentration have been explored, including cryocondensation and trapping of volatile species in aqueous media [83,84], new and powerful sampling strategies, such as solid phase micro extraction (SPME) [85,86] and single droplet micro extraction [87,88], have been pursued; new insights into the mechanism of one of the oldest VCG techniques, HG,

have emerged [89]. Elemental coverage continues to expand [90,91]. The sustained interest in VCG by atomic spectroscopists is driven by their quest for enhanced detection power. The majority of sample introduction strategies is currently based on aqueous solutions and, for those systems relying on the use of pneumatic nebulization for sample introduction, such as FAAS and most plasma-based techniques. In these types of systems, the transport efficiency of analyte from the solution to the spectroscopic source rarely exceeds 1–5%. Herein lies the stimulus for undertaking VCG, the vapor form of the analyte being efficiently separated from the liquid phase and transported quantitatively to the source. High generation efficiencies, achieved with aquo-ion reduction by sodium tetrahydroborate (III), can be routinely implemented for Hg, As, Sb, Bi and Se, frequently rendering VCG of these elements the preferred methodology for their determination by atomic spectrometry. However, HG of other elements, such as Te, Ge, Sn, In and Tl, is less frequently employed because optimum reaction conditions are not easily accomplished, inexpensive quartz tube atomizer used for atomic absorption detection systems suffers from inefficient atomization for these elements [79]. In order to take the best detection limits in HG, the atomization step should be optimized to obtain high signal to noise (S/N) ratio. More often, aqueous phase ethylation (as opposed to classical Grignard alkylation in non-aqueous media) is undertaken, not only for these particular elements, but because reaction conditions for ethylation are sufficiently generalized (pH 5 medium), many HG reactions would be achieved using tetraethylborate if the reagent were comparably priced to tetrahydroborate (III) [81]. Recent advances in understanding of the hydrolysis of the tetrahydroborate (III) reagent and discarding of the concept of ‘‘nascent’’ hydrogen as the mechanism of analyte reduction have been introduced [89] A schematic view of a hydride generation system is given in Figure 1.1.

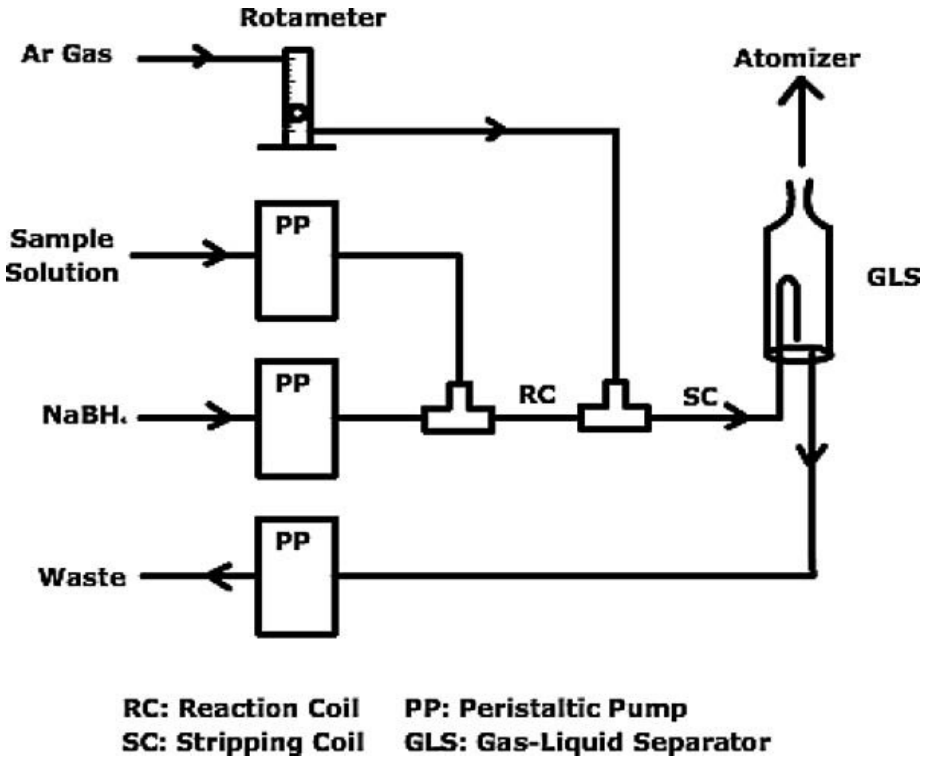


**Figure 1.1.** Schematic representation of a conventional laboratory-made hydride generation system.

Amongst the many methodologies noted above for effecting VCG, the application of photochemical reduction and alkylation is the one of the most significant recent developments [92]. Alkylation, as a method for VCG, became widespread when interest in the speciation analysis of trace metals emerged. The technique, inspired by synthetic organic chemists, was initially confined to non-aqueous media (Grignard reaction), but availability of sodium tetraalkylborates has permitted efficient alkylation reactions to be conducted in aqueous media. Photo-induced alkylation [82] and photo-reduction of valence states are emerging as powerful alternatives to conventional VCG that potentially provide for wide multielemental coverage such as As, Bi, Sb, Se, Sn, Pb, Cd, Te, Hg, Ni, Co, Cu, Fe, Ag, Au, Rh, Pd, Pt, I and S. It also remains to be seen whether the simplicity of this approach, a UV source and

inexpensive low molecular weight organic acids as chemical reagents, will permit it to functionally and analytically out-perform current HG and carbonylation methodologies [92,93].

The transient existence of free atoms of several transition and noble metals in solution following their reduction with sodium tetrahydroborate (III) suggests that many more elements may be amenable to HG for analytical application than earlier speculated. Moor *et al.* [94] reported analytical figures of merit for detection of volatile species of Rh, Pd, Ag, and Au following their solution-phase reduction by a stream of tetrahydroborate (III) and rapid introduction into an inductively coupled plasma mass spectrometer. In the case of the transition and noble metals, their reaction with tetrahydroborate (III) in aqueous solution generates unidentified volatile species, which makes comprehension of the reaction mechanism quite difficult. It is well known that the final products are the reduced metals or metal borides, depending on both the metal and the experimental parameters, and this reaction is widely employed for the preparation of nanoparticles of metals or metal borides [95,96]. This can be considered the result of a coalescence process, starting with the formation of free atoms in solution, as demonstrated by Panichev and Sturgeon [93]. However, with vapor generation of transition and noble metals, the resultant species are not chemically stable in solution [97,98], and thus extended reaction time leads to decreased product yield [97]. This is an important piece of evidence indicating that the volatile metal products are unstable. As an example, it has been suggested that the generation of the volatile Ag species proceeds in two steps [99]. The first step is that formation of the volatile species may correspond to the reduction of $Ag^{+}$ to $Ag^{0}$. This is the most probably a rather fast process. On the other hand, the second step, formation of the volatile species and/or its release from the liquid phase, is much slower. It has been found that only about 30% of the volatile species is released prior to or upon contact of the reaction mixture with the GLS surface [99].

#### 1.5.2.1 Most Frequently Used Hydride Atomizers

Most frequently used hydride atomizers are conventional quartz tube atomizers (QTA), miniature diffusion flame (MDF), flame-in-gas-shield (FIGS), multiple microflame quartz T-tube atomizers (MMQTA), graphite furnaces and metal furnaces.

In general, quartz tube atomizers are T-tubes with the horizontal arm (optical tube) aligned in the optical path of AA spectrometer. Volatile compounds and/or hydride carried by the gas flow from the hydride generator are delivered to the atomizer from the central arm of the T-tube of atomizer. Quartz tube atomizers can either be heated by flame, or more often and more conveniently, electrically. Electrically heated atomizer was introduced by Chu *et al.* [100]. The use of air–acetylene flame to heat the atomizer was first suggested by Thompson and Thomerson [101].

MDF has very simple design consisting of a vertical quartz tube (support tube) with i.d. varying between 3 and 8 mm as the burner of the argon/hydrogen mixture introduced to the atomizer together with the analyte hydride. Temperatures in the MDF are ranging from 150 $^{o}$C to 1300 $^{o}$C. The minimum temperature is in the support tube axis close to the top of the tube i.e. lower part of MDF near support tube. On the other hand, the maximum temperature is observed in the outer zones of the flame because of the fact that reactions take place between hydrogen and ambient oxygen in the outer zone of the flame. Its essential drawback is its high atomizer noise and the extrmelly short residence time of the free atoms in the optical path. In order to find best sensitivity in MDF, argon/hydrogen mixture, hydrogen fraction in mixture and “the observation height”, i.e. the distance of the atomizer top from the center of the optical beam cross section are important experimental parameters to be optimized. H radicals are formed in the outer zone of the flame by “radical generating reactions” between hydrogen and oxygen. H radicals can thus diffuse to the cooler

inner sections of the flame. They can eveen diffuse as deep as at least 3 mm inside the support tube. Outside the hot zone of the flame, H radicals tend to vanish by terminating chemical reactions. The main terminating reaction is that with molecular oxygen. In MDF, molecular oxygen access to the flame volume is prevented by the hot zone of outer flame shell where oxygen is consumed. Consequently, the whole flame volume contains a high concentration of H radicals. Hydride is, under optimum conditions, fully atomized in the H radical cloud by reactions with extremely energetic H radicals. Free analyte atoms are stable within the H radical cloud, i.e. in the presence of a sufficient excess of H radicals. Even if free analyte atoms reacted to form molecular species, they should be reatomized by the interaction with the excess of H radicals. The species formed by the decay of free analyte atoms can be reatomized but only by an interaction with H radicals [102-105]. A schematic view of a MDF system is given in Figure 1.2.

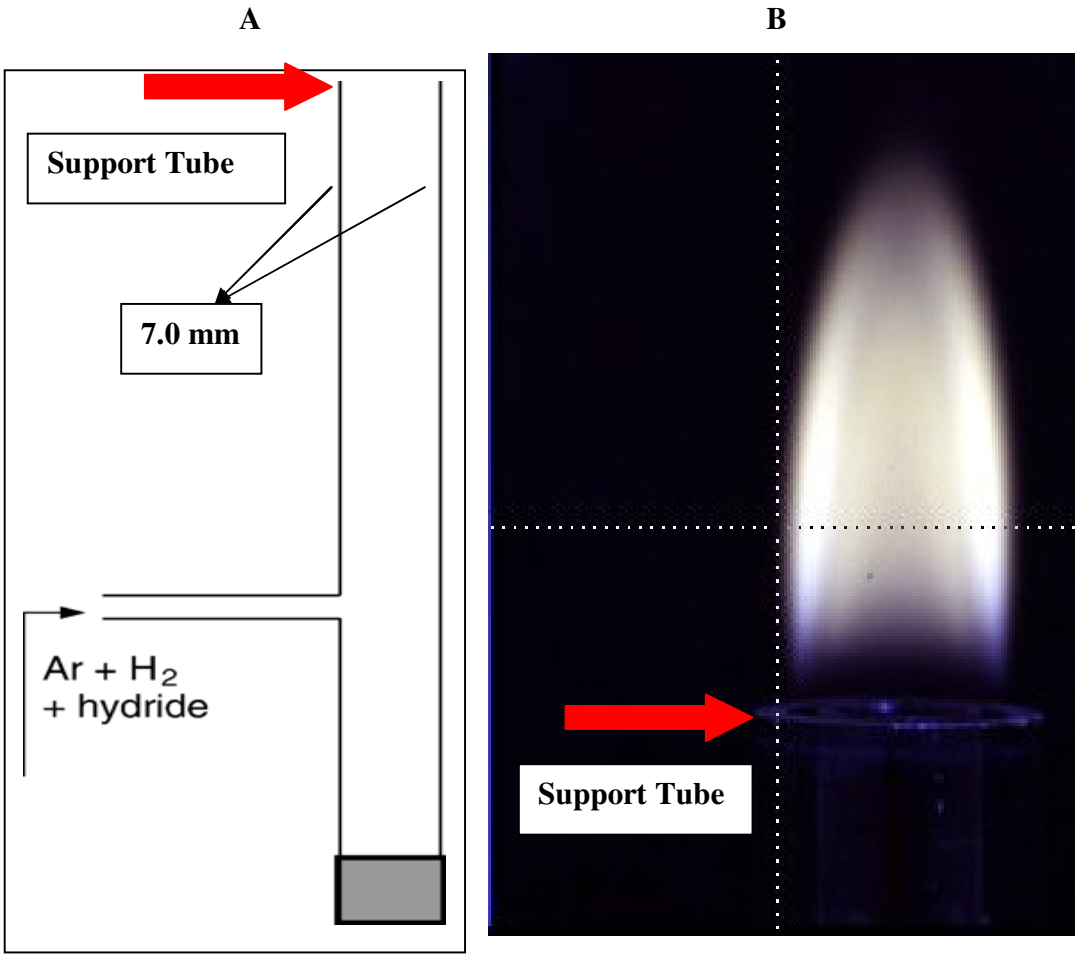


**Figure 1.2.** Miniature diffusion flame **(A)** Schematic representation **(B)** Photograph of MDF.

The FIGS atomizer can be used with both AFS and AAS. The scheme of typical FIGS was given in literature. In the FIGS, argon shielded, highly fuel-rich hydrogen oxygen micro flame was used [102]. In principle, FIGS atomizer is identical to the MDF. It is the same quartz support tube with the inlet of the mixture of hydrogen in argon containing the hydride. The main difference from the MDF is that the capillary whose i.d. 0.53 mm serves to introduce a very small flow of oxygen inserted inside

the quartz support tube. Inside the microflame, oxygen burns in the excess of hydrogen at the end of the capillary to form H radicals. By the effect of the argon flow which is typically at the rate around 2 L $min^{-1}$, the observation volume above the top of the support tube must be protected from the ambient atmosphere [106]. A schematic view of a MDF system is given in Figure 1.3.

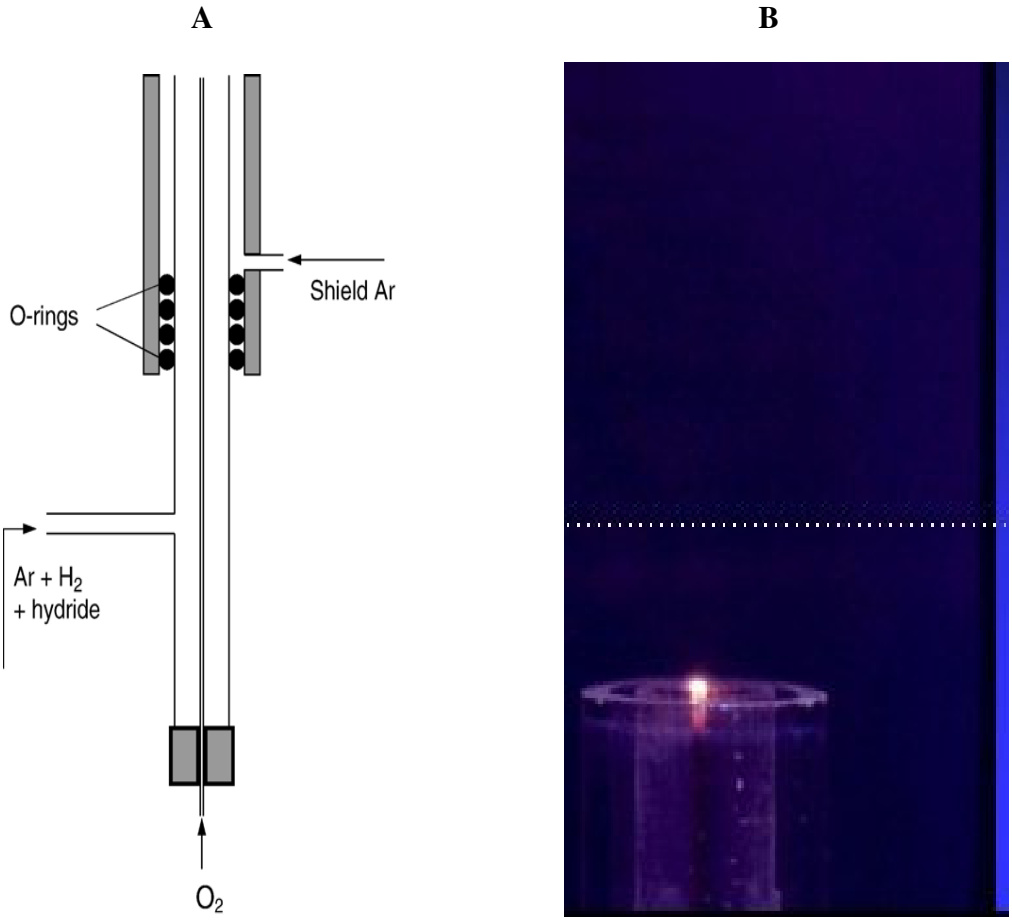


**Figure 1.3.** Flame in gas shield atomizer **(A)** Schematic representation **(B)** Photograph of FIGS.

As described above, MDF has low sensitivity when compared with conventional QTA because the residence time of free analyte atoms in the optical path is rather short. When the combination of the conventional QTA and MDF was made, the disadvantages of the both atomizers were prevented. In this respect, a nearly ideal atomizer which was called as MMQTA or multiatomizer whose whole volume of a optical tube was filled with H radicals which was explained in MDF was designed by Dědina and co-workers [106,107]. In this manner, the analyte would be maintained in the free atomic state by a permanent interaction with H radicals similar as in MDF along the whole optical tube length. The scheme of the multiatomizer design is shown in Figure 1.4. [106].

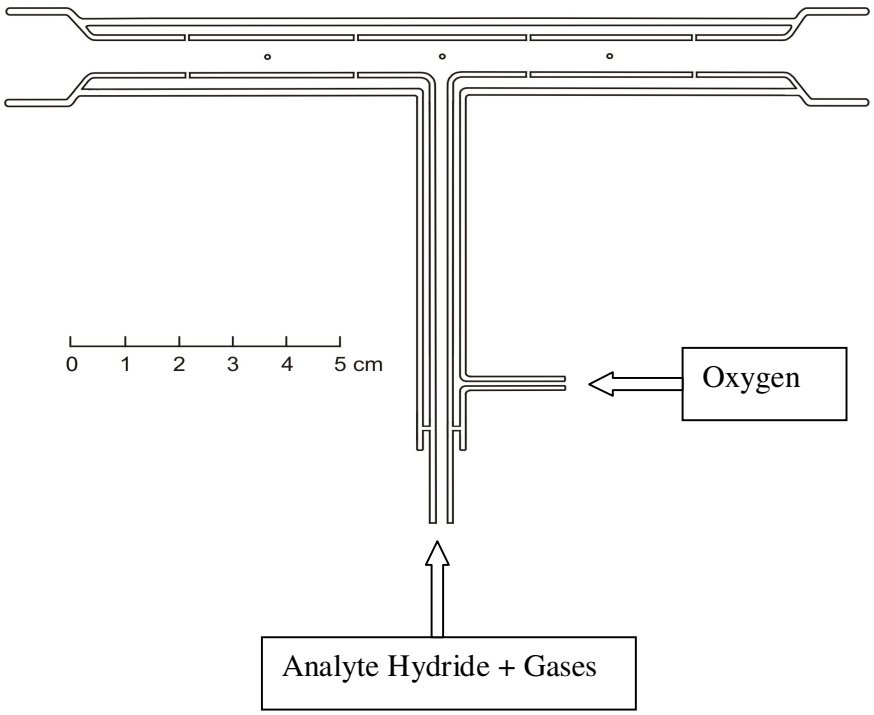


**Figure 1.4.** Schematic representation of a mulltiatomizer system [106].

Graphite furnaces have been widely used for hydride atomization. L'vov was the first person who used an electrically heated furnace as an atomizer for AAS in general and published his works in 1959 which was written in Welz *et. al* [1]. In this technique called as graphite furnace atomic absorption spectrometry (GFAAS) or electrothermal atomic absorption spectrometry (ETAAS) since the nebulization is eliminated and residence time of the atoms in the graphite tube are longer than FAAS, the sensitivity is usually about 2-3 orders of magnitude higher than that obtained by FAAS.

A flame heated metal tube which was made of Ni, Cr and Fe [108-109]. Metal furnace heated by flame as a hydride atomizer was used for the determination of Sb in environmental and pharmaceutical samples [108]. The method has a linear Sb concentration range from 2 to 80 ng $mL^{-1}$ and the LOD is 0.23 ng $mL^{-1}$. The authors report that the metal furnace has low cost and a longer lifetime as compared to a quartz tube atomizer; therfore, it can be used for hydride atomization [108].

#### 1.5.2.2 Trapping Techniques Used in Literature

A tremendous amount of work has been done in the literature to increase the sensitivity of the present systems. The easiest way of increasing sensitivity using relatively simple and low-cost instruments is using trapping techniques. The basic idea of trapping is collecting the analyte atoms in a predetermined amount of sample solution by using the proper medium and sending the atoms to the detector as rapidly as possible. In this way a transient signal can be obtained and either the height or the area can be used as the analyte signal. Analyte atoms can be trapped in an environment as solid, liquid, or gas. In principle, an adsorbing medium that is capable of trapping, storing, and releasing analyte atoms without any or with minimum loss in

physical and chemical form is needed. Thousands of materials have been found and synthesized that are more efficient and have low cost.

#### 1.5.2.2.1 Graphite Furnace Trap

Trapping of volatile species on the surface of a graphite tube is an easy and efficient task as applied in the literature. Drasch et al. [110] used a preheated commercially available graphite tube for the trapping of As. In this technique, volatile species are formed and sent to the graphite tube using glass or quartz capillaries. A schematic diagram showing the application of the system is given in Figure 1.5. There are two important approaches for graphite furnaces (i) *in-situ* trapping of hydrides in the furnace, (ii) on-line atomization. *In-situ* trapping techniques coupling HG with the graphite furnace permit significant enhancement in relative detection power over conventional batch and continuous generation approaches for the ultra trace determination of metallic hydrides. Graphite furnace is used to decompose the volatile hydride and trap analyte species on the graphite tube surface, thereby effecting a clean, rapid separation from the matrix as well as collection. The generated hydrides are introduced to the internal gas line of commercial furnaces. This arrangement, though very simple, has the same disadvantage as in-situ trapping: hydrides can be captured on cooler metal or graphite parts. Naturally, sensitivity for on-line atomization is generally lower than with in-situ trapping. It is also lower than those in quartz tube atomizers [79].

The surface of the tube is usually modified with carbide-forming metals with high boiling points, such as Ir [111], W, Zr [112], and Nb [113], or metals that exibit catalytic activities like Pd [114] or Pt [115]. After the collection stage, temperature of the tube is increased to an elevated temperature and analyte atoms are both revolatilized and atomized. In this way, a transient signal can be obtained. The

efficieny of the system is dependent on the design of the trapping system. Lee [116] studied the deposition of bismuthine and determined that 61% of the generated bismuthine was trapped in the graphite interface, 11% in the atomizer tube, and the rest was lost through the hydride generation and transport system. The method is very popular because it does not require much expertise, is easy to operate, and has high sensitivity and stable signal and background values. Disadvantages of the method include low dynamic range due to limited surface area, high cost of the graphite tubes, and possible transfer losses. In addition, the presence of hydrogen gas coming from the reaction of $NaBH_4$ and acid reduces the lifetime of the tube by reacting with graphite and forming methane gas [117].

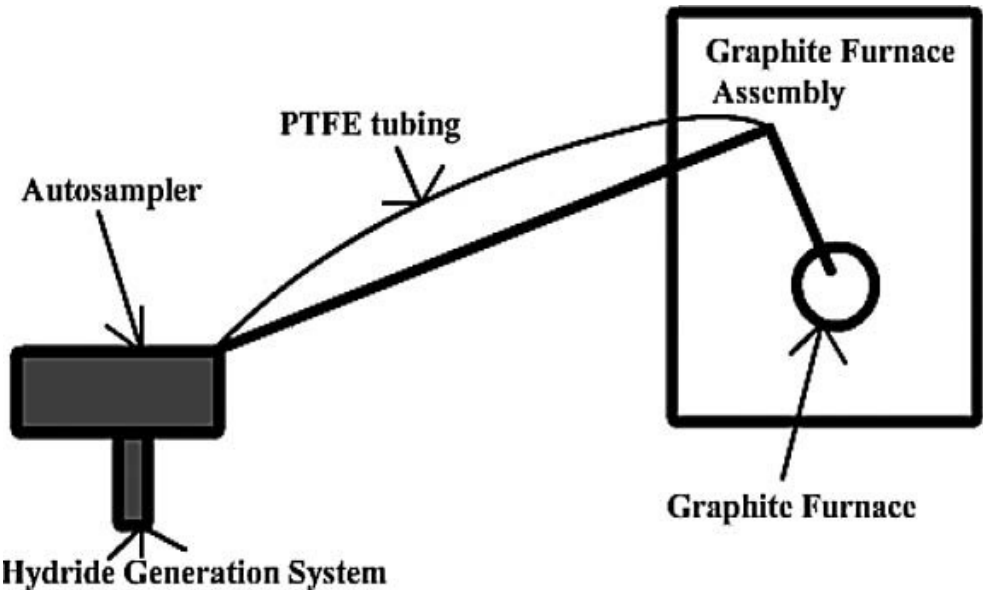


**Figure 1.5.** Schematic representation of graphite furnace atom trapping system.

#### 1.5.2.2.2 Quartz Trap

Another approach for the trapping of hydride is the use of quartz traps. In this approach, externally heated quartz pieces are used as the trapping medium. Either the inlet arm of the T-tube is used directly or some additional quartz pieces are placed to increase the surface area [118]. When the collection stage is completed, the temperature of the system is further increased to a predetermined revolatilization temperature. At this temperature, analyte molecules are released from the surface either as atoms or molecular species. It is not necessary to atomize the atoms at this stage because they are then sent to the T-tube and molecular species can be atomized there. For the revolatilization stage, usually $H_2$ gas is sent to the system to create a reducing environment that helps the revolatilization of the species [119]. The distance between the trap and the optical path is important and should be optimized. The distance should be short enough to prevent decay of the volatile species through transfer lines. External heating is the weakest point of the system because it takes a relatively long period of time, between 30 to 90 s, to reach the desired temperature due to low thermal conductivity. To minimize this problem, Kratzer and Dědina [120] used a hydrogen microflame in addition to the external heating. The microflame was created at the tip of a capillary by sending $O_2$ gas to the system. Revolatilization was achieved by increasing the external heating and extinguishing the microflame and creating a reducing atmosphere. A schematic view of the system is given in Figure 1.6.

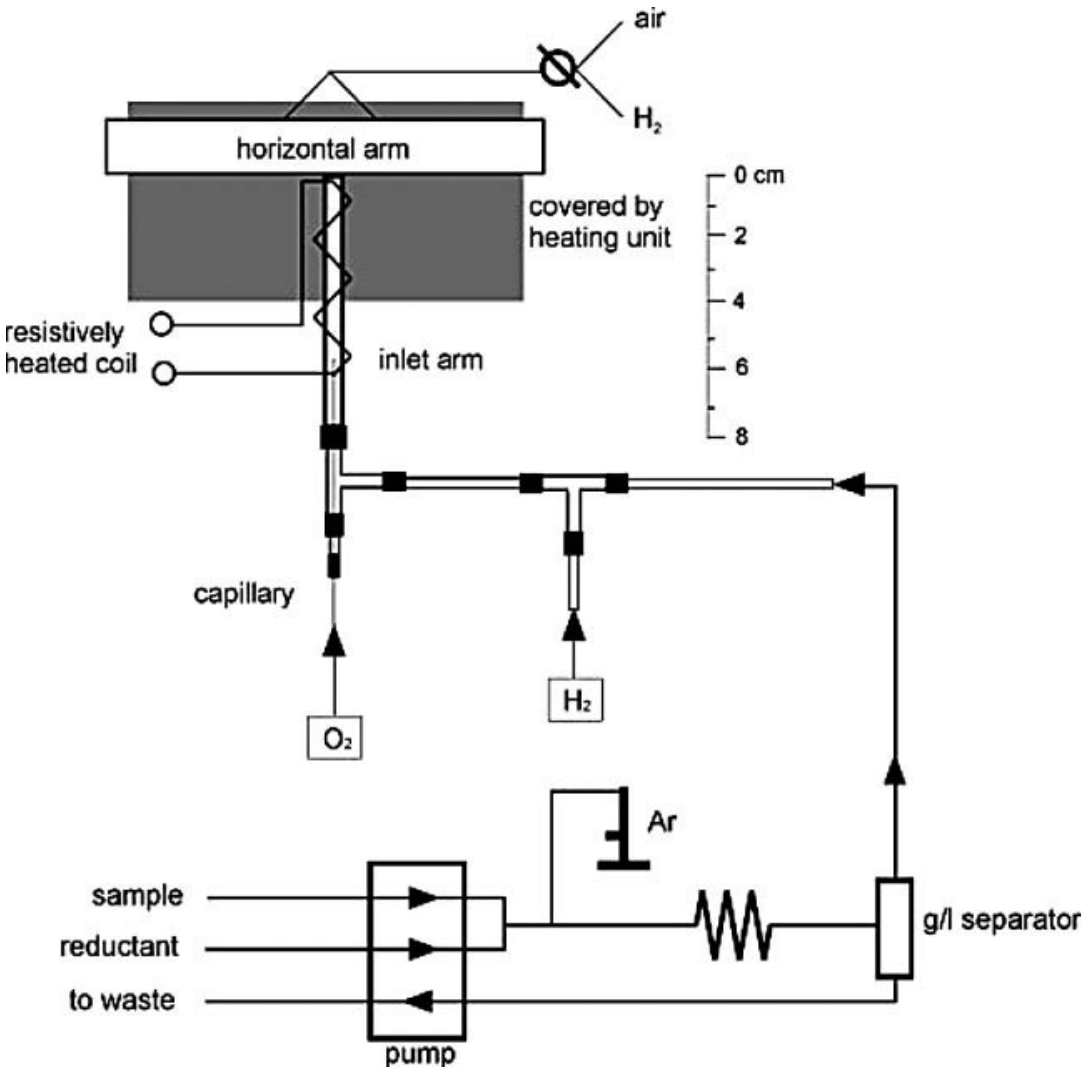


**Figure 1.6.** Schematic representation of quartz atom trapping system [120].

#### 1.5.2.2.3 Metal Traps

Another technique used in the literature is the use of metal surfaces as trapping medium. The idea of metal trapping is more or less the same as the quartz trap, with

some exceptions. In the metal trapping system, metal itself is resistively heated, so no external heating mechanism is necessary. Because the thermal conductivity of metals is much higher than quartz, setting the temperature of the system to the desired values is much easier and takes less than few seconds. Among the metals, W is the most popular one due to its high melting point, high heating rate, and low cost. The system was first proposed by two different groups independently at the same time [121,122]. The first group used W in combination with a T-tube atomizer, whereas the second group used W as both as trapping medium and as atomizer. In the system the temperature of the coil is controlled by adjusting the voltage passing through the coil. One of the problems that should be overcome is the oxidation of the Wcoil. Even though the systems are usually closed, molecular $O_2$ diffuses the system from the connections. This $O_2$ causes oxidation of W-coil trap and reduces the performance of the system. To prevent oxidation, $H_2$ gas is sent to the system to create a reducing medium. By the use of $H_2$ gas, oxidation is prevented or the rate of oxidation is reduced.

The use of W-coil as an atomizer for analytical purposes can be dated back to 1972 [123]. After this first application, there have been other studies on W-coil as a device where analyte can be dried, ashed and atomized. Then, a wide interest in use of a W-coil as an atomizer arose mostly an alternative to the graphite furnace [124,125]. The schematic representation of W-coil trap together with quartz T-tube atomizer is shown in Figure 2.1.

Trapping of hydrides of Se and As in a W tube atomizer was studied by Dočekal *et al*. and it was found that coating with Pt, Ir or Re was a good way to increase the trapping efficiency of W atomizer [126]. When the W tube was treated with Pt, trapping temperatures of 100-200 $^0$C gave the most efficient trapping approaching to 100%. The collection temperature on Ir and Re coated tubes was as high as 700-900

$^{o}$C and the trapping efficiency was only 10%. In another study, for in-situ trapping of selenium hydride, Rh coated W-coil atomizer was also used [122].

For on-line trapping and vapor generation systems, some alternative metal traps; a molybdenum strip in order to determine As and Se [127] and Sb and Bi [128], resistively heated Pt for Cd have also been suggested [129]. Recently, the similar approach was employed to preconcentrate volatile forms of Cd on quartz surface yielding an LOD of 1.8 pg $mL^{-1}$ ($m_o$ was 1.2 pg) [130].

## 1.6 Application of Analytes

### 1.6.1 Selenium

Selenium was discovered by Jöns Jakob Berzelius in 1817. It was discovered as a byproduct of sulfuric acid production. It is a nonmetal, chemically related to sulfur and tellurium, and rarely occurs in its elemental state in nature. Its electrical conductivity is better in the light than in the dark, and this property is used in photocells. Because of its photovoltaic and photoconductive properties, selenium is used in photocopying, photocells, light meters and solar cells. Selenium was once widely used in rectifiers. [131].

Selenium occurs naturally in a number of inorganic forms, including selenide, selenate, and selenite. In soils, selenium most often occurs in soluble forms such as selenate (analogous to sulfate), which are leached into rivers very easily by runoff. Selenium is most commonly produced from selenide in many sulfide ores, such as those of copper, silver, or lead. It is obtained as a byproduct of the processing of these ores, from the anode mud of copper refineries and the mud from the lead chambers of sulfuric acid plants. These muds can be processed by a number of means to obtain

free selenium. Natural sources of selenium include certain selenium-rich soils, and selenium that has been bioconcentrated by certain plants. Anthropogenic sources of selenium include coal burning and the mining and smelting of sulfide ores [132].

#### 1.6.1.1 Determination of Selenium

Selenium determination has been possible by a series of analytical techniques; regarding its rather low concentration in biological systems and environment adequate sensitivity could be supplied most frequently by powerful and commonly used techniques such as ETAAS, HGAAS and ICP-MS. Although the literature is very rich regarding Se determination, in this section only the approaches using HG and on-line preconcentration will be emphasized. Combining the advantages of hydride generation and electrothermal AAS has been suggested in several occasions [133]. Several researchers have used the approach of *in situ* trapping of volatile analyte hydride species in graphite furnace atomizers with subsequent atomization [134-137]. It has been shown that selenium hydride could be trapped and preconcentrated on platinum-treated tungsten surface where the workers used a Wolfram electrothermal atomizer (WETA) device [126]. A tungsten coil usually extracted from a commercial visible lamp provides another alternative as an electrothermal device. The use of W-coil as an atomizer for analytical purposes can be dated back to 1972 [138]. After this first application there has been other studies on W-coil as a device where analyte can be dried, ashed and atomized [139,140]. W-coil requires a relatively simple power supply when compared with a graphite furnace; the latter device has a relatively complicated and bulky power system. In one of the earlier applications, iridium coated W-coil was used for determination of selenium [141]. The use of W-coil as a trapping device for selenium determination has been reported [122]. Gold surface has also been used as an atom trap for selenium determination where external heating for trap was used [142]. In this study,

chemically generated $H_2Se$ was collected on the gold wire trap at 200 °C; following preconcentration step, the trap was heated to 900 °C, the analyte was released, transported to and detected by AFS; although AAS determination in the same work was mentioned, no relevant results were provided. Among the other efforts to trap selenium from its hydride, a quartz trap used with HGAAS [143], molybdenum foil [127] and graphite surfaces with HGAAS [144] and the use of an integrated atom trap with hydride generation and a flame atomizer [145] should be noted.

### 1.6.2 Gold

Gold (Au) is a transition metal. Compared with other metals, pure Au is significantly less reactive, but it is attacked by aqua regia, forming chloroauric acid, and by alkaline solutions of cyanide but not by single acids such as HCl, $HNO_3$ or $H_2SO_4$. Au dissolves in mercury, forming amalgam alloys, but does not react with it. Au is insoluble in $HNO_3$, which dissolves silver and base metals. This property is exploited in the Au refining technique known as "inquartation and parting". Nitric acid has long been used to confirm the presence of Au in items, and this is the origin of the colloquial term "acid test", referring to an *Au standard* test for its genuine value. The transmitted light through a gold dispersion in water appears greenish blue, because Au strongly reflects yellow and red. Such semi-transparent sheets also strongly reflect infrared light, making them useful as infrared (radiant heat) shields in visors of heat-resistant suits, and in sun-visors for space suits [146,147].

Au readily forms alloys with many other metals. These alloys can be produced to modify the hardness and other metallurgical properties or to control the melting point. Au is also a good conductor of heat and electricity. Gold is unaffected by air, moisture and most corrosive reagents, and is therefore well-suited for use in coins and jewelry and as a protective coating on other, more reactive, metals. Au also dissolves

in alkaline solutions of potassium cyanide. Common oxidation states of Au include +1 (Au (I) or aurous compounds) and +3 (Au (III) or auric compounds). Au ions in solution are readily reduced and precipitated out as Au metal by addition of any other metal as the reducing agent. The added metal is oxidized and dissolves allowing the Au to be displaced from solution and be recovered as a solid precipitate. In addition, Au is very dense, its density is 19.7 g $cm^{-3}$. By comparison, the density of lead is 11.3 g $cm^{-3}$, and that of the densest element, osmium, is 22.6 g $cm^{-3}$. In modern times, injectable gold has been proven to help to reduce the pain and swelling of rheumatoid arthritis and tuberculosis [148,149].

Gold can be manufactured as layers so thin that it appears transparent. It is used in some aircraft cockpit windows for de-icing or anti-icing by passing electricity through it. The heat produced by the resistance of the gold is enough to prevent freezing of water [150]. Although gold is a noble metal, it forms many and diverse compounds. The oxidation state of gold in its compound ranges from −1 to +5 but Au (I) and Au (III) dominate. Au (I) compounds are typically linear. A good example is $Au(CN)_2^-$, which is the soluble form of gold encountered in mining. Curiously, aurous complexes of water are rare. The binary gold halides, such as AuCl, form zig-zag polymeric chains, again featuring linear coordination at Au. Most drugs based on gold are Au (I) derivatives. Gold (III) ("auric") is also a common oxidation state as in gold (III) chloride, $AuCl_3$. Its derivative is chloroauric acid, $HAuCl_4$, which forms when Au dissolves in aqua regia. Au (III) complexes, like other $d^8$ compounds, are typically square planar [151]. Au is the classical noble metal as shown by its use for valued ornaments through the ages. Because of the fact that it has commercial value, high electrical and thermal conductivity, gold is one of the most important noble metals.

### 1.6.2.1 Determination of Gold

In literature, there are several analytical techniques such as electrochemical methods, neutron activation analysis and spectrophotometry in order to determine Au [152].

Luna *et al*. [98] described a batch procedure for the generation of volatile Au species by reduction with tetrahydroborate. The sensitivity, however, was poor with a LOD of 23 ng corresponding to 2.3 mg $L^{-1}$ and a characteristic mass of 29 ng corresponding to 2.9 mg $L^{-1}$. The precision was also poor, i.e., 12% for 1000 ng, corresponding to 100 mg $L^{-1}$. A method was reported for the flow injection volatile compound generation (FI-VCG) of Au in an acidified medium using $NaBH_4$ reductant in the presence of micro amounts of sodium diethyldithiocarbamate (DDTC) [153]. The system was used for the determination of Au in digests of ore samples. A precision of 2.0% RSD ($n$=11, at 2.0 mg $L^{-1}$) was obtained at a sampling frequency of 180/h, yielding a detection limit of 24 ng $mL^{-1}$ ($3\sigma$) by using 2.0 mg $L^{-1}$ based on a 300 μL sample volume corresponding to 600ng. Sodium tetraethylborohydride was used to enhance the VCG efficiency of Au. Volatile species of Au in a weakly acidified buffer medium were generated at room temperature by reaction with a mixed reductant containing 0.1% $NaBH_4$ and 0.01% $NaBEt_4$ in the presence of 0.03% sodium diethyldithiocarbamate (NaDDTC) [154]. A flow injection (FI) system was coupled to a heated quartz tube atomizer for atomic absorption spectrometry (AAS) detection. A precision of 2.5% RSD ($n$=11, 0.4 mg $L^{-1}$ level) was realized at sampling frequencies of 110/h. A detection limit of 2.8 ng $mL^{-1}$ ($3\sigma$) was obtained by using 0.4 mg $L^{-1}$ Au solution based on a 500-μL sample volume corresponding to 200 ng. Also calibration plot is from 0.04 to 0.4 mg $L^{-1}$. Compared with FI-VCG-AAS using $NaBH_4$ as the sole reductant, sensitivity was increased 8- to 10-fold [154]. In a flow-injection vapor-generation atomic absorption spectrometry (FI-VGAAS) system, it was shown that the volatile species of Au can be generated in acidified aqueous medium by reduction with $NaBH_4$. The volatile

species of Au have been generated by FI-VGAAS and then trapped in situ in a graphite furnace to obtain ETAAS detection. The inside surfaces of the gas–liquid separator (GLS) and quartz probe were silanized in order to minimize the memory effects. The detection limit of 2.6 ng $mL^{-1}$ (3 s) was obtained with a 5.0 mL sample volume. The method was applied to the analysis of Au containing ore sample digests [135]. In an another study [155], VCG system was used for the in situ trapping on graphite furnace AAS determination of Au, providing a detection limit of 0.8 ng $ml^{-1}$ ($3\sigma$) with a 40 s trapping time and a sampling frequency of 50/h.

### 1.6.3 Silver

Silver is a very ductile and malleable metal with a brilliant white metallic luster; it can take a high degree of polish. Silver is slightly harder than gold. Among metals, pure silver has the highest thermal conductivity and one of the highest optical reflectivity. It has the highest electrical conductivity of all metals even higher than copper, but its higher cost and tendency to tarnish have prevented it from being widely used instead of copper for electrical purposes. Despite this, 13,540 tons of silver were used in the electromagnets while enriching uranium during World War II, mainly because of the wartime shortage of copper [156]. Another notable exception is in high-end audio cables [157,158].

Small devices such as hearing aids and watches commonly use silver oxide batteries due to their long life and high energy/weight ratio. Another usage is in high-capacity silver-zinc and silver-cadmium batteries. Mirrors which need superior reflectivity for visible light are made with silver as the reflecting material in a process called silvering, though common mirrors are backed with aluminum. Using a process called sputtering, silver (and sometimes gold) can be applied to glass at various thicknesses, allowing different amounts of light to penetrate. Silver is usually reserved for

coatings of specialized optics, and the silvering most often seen in architectural glass [159].

Silver ions and silver compounds have a toxic effect on some bacteria, viruses, algae and fungi, typical for heavy metals like lead or mercury, but without the high toxicity to humans that are normally associated with these other metals. Its germicidal effects kill many microbial organisms *in vitro*, but testing and standardization of silver products is difficult [160].

#### 1.6.3.1 Determination of Silver

As explained in the preceding sections, VCG or HG in atomic spectrometry is commonly used as the analyte introduction technique for the determination of low levels of hydride forming elements, i.e., Sb, Bi, Se, As, Tl, Ge, Sn, Pb and Te [161-166]. Luna *et al*. [98] described a batch procedure for the generation of volatile Ag species by reduction with tetrahydroborate. The sensitivity, however, was rather low with an LOD of 33 ng (corresponding to 3.3 mg $L^{-1}$) and a characteristic mass of 37 ng (corresponding to 3.7 mg $L^{-1}$). The precision was also not very high, i.e., 8% for 50 ng, corresponding to 5 mg $L^{-1}$. Matoušek *et al*. [167] used Continuous Flow Chemical Vapor Generation CF-CVG and Multiple Microflame Quartz Tube Atomizer, (MMQTA) techniques and they found the detection limits of 0.015 mg $L^{-1}$ and 0.33 mg $L^{-1}$ respectively. Matoušek *et al*. developed a chemical vapour generation (CVG) procedure for the production of volatile species of Ag using AAS and ICP-OES detection. A characteristic mass of 0.12 ng was achieved using a miniature diffusion flame atomizer-AAS system; whereas a 38-fold higher sensitivity compared with conventional liquid nebulization was obtained with ICP-OES [168]. The same authors proposed both a remedy for some of the difficulties encountered, i.e., avoidance of pronounced sensitivity drifts and increase in the CVG efficiency

through modification of the inner generator surface by deposits of finely reduced metal (Ni or Pd), as well as providing deeper insight into the mechanism of the process for Ag [168].

### 1.6.4 Indium

The German chemists Ferdinand Reich and Hieronymous were testing ores from the mines around Freiberg, Saxony in 1863. They dissolved the minerals pyrite, arsenopyrite galena and sphalerite in HCl and distilled the raw zinc chloride. As it was known that ores from that region sometimes contain thallium they searched for the green emission lines with spectroscopic methods. The green lines were absent but a blue line was present in the spectrum. As no element was known with a bright blue emission they concluded that a new element was present in the minerals. They named the element with the blue spectral line as indium, from the indigo color seen in its spectrum [169,170]. Indium rank 61st in abundance in the Earth's crust at approximately 0.25 ppm which means it is more than three times as abundant as silver, which occurs at 0.075 ppm. Fewer than 10 indium minerals are known, none occurring in significant deposits. Examples are the dzhalindite ($In(OH)_3$) and indite ($FeIn_2S_4$) [171].

In the electronics, indium oxide ($In_2O_3$) and indium tin oxide (ITO) are used as a transparent conductive coating applied to glass substrates in the making of electroluminescent panels. Some indium compounds such as indium antimonide, indium phosphide [172] and indium nitride [173] are semiconductors with useful properties. Indium is used in the synthesis of the semiconductor copper indium gallium selenide (CIGS), which is used for the manufacture of thin film solar cells [174]. Indium is also used in light-emitting diodes (LEDs) and laser diodes based on

compound semiconductors such as InGaN, InGaP that are fabricated by Metalorganic Vapor Phase Epitaxy (MOVPE) technology [174].

### 1.6.4.1 Determination of Indium

In principle, indium is the one of the less studied elements in literature by using FAAS, HG-AAS and ETAAS, [1,79,175]. Because of the trace concentrations, determination of In at endogenous level in analytical samples is a difficult task. Therefore in In determination, preconcentration stage is essential [175]. In 1982, Busheina *et al.* found that Indium could be determined by AAS with HG from aqueous solution [176]. In order to improve the sensitivity, Yan *et al.* modified the reaction conditions. The best sensitivity reported was 0.13 µg as characteristic mass; they used an electrically heated quartz tube atomizer [177]. In 1988, Castillo *et al.* reported a similar procedure where the quartz atomizer used was heated by flame [178]. Liao *et al.* used the HG-AAS with *in situ* preconcentration in a palladium coated graphite furnace for the determination of In. In this study Palladium was found to be a very efficient adsorbent for indium hydride. X-ray photoelectron spectroscopy was used to characterize the sample deposits on the graphite platform surface. The method is linear up to 50 ng and characteristic mass for In was found as 0.63 ng [179]. Matusiewicz *et al.* evaluated the analytical performance of coupled hydride generation-integrated atom trap (HG-IAT) atomizer flame atomic absorption spectrometry system for determination of In. The detection limit, defined 3 times the standard deviation of blank (3 s), was 0.6 ng $mL^{-1}$. The designs studied included slotted tube, single silica tube and integrated atom trap-cooled atom traps [175].

## 1.7 Purpose of This Study

In this study, Selenium (Se), Gold (Au), Silver (Ag) and Indium (In) were determined by using analyte vapour generation atomic absorption spectrometry. Although there are many studies for Se determination, applications for Au, Ag and In are rather rare. For sensitivity improvement, atom trapping technique is used. W-coil atom trap is used for all the analytes. In addition, for Au, the studies also involve the use of multiatomizer, in-situ trapping in graphite furnace and the investigations of the nature of volatile species; which have been conducted in Prague at Institute of Analytical Chemistry of the Analytical Science of the Czech Republic, Prague , during a visit to Prof. Dr. J. Dědina's laboratories.

# CHAPTER 2

# EXPERIMENTAL

## 2.1 Selenium Determination byVCG-AAS

### 2.1.1 Reagents

All reagents were at least of analytical grade. Working solutions of Se (IV) were prepared by making necessary dilutions from their standard solutions: 1000 mg $L^{-1}$ Se (Merck, Germany). For the acidification of analyte solutions, 37% (w/w) HCl (Merck, Germany) was used. Reductant solutions were prepared daily from the powder sodium tetrahydroborate (Merck, min. purity 96%). For the stabilization of the $NaBH_4$ solution, NaOH (Carlo Erba, Milano, Italy) was used. Dilutions were made using 18 MΩ cm ultra pure water obtained from Milli-Q water purification system (Millipore Bedford, MA, USA). All the solutions were prepared in high density polyethylene containers and were kept refrigerated.

For coating W-coil surface with Au, gold solution was prepared by making necessary dilutions from their stock standard solution: 1000 mg $L^{-1}$ Au (Merck, Germany). Stock solution of 1.0% (m/v) sodium diethydithiocarbamate (NaDDTC) (Merck) was prepared in ethanol (Merck) in order to increase the efficiency of volatile gold species. For the acidification of gold solutions, 64% (w/w) $HNO_3$ (Merck, Germany) was used.

### 2.1.2 Instrumentation

An ATI Unicam 929 atomic absorption spectrometer equipped with a deuterium background correction system was used. A Philips data coded hollow cathode lamp was operated at 7.0 mA; the analytical line at 196.0 nm was used in the measurements with 0.5 nm as the spectral bandwidth. Flow system for VCG is given in Figure 1.1.

Quartz T-tube atomizer (QTA) heated by a stoichiometric air/acetylene flame was used as atomizer. QTA consisted of a horizontal arm with dimensions of 115 mm in length, 15 mm in o.d. and 13 mm in i.d.; inlet arm was 110 mm in length, 10 mm in o.d. and 7.0 mm in i.d. Another smaller quartz tube was inserted and fixed in the inlet arm with dimensions of 6.0 mm in o.d. and 4.0 mm in i.d.; it extended between the open end of the inlet arm and a point that was 5.0 mm away from the W-coil; analyte vapor was transported through this inner tube. Hydride generation for both conventional and W-coil trap systems were carried out in continuous flow (CF) mode using a Gilson Minipuls 3 (Villers le Bell, France) 4-channel peristaltic pump. Tygon peristaltic pump tubing of 0.8 mm i.d. (Ismatec, Germany) was used for pumping the analyte and reductant solutions that are mixed in a 3- way polytetrafluoroethylene PTFE connector (Cole Parmer Instrument Co. USA). For the separation of hydrogen selenide from the liquid phase, a laboratory made cylindrical gas liquid separator (GLS) was employed. Tygon tubing of length of 4.0 cm and 6.0 mm i.d. (Masterflex, Cole Parmer Instrument Co.) was used between the GLS and the inlet arm of the silica T-tube atomizer. The composition of the gas mixture was the same for both conventional HGAAS and collection stage on trap while additional $H_2$ was used for revolatilization stage. A mixture of $H_2$ and Ar was used in both conventional HGAAS and W-coil trap studies. The flow rates of these gases were measured by two separate flow meters (Cole Parmer Instrument Co. USA). The W-coil used for trapping was obtained from a 15 V, 150W projector bulb (Halogen Photo optic Lamp Xenophot,

Osram, Germany) and placed in the inlet arm of a silica T-tube, 50 mm away from the connection point to the horizontal arm. The experimental setup for hydride generation and trap was as reported previously [180] except for the way W-coil was inserted into the inlet arm. A laboratory-made quartz female joint was attached to the inlet arm. The W-coil with its socket base was fixed inside the male portion of the glass joint; in order to assure immobilization of the setup, ordinary silicone type glue was used. This configuration is shown in Figure 2.1. Quartz T-tube and W-coil trap allows a very rapid and convenient change of W-coil when needed. The W-coil was positioned so that its longer axis was perpendicular to the gas flow that is reaching to it through the smaller quartz tube in the inlet arm. The coil temperature was manually controlled by a variable potential power supply (Variac) and a 750 W transformer connected to mains electricity (220 V ac) through a power switch. The input voltage of the variable potential power supply was 220 V. The temperature measurements were carried out with a Ni–Cr thermocouple.

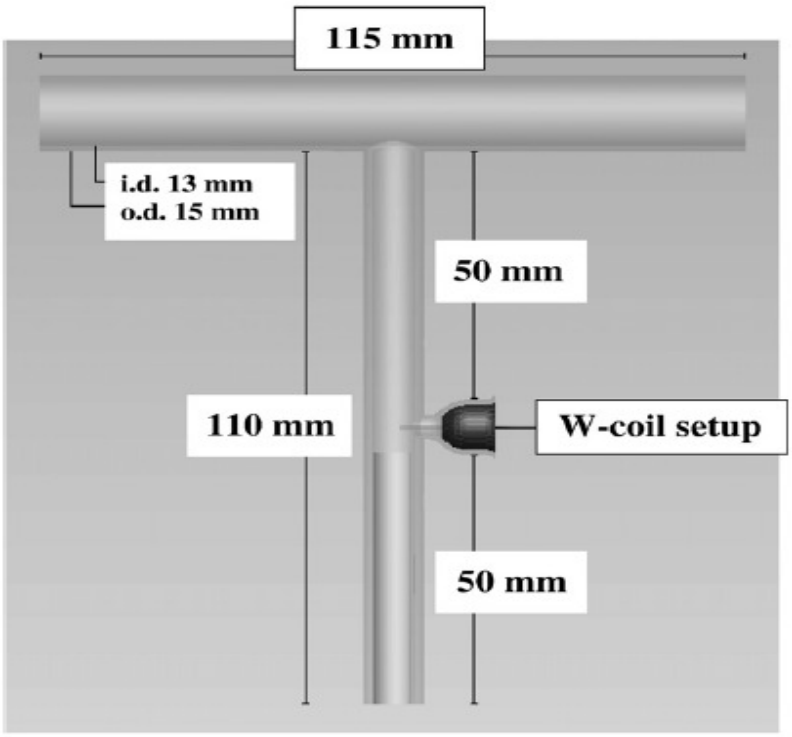


**Figure 2.1.** Quartz T-tube and W-coil trap.

For the characterization of the Au coated W-coil atom trap surface, a Philips scanning electron microscopy (SEM) XL-30S FEG microscope equipped with an EDX PW 900 microprobe system for element specific mapping was used.

### 2.1.3 Procedures

#### 2.1.3.1 Coating of W-coil Surface by Gold

In order to coat W-coil surface by Au, volatile species of Au formed by VCG were sent through W-coil which was heated at around 675 $^{o}$C. Design of QTA and W-coil

was the same as those given in section 2.1.2. Prior to coating W-coil was washed with ethanol and then deionized water. For Au-VCG, the optimization of the some experimental parameters which are length of reaction and stripping coils, concentration of reductant solution, flow rates and composition of gases, flow rates of gold and reductant solutions and collection temperature of W-coil atom trap were carried out by using a 1.0 mg $L^{-1}$ of Au solution. During the optimization studies, one parameter was varied while the others were kept constant. Optimization cycles were repeated until efficient collection of gold is taken place on the W-coil atom trap. During any optimization as the value of the parameter in question was varied, all the other parameters were kept in their optimized values.

For the separation of generated gold volatile species from the liquid phase, a laboratory-made cylindrical gas-liquid separator (GLS) was employed. After GLS, the volatile species were transferred to QTA through a Tygon tubing of length of 4.0 cm and 6.0 mm id (Masterflex, Cole Parmer Instrument Co.) using a carrier gas mixture composed of Hydrogen and Argon at flow rates of 155 mL $min^{-1}$ and 206 mL $min^{-1}$, respectively. Initially, this carrier gas mixture was sent through the system. Then, W-coil atom trap was brought to its optimum collection temperature and peristaltic pumps were activated to iniate the flow of gold solution and reductant solutions that are mixed in a 3-way PTFE connector. The transferred gold volatile species were trapped on the W-coil atom trap placed in the inlet arm of QTA as explained above.

#### 2.1.3.2 Selenium Determination by VCG-AAS and Gold Coated W-coil Trap

The experiments were carried out in CF mode in both conventional HGAAS and W-coil trap HGAAS studies. A schematic view of a hydride generation system is given in Figure 1.1. The HCl and $NaBH_4$ concentrations were optimized in conventional

HGAAS studies by using a 10.0 ng $mL^{-1}$ Se solution containing 7.0 mol $L^{-1}$ HCl. The blank was 7.0 mol $L^{-1}$ HCl solution. The reductant and analyte solutions were pumped at the flow rates of 1.88 mL $min^{-1}$ and 6.75 mL $min^{-1}$, respectively.

The generated hydrogen selenide was separated from the liquid phase by the GLS and was transferred to QTA through Tygon tubing using a carrier gas mixture composed of $H_2$ and Ar at flow rates of 112.5 mL $min^{-1}$ and 75 mL $min^{-1}$, respectively. In the W-coil trap study, the W-coil trap was resistively heated to 165 °C before turning the pumps on to deliver the analyte and reductant solutions for subsequent trapping; hydrogen selenide was trapped on the gold coated W-coil trap. During trapping, the carrier gas consisted of 112.5 mL $min^{-1}$ Ar with 75 mL $min^{-1}$ $H_2$. After the collection step for a chosen period of time, the pumps were stopped but the gas flow was continued. The W-coil trap temperature was increased to 675 °C for about 1.0 s; and then the flow of $H_2$ gas was increased to 450 mL $min^{-1}$. Analytical parameters for the gold-coated W-coil trap HGAAS technique are given in Table 2.1.

**Table 2.1.** Optimized analytical parameters for Se determination by VCG and the gold-coated W-coil trap VCG-AAS system.

| **Optimized Parameters** | **Optimum Values** |
|---|---|
| Carrier Solution | 7.0 mol $L^{-1}$ HCl, 6.75 mL $min^{-1}$ |
| Reductant Solution | 0.30% (w/v) $NaBH_4$, in 0.5% (w/v) NaOH, 1.88 mL $min^{-1}$ |
| Length of Reaction Coil | 20.0 cm |
| Length of Stripping Coil | 35.0 cm |
| Collection Carrier Gas | 112.5 mL $min^{-1}$ Ar, 75 mL $min^{-1}$ $H_2$ |
| Revolatilization Carrier Gas | 112.5 mL $min^{-1}$ Ar, 450 mL $min^{-1}$ $H_2$ |
| Collection Trap Temperature | 165 $^oC$ |
| Revolatilization Trap Temperature | 675 $^oC$ |

## 2.2 Gold Determination by VCG-AAS

### 2.2.1 Reagents

The working solutions of Au were prepared by making necessary dilutions from their stock standard solutions: 1000 mg $L^{-1}$ Au (Merck, Germany). Stock solution of 1.0% (w/v) sodiumdiethydithiocarbamate (NaDDTC, Merck) was prepared in ethanol (Merck) [135]. For the acidification of analyte solutions, 64% (v/v) $HNO_3$ (Merck, Germany) was used. Reductant solutions were prepared daily from the powder $NaBH_4$ (Merck, min. Purity 96%). For the stabilization of the $NaBH_4$ solution, NaOH (Carlo Erba, Milano, Italy) was used. Dilutions were made using 18 MΩ cm ultra pure water obtained from Milli-Q water purification system (Millipore, Bedford, MA, USA). All the solutions were prepared in high density polyethylene containers and were kept refrigerated.

### 2.2.2 Instrumentation

An ATI Unicam 929 atomic absorption spectrometer equipped with a deuterium background correction system was used. A Philips data coded hollow cathode lamp was operated at 7.0 mA; the analytical line at 242.8 nm was used in the measurements with 0.5 nm as the spectral bandwidth. QTA heated by a stoichiometric air/acetylene flame was used as atomizer. The dimentions of horizontal and inlet arm of QTA and placing of W-coil trap in the QTA were explained in Section 2.1.2. Solutions for both conventional and W-coil trap systems were sent continuously into the high volume gas liquid separator (HVGLS) shown in Figure 2.2 using a Gilson Minipuls 3 (Villers le Bell, France) 4-channel peristaltic pump. Main body of HVGLS is a cylinder with a height of 180 mm and a diameter of 50 mm. Tygon peristaltic pump tubing of 0.8 mm id (Ismatec, Germany) was used for pumping the analyte and reductant solutions that are mixed in a 3-way PTFE connector (Cole Parmer Instrument Co. USA).

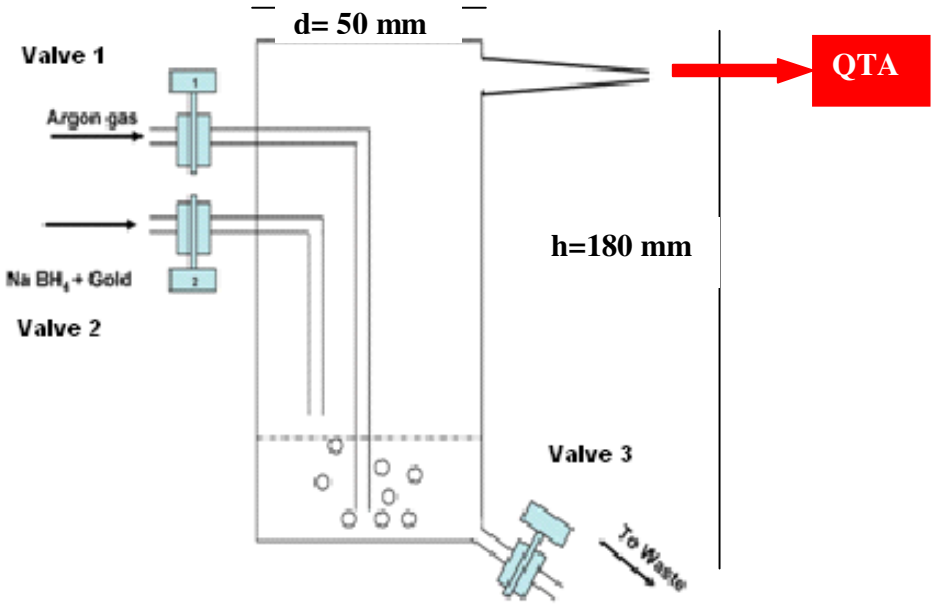


**Figure 2.2.** High Volume Gas Liquid Separator (HVGLS).

PTFE tubing of length of 40 mm and 6.0 mm id (Masterflex, Cole Parmer Instrument Co.) was used between the HVGLS and upstream of the inlet arm of the silica T-tube atomizer. During the experiment, two types of VCG systems have been used. One of them was the HVGLS itself shown in Figure 2.2.

The other includes the same HVGLS connected to W-coil trap shown in Figure 2.3. In the HVGLS without W-coil trap experiment, different type of gases such as Ar, $H_2$, $N_2$ and air were used in order to compare the sensitivities with different gases. On the other hand, in the W-coil trap study, a mixture of Ar and $H_2$ gases were applied for collection of analyte species on the W-coil trap while only $H_2$ gas was used for the revolatilization of the analyte species on the W-coil trap surface. The flow rates of these gases were measured by two separate flow meters (Cole Parmer Instrument Co. USA). As explained in Section 2.1.2., the W-coil temperature was manually

controlled by a variable potential power supply (Variac) and a 750 W transformer connected to mains electricity (220 V ac) through a power switch. The input voltage of the variable potential power supply was 220 V [181,182]. The temperature measurements were carried out by using both a Ni-Cr thermocouple and a Pyrometer (IRCON Niles, IL USA).

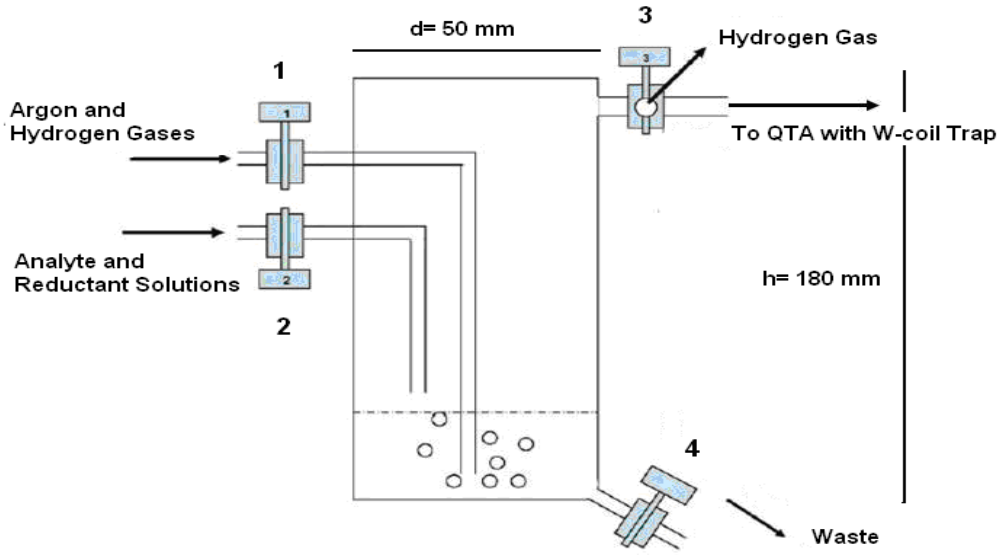


**Figure 2.3.** Modified HVGLS with the W-coil atom trap

### 2.2.3 Procedure

The experiments were carried out both HVGLS itself and W-coil trap with a HVGLS. The $HNO_3$ and $NaBH_4$ concentrations were optimized for both VCG systems with HVGLS only and HVGLS having W-coil trap by using a 100.0 ng $mL^{-1}$ and 10.0 ng $mL^{-1}$ Au solutions containing 1.0 mol $L^{-1}$ $HNO_3$, respectively. The blank solution was 1.0 mol $L^{-1}$ $HNO_3$ and 0.0006% NaDDTC [135]. The reductant and analyte solutions were pumped at the flow rates of 8.31 mL $min^{-1}$ and 11.03 mL $min^{-1}$, respectively. In

the first procedure, by the effect of the peristaltic pumps, around 20 mL of analyte solution (total volume 35 mL) were collected in the HVGLS and then a flow rate of 76 mL $min^{-1}$ Ar gas was bubbled through into the solution for 30 seconds; this stage is called as *bubbling period*. After this step, Ar gas flow was turned off for 2 minutes, which is called *waiting period*. Immediately at the end of this period, Ar gas at the flow rate (376 mL $min^{-1}$) was sent through the solution and slowly generated Au volatile species were transferred to QTA through PTFE tubing; the peak shaped signal was recorded.

In the W-coil trap study, the W-coil trap was resistively heated to 750 $^{o}$C; then pumps were turned on to deliver the analyte and reductant solutions into HVGLS for subsequent trapping. During the collection of the Au and $NaBH_4$ solutions into the HVGLS, the carrier gas consisted of 76 mL $min^{-1}$ Ar and 146 mL $min^{-1}$ $H_2$ is bubbled into the contents of HVGLS for 2 minutes and generated volatile Au species were collected on the W-coil. The function of bubbling is to transport all of the slowly generated volatile Au species to the W-coil trap. After 2 min bubbling/collection time, as the Au signal was almost same, 2 min was chosen as an optimized *bubbling/collection period*. If the *bubbling/collection period* is less than 2 minute, the Au signal is decreased. After the collection step for a chosen period of time, only $H_2$ gas with the flow rate of 376 mL $min^{-1}$ was sent through the 3-way valve shown in Figure 2.3 and W-coil trap temperature was simultaneously increased to 1400 $^{o}$C for about 1.0 second for revolatilization of the Au species on the W-coil trap; peak shaped signal was recorded. At the revolatilization stage, the function of the $H_2$ gas is not only for eliminating the probability of the oxidation of the W-coil trap but also for transporting the revolatilized Au species to the atomizer. The optimum analytical parameters for gold both HVGLS itself and W-coil atom trap with HVGLS system are given in Table 2.2 and Table 2.3, respectively.

**Table 2.2.** Optimized analytical parameters for Au determination using VCG-AAS with HVGLS itself.

| **Optimized Parameters** | **Optimum Values** |
|---|---|
| Carrier solution | 1.0 mol $L^{-1}$ $HNO_3$, 11.03 mL $min^{-1}$ |
| Reductant solution | 1.00% (w/v) $NaBH_4$, in 0.50% (w/v) NaOH, 8.31 mL $min^{-1}$ |
| Length of reaction coil | 23.0 cm |
| Bubbling period | 30 s |
| Waiting period | 120 s |

**Table 2.3.** Optimized analytical parameters for Au determination using VCG-AAS with HVGLS and W-coil trap.

| **Optimized Parameters** | **Optimum Values** |
|---|---|
| Carrier solution | 1.0 mol $L^{-1}$ $HNO_3$, 11.03 mL $min^{-1}$ |
| Reductant solution | 1.00% (w/v) $NaBH_4$, in 0.50% (w/v) NaOH, 8.31 mL $min^{-1}$ |
| Length of reaction coil | 23.0 cm |
| Collection carrier gases | 76 mL $min^{-1}$ Ar , 146 mL $min^{-1}$ $H_2$ |
| Revolatilization carrier gas | 376 mL $min^{-1}$ $H_2$ |
| Collection trap temperature | 750 $^oC$ |
| Revolatilization trap temperature | 1400 $^oC$ |
| Collection Period | 120 seconds |

## 2.3 Gold Determination by Flow Injection Volatile Compound Generation Atomic Absorption Spectrometry (FI-VCG-AAS)

This part of study has been conducted in Prague at the Institute of Analytical Chmistry in Czech Republic.

### 2.3.1 Reagents

All reagents were at least of analytical grade. Deionized water (< 0.2 µS $cm^{-1}$, Ultrapure, Watrex) was used for all dilutions. The working solutions of Au were prepared by making a series of dilutions from their stock standard solutions: 1000 µg $ml^{-1}$ Au (BDH, England) in 0.6 mol $L^{-1}$ $HNO_3$ (p.a., Lach-Ner, Czech Rep.) used also as the carrier liquid. If not stated otherwise all measurements were done with working solutions containing 1 µg $mL^{-1}$ Au. Stock solution of 1.0% (m/v) sodium diethyldithiocarbamate trihydrate (DDTC) (Sigma) was prepared in ethanol (reagent grade, Severochema, Czech Rep.). Reductant solution of 2.4% (m/v) sodium THB (Fluka, Switzerland) was prepared fresh daily in 0.1% (m/v) KOH (p.a., Lachema, Czech Republic) with antifoaming agent - 133 µL of 10% (m/v) solution of Antifoam B emulsion (Sigma) per 100 mL. 20 µg $mL^{-1}$ of Triton X-100 (Aldrich Chemical Co., USA) in 0.1 mol $L^{-1}$ $HNO_3$ was used as a reaction modifier. 0.5 mol $L^{-1}$ NaOH solution (Lach-Ner, s.r.o., Czech Rep.) served as a waste stabilizer.

### 2.3.2 Instrumentation

Perkin Elmer 503 AAS spectrometer (Perkin Elmer, Bodenseewerk, Germany) was used in the case of on-line atomization of the generated Au form. Pye-Unicam Au hollow cathode lamp was operated at 10.0 mA; the analytical line at 242.8 nm was

used in the measurements with 0.7 nm as the spectral bandwidth. Spectrometer output signals were AD converted in a PC as ASCII files for further processing in Microsoft Excel software.

For GF AAS measurements, a Varian SpectrAA 30 atomic absorption spectrometer equipped with a Zeeman background correction system was used. Varian Techtron Au hollow cathode lamp at 242.8 nm line, using 1 nm spectral bandwidth, operated at 15 mA was the radiation source.

### 2.3.3 VCG/on-line Atomization

The details of the flow injection (FI) generator are given in Figure 2.4 [183]. It was constructed of 1/16" o.d. polytetraflouroethylene (PTFE) tubing connected by 1/4-28 polyether ether ketone (PEEK) connectors. Sample was injected into the flow system by a manual injection valve (5020 sample injection valve, Rheodyne, CA, U.S.A.) with a 500 µL sample loop. The core of the system is the mixing manifold based on 3 concentric capillaries and a gas-liquid separator (GLS) [184,185]. Innermost capillary (quartz, 0.25 mm i.d.) leads carrier liquid with sample plug and reaction modifier, middle one (quartz, 0.53 mm i.d.) the reductant solution and the outer one (PTFE, 1mm i.d.) carrier Ar. The capillaries end in 1 mm distances and protrude 5 mm inside the GLS (glass, volume 3 mL). Mixing of reagent solutions therefore proceeds in a very small volume. In order to eliminate $H_2$ evolution (28 mL $min^{-1}$ of hydrogen was produced from THB decomposition) inside the waste liquid tubing, 0.5 mol $L^{-1}$ NaOH as waste stabilizer which was pumped to the waste outlet of the GLS. Peristaltic pumps (Reglo Digital 4-11, Ismatec, Switzerland) were used to pump reagents at the flow rate of 0.5 mL $min^{-1}$ and to remove the waste liquid at arbitrary rate. Mass flowmeters (FMA-2400 or 2600 Series, Omega Engineering, Stamford, CT, USA) were used to control gas flows for the system.

The on-line atomization of the analyte VC, transported from GLS by the flow of carrier Ar via a PTFE tubing (1.6 mm i.d., 4 cm in length), was performed in the multiatomizer described previously - model MM5 in Ref [107]. If not stated otherwise, the Ar carrier flow rate was 240 mL $min^{-1}$. The multiatomizer consisted of a horizontal arm aligned in the optical path of the AAS spectrometer and of an inlet arm 90 mm long with 2 mm i.d. The horizontal arm of the atomizer was made of two concentric tubes: the inner one (optical, 130 mm long, 7 mm i.d.) was evenly perforated with 14 holes of approximately 0.5 to 1 mm in diameter. A flow of gas (outer gas) was introduced from the sides into the cavity between the two tubes of the horizontal arm and then passed through the holes into the optical tube. If not stated otherwise, 30 mL $min^{-1}$ of air was employed as the outer gas.

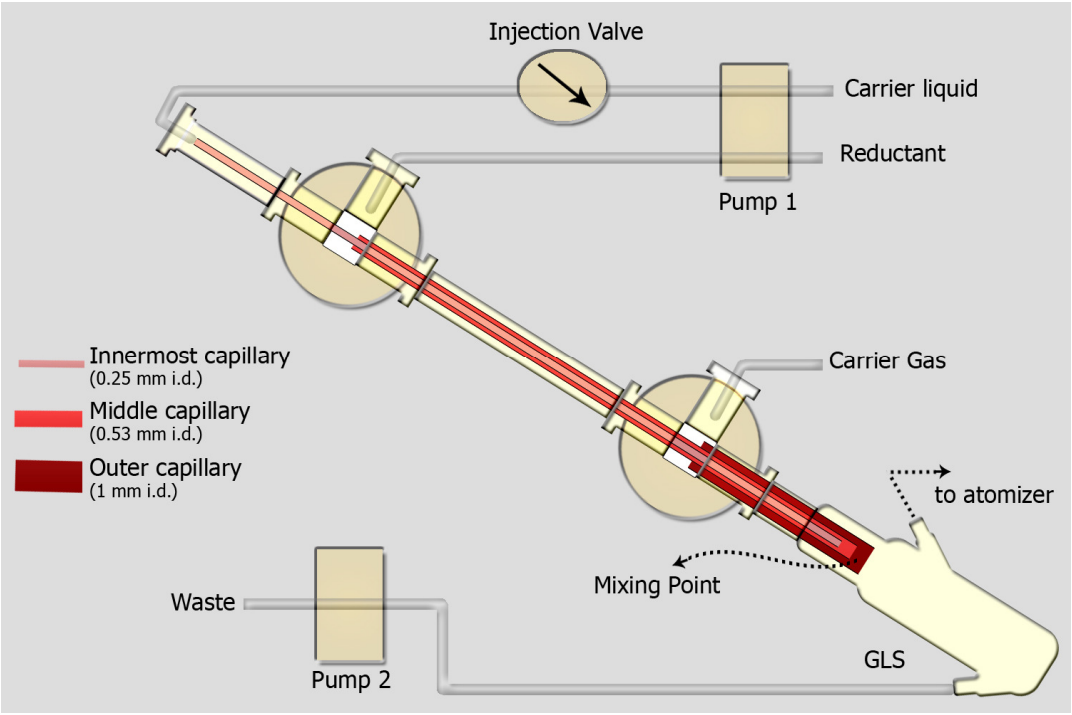


**Figure 2.4.** The scheme of the FI generator

### 2.3.4 Au Determination in Filter Leaches and in the Reaction Mixture Waste by the Liquid Sample Introduction GF AAS

The permanent Ir modification by 40 µL of 1000 µg $mL^{-1}$ Ir was used [135]. The coating Ir solution was dried and pretreated at 500 °C.

1 mL of aqua regia filter leach was diluted to 10 mL and determined using calibration standards prepared in aqua regia/matching matrix. 15 µL of sample was injected. Sample was dried (5 s at 85 °C, 40 s at 95 °C and 10 s at 120 °C), thermally pretreated 7 s at 500 °C and atomized at 2200 °C (3 s). It has been checked that analyte additions yielded results which did not significantly differ from those based on the calibration employing aqua regia/matching standards.

Samples of reaction mixture were diluted 10 times; method of analyte additions was used with 15 µL sample injections. The furnace program was the same as used to determine Au in filter leaches.

### 2.3.5 VCG/in-situ Trapping in GF AAS

VCG of Au has been carried out using the above described FI generator and then trapped in-situ in GF. The above described Ir permanent modification of the graphite was used.

*Procedure.* After the 0.500 mL loop of the injection valve was filled with sample solution, the tip of the quartz capillary (1.65 mm o.d., 0.7 mm i.d.) connected to GLS by 150 mm of 1 mm i.d. PTFE tubing was inserted manually into the injection hole of the graphite tube, 1 mm from the bottom wall of the tube. The FI system was then actuated when the furnace temperature was reached to 500 $^{o}$C. The generated VC of

Au was separated and transferred by the Ar carrier gas of the flow rate of 125 mL $min^{-1}$ and hydrogen evolved from the THB (around 30 mL $min^{-1}$) and was deposited on the tube inner wall. At the end of a 200 s trapping period, the quartz probe was removed from the graphite tube manually and immediately the GF was heated to atomization temperature of 2200 $^{o}$C (ramp 1.1 s, hold 2 s). After recording the signal, the furnace was cleaned at the same temperature for additional 1 s. Furnace Ar flow of 3 L $min^{-1}$ was used throughout the program except trapping and atomization step when gas stop conditions were used.

### 2.3.6 Conventions

Peak areas of AAS signals are invariably employed as the analytical quantity. If sensitivity is mentioned it always stands for peak area related to the analyte mass taken for the measurement, i.e. introduced either to the generator in the case of VCG or to the GF in the case of the liquid sample introduction GF. Since the analyte volumes were always 500 µL and 15 µL, respectively, in the case of VCG and liquid sample introduction to GF, the relation between analyte concentration and mass is unambiguous. The peak area characteristic mass, $m_0$, is here invariably related to the analyte mass transported to the atomizer. Consequently, $m_0$ is fully independent of the generator - it is controlled exclusively by spectrometer and atomizer parameters (including, however, gas flow rate to the atomizer [106,186].

Averages of at least 3 replicates of peak area values are presented in Figures and in the text. Uncertainties are presented as ± standard deviation. If not explicitly given otherwise the precision of measurements was better than 3.5% (RSD).

### 2.3.7 Studies with Electron Microscopy

In order to prepare the microscopic measurements, VC of Au was continuously generated from 10 µg $mL^{-1}$ Au solutions and transported to be adsorbed onto carbon/formvar coated Cu grids. The grids had been glow discharge activated immediately prior to sampling to make them hydrophilic and attractive for positively charged particles as well [184,187]. Grids were placed downstream of GLS to sample particles from the gaseous phase for 60 seconds and then air dried.

The samples were examined in transmission electron microscope (TEM) Philips CM100 (FEI, formerly Philips EO, The Netherlands) equipped with slow-scan CCD camera Mega ViewII (Olympus, formerly Soft Imaging Systems, GmbH, Germany). Digitally recorded images were taken at the magnification of 64 000, which corresponds to pixel size of 1 nm. The Energy Dispersive X-ray Spectroscopy (EDS) microanalysis was performed in Philips CM12/STEM electron microscope (FEI, formerly Philips EO, The Netherlands) equipped with EDAX DX4 X-ray analytical system (EDAX, AMETEK, Inc.). The spectra from individual particles or particle clusters were recorded in Scanning Transmission Electron Microscopy (STEM) bright-field spot-mode at magnification of 50 000, 80 kV and spot-size of 7 (10 nm) for 300 ls (live seconds). The corresponding images of analyzed samples were recorded in STEM bright-field spot-mode at the same magnification.

## 2.4 Silver Determination by VCG-AAS

### 2.4.1 Reagents

The working solutions of Ag were prepared by making necessary dilutions from their stock standard solution: 1000 mg $L^{-1}$ Ag (Merck, Germany). For the acidification of

analyte solutions, 64% (w/v) $HNO_3$ (Merck, Germany) was used.

Reductant solutions were prepared daily from the powder sodium tetrahydroborate (III) (Merck, min. Purity 96%). For the stabilization of the $NaBH_4$ solution, NaOH (Carlo Erba, Milano, Italy) was used. Dilutions were made using 18 MΩ.cm ultra pure water obtained from a Milli-Q water purification system (Millipore, Bedford, MA, USA). All the solutions were prepared in high density polyethylene containers and were kept refrigerated.

### 2.4.2 Instrumentation

An ATI Unicam 929 atomic absorption spectrometer equipped with a deuterium background correction system was used. A Philips data coded hollow cathode lamp was operated at 7.0 mA; the analytical line at 328.1 nm was used in the measurements with 0.5 nm as the spectral bandwidth. Quartz T-tube atomizer (QTA) which was explained in section 2.1.2.

In this system, the W-coil trap obtained from a 15 V, 150 W projector bulb (Halogen Photooptic Lamp Xenophot, Osram, Germany) was inserted inside the QTA as the same procedure which was explained in the Section 2.1.1. As outlined before, this configuration allows a very rapid and convenient change of W-coil when needed [181]. The temperature measurements were carried out with a Ni–Cr thermocouple.

In the W-coil trap studies, two types of the GLS were used in turn for the separation of volatile Ag species from the liquid phase. The first one is called as the cylindrical GLS. The second system used is the HVGLS shown in Figure 2.3. Prior to use of these GLSs for both W-coil trap and without W-coil trap systems, they were silanized to deactivate the internal surfaces [135]. For this purpose, a 10% (v/v) solution of

dichlorodimethylsilane (Aldrich, 99%) in toluene was prepared and the glass parts were kept in this solution for 24 hours and then oven dried at 100 $^{o}$C and finally washed with methanol. After silanization, the GLSs were used until the blank values started to increase; then, another silanization was required. A typical lifetime for silanization was about 50-100 uses [135].

VCG for both conventional and W-coil trap systems were carried out in CF mode using a Gilson Minipuls 3 (Villers le Bell, France) 4-channel peristaltic pump. Tygon peristaltic pump tubing of 0.8 mm id (Ismatec, Germany) was used for pumping the analyte and reductant solutions that are mixed in a 3-way PTFE connector (Cole Parmer Instrument Co. USA). Without W-coil study, only $H_2$ gas which was evolved from the $NaBH_4$ by the reaction with acidic solutions i.e. no additional gas was used to eliminate the dilution of the analyte with gases. HVGLS design was not used without a W-coil because the control of the signals in HVGLS without W-coil trap was difficult; therefore, the reproducibility was poor. Owing to this reason, W-coil trap was connected to downstream of the HVGLS for the further studies.

### 2.4.3 Procedures

The experiments were carried out in CF mode in the both conventional VCG-AAS and W-coil-VCG-AAS studies. In conventional VCG-AAS studies with U-shaped GLS and cylindrical GLS, $HNO_3$ and $NaBH_4$ concentrations and their flow rates and length of the reaction and stripping coils were optimized using 250 ng mL$^{-1}$ and 10.0 ng mL$^{-1}$ Ag solutions containing 1.0 mol L$^{-1}$ $HNO_3$, respectively. Blank solution was 1.0 mol L$^{-1}$ $HNO_3$ solution which was the optimized value for carrier solution. The reductant and Ag solutions were pumped at the flow rates of 4.24 mL min$^{-1}$ and 30.00 mL min$^{-1}$, respectively. The experimental set-up is shown in Figure 2.5.

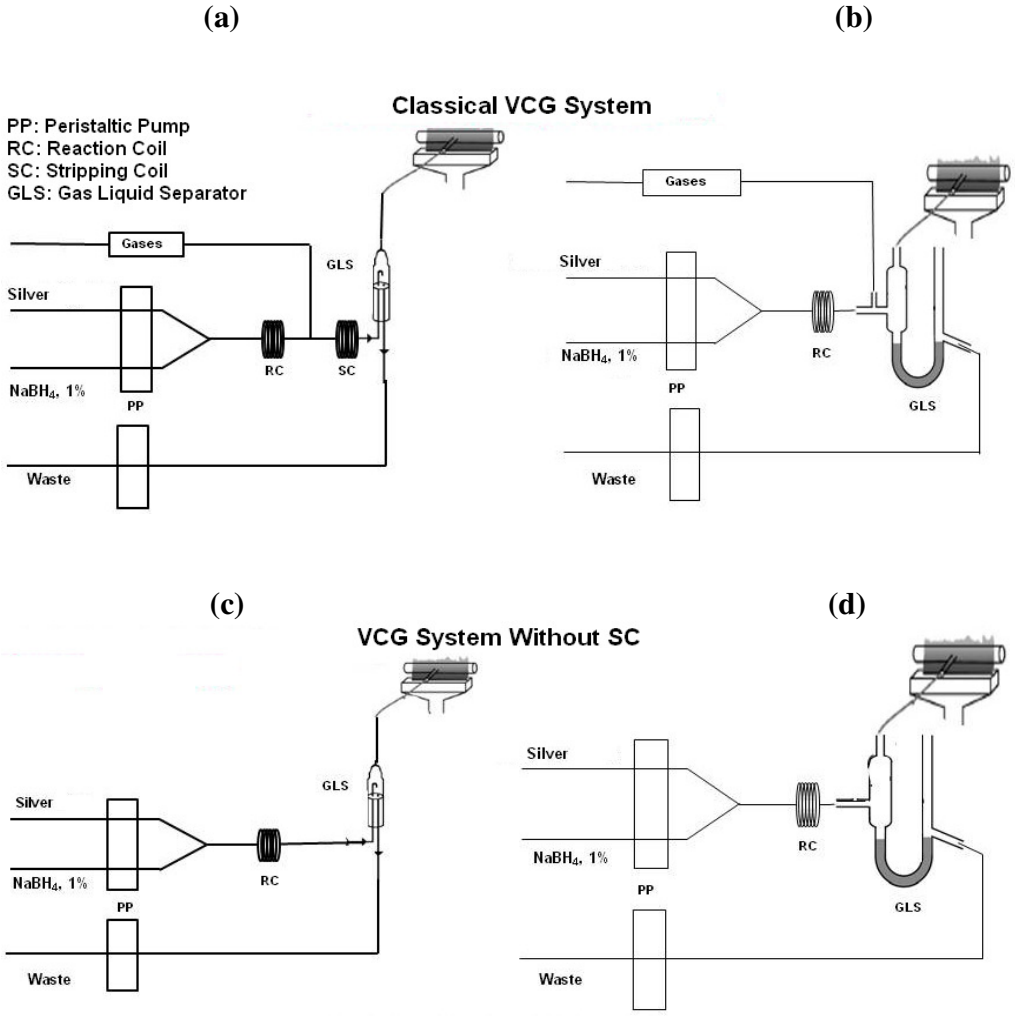


**Figure 2.5.** (a) Scheme of classical VCG system using cylindrical GLS. (b) Scheme of classical VCG system using U-shaped GLS. (c) Scheme of classical VCG system without SC using cylindrical GLS and no carrier gas flow. (d) Scheme of classical VCG system without SC using U-shaped GLS and no carrier gas flow.

In studies without W-coil trap, the generated volatile Ag species were separated from the liquid phase by a laboratory made U-shaped GLS or a cylindrical GLS and then transferred to QTA through a Tygon tubing. In this stage, as the gases caused the

dilution of the analyte and decreased the sensitivity, they were not used.

In the W-coil trap study, the generated volatile Ag species were separated from the liquid phase by using a cylindrical GLS or HVGLS and then transferred to the W-coil trap. For both of the systems, flow rates of the gases, collection and revolatilization temperatures were optimized separately. In the cylindrical GLS system, to collect the generated volatile Ag species, only $H_2$ gas at a flow rate of 146 mL $min^{-1}$ was used. During the revolatilization stage, the flow rate of the $H_2$ gas was increased to 376 mL $min^{-1}$ to help the release of the collected Ag species on the W-coil trap. In both of the stages, Ar gas was not used. The optimum collection and revolatilization temperatures were found in turn as 750 $^oC$ and 1800 $^oC$ on W-coil trap surface. To improve the sensitivity and reach lower LOD values, W-coil trap was also employed with HVGLS shown in Figure 2.3 instead of cylindrical shape GLS. In this system, the W-coil was resistively heated to 750 $^oC$ which is the optimum collection temperature. Then, the pumps are turned on to send Ag and $NaBH_4$ solutions into HVGLS. During the collection of Ag and $NaBH_4$ solutions into the HVGLS, the carrier gas consisted of 76 mL $min^{-1}$ Ar and 146 mL $min^{-1}$ $H_2$ was bubbled through the contents of HVGLS for 30 s and generated volatile Ag species were started to collect on the W-coil trap. After the collection step for a chosen period of time, only $H_2$ gas with the flow rate of 376 mL $min^{-1}$ was sent through the 3-way valve which was placed the downstream of the HVGLS and then W-coil trap temperature was increased to 1800 $^oC$ which is the optimum revolatilization temperature and Ag signal was taken. At the revolatilization stage, function of the $H_2$ gas is not only to eliminate the probability of the oxidation on the W-coil trap but also to help transferring the revolatilized species to the QTA. Analytical parameters for Ag determination using VCG-AAS system with or without W-coil trap are given in Table 2.4 and Table 2.5.

**Table 2.4** Optimized analytical parameters for Ag determination using VCG-AAS system with U-shaped and cylindrical GLS without W-coil trap.

| **Optimized Parameters** | **Optimum Values** |
|---|---|
| Carrier solution | 1.0 mol $L^{-1}$ $HNO_3$, 30.0 mL $min^{-1}$ |
| Reductant solution | 1.00% (w/v) $NaBH_4$, in 0.50% (w/v) NaOH, 4.24 mL $min^{-1}$ |
| Length of reaction coil | 30.0 cm |
| Collection carrier gas | Only $H_2$ evolved from $NaBH_4$ |

**Table 2.5.** Optimized analytical parameters for Ag determination using VCG-AAS system with cylindrical and HVGLS with W-coil trap.

| **Optimized Parameters** | **Optimum Values** |
|---|---|
| Carrier solution | 1.0 mol $L^{-1}$ $HNO_3$, 30.0 mL $min^{-1}$ |
| Reductant solution | 1.00% (w/v) $NaBH_4$, in 0.50% (w/v) NaOH, 4.24 mL $min^{-1}$ |
| Length of reaction coil | 30.0 cm |
| Collection carrier gas | 76 mL $min^{-1}$ Ar , 146 mL $min^{-1}$ $H_2$ |
| Revolatilization carrier gas | 376 mL $min^{-1}$ $H_2$ |
| Collection trap temperature | 750 $^oC$ |
| Revolatilization trap temperature | 1800 $^oC$ |

## 2.5 Indium Determination by VCG-AAS

### 2.5.1 Reagents

The working solutions of In were prepared by making necessary dilutions from their stock standard solution: 1000 mg $L^{-1}$ In (Merck, Germany). For the acidification of analyte solutions, 37% (v/v) HCl (Merck, Germany) was used.

Reductant solutions were prepared daily from the powder sodium tetrahydroborate (III) (Merck, min. Purity 96%). For the stabilization of the $NaBH_4$ solution, NaOH (Carlo Erba, Milano, Italy) was used. Dilutions were made using 18 MΩ cm ultra pure water obtained from Milli-Q water purification system (Millipore, Bedford, MA, USA). All the solutions were prepared in high density polyethylene containers and were kept refrigerated.

### 2.5.2 Instrumentation

An ATI Unicam 929 atomic absorption spectrometer equipped with a deuterium background correction system was used. A Philips data coded hollow cathode lamp was operated at 10.0 mA; the analytical line at 303.9 nm was used in the measurements with 0.7 nm as the spectral bandwidth. Quartz T-tube atomizer (QTA) heated by a stoichiometric air/acetylene flame was used as atomizer. Dimentions of QTA and W-coil trap were explained in section 2.1.2.

### 2.5.3 Procedures

The experiments were carried out in CF mode in the both conventional VCG-AAS and W-coil-VCG-AAS studies. The experimental set-up was the same as shown in Figure 2.5. In conventional VCG-AAS studies without W-coil trap, a cylindrical GLS was employed. In this stage, HCl and $NaBH_4$ concentrations and their flow rates and length of the reaction and stripping coils were optimized using 4.0 mg $L^{-1}$ In solutions. Blank solution was 3.0 mol $L^{-1}$ HCl. The reductant and In solutions were pumped at the flow rates of 10.0 mL $min^{-1}$ and 15.0 mL $min^{-1}$, respectively.

In without W-coil trap studies, the generated volatile In species were separated from the liquid phase by a laboratory made cylindrical GLS and then transferred to QTA through a Tygon tubing. In this stage, as the gases caused the dilution of the analyte and decreased the sensitivity, they were not used.

In the W-coil trap study, the generated In species were separated from the liquid phase by using HVGLS and transferred to the W-coil trap by a mixture of Ar and $H_2$ gases. The W-coil was resistively heated to 750 $^0$C before turning the pumps on to deliver solutions into a HVGLS for subsequent trapping; then pumps are turned on to send In and reductant solutions into HVGLS. During the collection of In and $NaBH_4$ solutions into the HVGLS, the carrier gas consisted of 76 mL $min^{-1}$ Ar and 146 mL $min^{-1}$ $H_2$ was bubbled into the HVGLS for 60 s and generated volatile In species were collected on the W-coil trap. After the collection step for a chosen period of time, only a $H_2$ gas with the flow rate of 376 mL $min^{-1}$ was sent through the 3-way valve which was placed the downstream of the HVGLS shown in Figure 2.3 and then W-coil trap temperature was increased to 1800 $^o$C which is the optimum revolatilization temperature and In signal was taken. At the revolatilization stage, function of the $H_2$ gas is not only to eliminate the probability of the oxidation on the W-coil trap but also to help transferring the revolatilized species to the QTA. Analytical parameters for In

determination using VCG-AAS system with or without W-coil trap are given in Table 2.6 and Table 2.7, respectively.

**Table 2.6.** Optimized analytical parameters for In determination using VCG-AAS system and cylindrical GLS without W-coil trap

| **Optimized Parameters** | **Optimum Values** |
|---|---|
| Carrier solution | 3.0 mol $L^{-1}$ HCl, 15.0 mL $min^{-1}$ |
| Reductant solution | 1.00% (w/v) $NaBH_4$, in 0.50% (w/v) NaOH, 10.0 mL $min^{-1}$ |
| Length of reaction coil | 23.0 cm |

**Table 2.7.** Optimized analytical parameters for Ag determination using VCG-AAS system and HVGLS with W-coil trap.

| **Optimized Parameters** | **Optimum Values** |
|---|---|
| Carrier solution | 3.0 mol $L^{-1}$ HCl, 15.0 mL $min^{-1}$ |
| Reductant solution | 1.00% (w/v) $NaBH_4$, in 0.50% (w/v) NaOH, 10.0 mL $min^{-1}$ |
| Length of reaction coil | 23.0 cm |
| Collection carrier gas | 76 mL $min^{-1}$ Ar , 146 mL $min^{-1}$ $H_2$ |
| Revolatilization carrier gas | 376 mL $min^{-1}$ $H_2$ |
| Collection trap temperature | 750 $^oC$ |
| Revolatilization trap temperature | 1800 $^oC$ |

# CHAPTER 3

# RESULTS AND DISCUSSION

## 3.1 Selenium Determination by VCG-AAS

According to the preliminary results obtained in our laboratory, *in situ* trapping of selenium was realized successfully on bare W-coil; however, revolatilization did not take place even at about 2000 ºC. It has been reported that trapping of hydrogen selenide on bare tungsten surface could be obtained only with low efficiency by workers who used a WETA tungsten electrothermal atomizer [126]. On the other hand, other workers who used pure gold as a trap was successful in both trapping and revolatilization [142]. According to our previous findings, however, when heated to high temperatures, pure gold slowly vaporizes until it completely vanishes. Therefore, gold-coated W-coil was preferred in this study. W-coil has been designed to be resistively heated; and since for sufficiently thin coatings the gold layer will not be conducting, the resistive heating will be realized through the tungsten although it has a higher resistivity as compared to gold. The resistivity values in μΩ·cm are 2.2 and 5.4 for Au and W, respectively. Therefore, in a gold-coated W-coil, tungsten provides the convenient means for heating while the gold layer functions as the proper trap surface that provides both efficient trapping and revolatilization that are necessary for a feasible trap system. Since gold coating was realized in an oxygen-free organic solvent medium, no oxidation and deterioration was observed on W surface. In this study, it has been tested that after at least 200 firing, the change in

sensitivity is not significant for selenium signal.

### 3.1.1 Optimization of $NaBH_4$ and HCl Concentrations

Optimization of $NaBH_4$ concentration was made in order to obtain the maximum sensitivity for selenium determination using conventional HGAAS measurements. The $NaBH_4$ flow rate was fixed at 1.88 mL $min^{-1}$ and the optimum concentration of $NaBH_4$ was found to be 0.3% (w/v). $NaBH_4$ solutions were prepared by dilution with 0.5% (w/v) NaOH for better stability. Nevertheless, only freshly prepared solutions were used. For concentrations of reductant higher than the optimum value, a slight decrease in sensitivity was observed. The best concentration for HCl in the blank and sample solutions was selected as 7.0 mol $L^{-1}$; this value, in addition to the fact that it assured the best sensitivity in hydride generation, also kept Se in +4 state during the experiments.

### 3.1.2 Effects of the Carrier Gas Composition and Flow Rate

Carrier gas composition and its flow rate is one of the most important variables in the trapping and revolatilization efficiency for *in situ* hydride collection. The carrier gas was a mixture of Ar and $H_2$ where the flow rates were optimized and fixed at 112.5 mL $min^{-1}$ and 75 mL $min^{-1}$, respectively, during the collection step. Presence of hydrogen in the system is needed to provide the medium that will protect W-coil from oxidation by oxygen impurities in gases and oxidizing species that could be transported to the trap in the aerosol reaching from GLS. In the revolatilization step, the flow rate of $H_2$ was increased from 75 mL $min^{-1}$ to 450 mL $min^{-1}$. Although a signal could be obtained with the former carrier gas composition, this change in composition provided an increase in sensitivity by a factor of 2.1 fold and sharper

peaks were obtained. For some experiments during revolatilization when only Ar gas was used with a flow of 525 mL $min^{-1}$, a value that is equal to the sum of the individual gases used in revolatilization, no selenium signal could be obtained. This shows that $H_2$ should be used not only for the protection of trap but it also is functional in the mechanism that is responsible for the stripping of analyte species from the trap surface during the revolatilization step.

In this study, it was also observed that during the revolatilization step if the hydrogen gas flow was increased immediately after increasing the trap temperature, the sensitivity was improved by 15% as compared with increasing the hydrogen gas flow before increasing the trap temperature.

### 3.1.3 Nature of Analyte Species on Trap and after Revolatilization

There is no direct evidence regarding the nature of analyte species that are trapped and that are revolatilized. During the revolatilization step, when the flame heating QTA was extinguished, no signal could be obtained. Therefore, it could be concluded that revolatilized species are not in atomic form, at least not in a stable atomic form with a life-time that is long enough to reach the QTA. It should be noted that while some other researchers [122,188] use W-coil as an atomizer by heating it as high as 2200 ºC, in this study the similar device is used as an electrothermal vaporizer rather than the atomizer since atomization takes place in QTA; significantly lower temperatures are used, 675 ºC in this case while using the similar technique it was 1200 ºC for Bi determination [121] and only 1000 ºC for determination of Cd [180]. On the other hand, the effect of hydrogen during revolatilization clearly shows that the process of stripping the analyte from trap surface is not totally a thermal process, some chemistry is involved. The nature of species involved requires further and deeper studies on the subject.

### 3.1.4 Analytical Figures of Merit

The analytical figures of merit for the suggested technique are given in Table 3.1. The calibration plot is linear ($R^2$= 0.9976) from 0.10 to 2.0 ng $mL^{-1}$ shown in Figure 3.1 for gold coated W-coil trap HGAAS measurements; the limit of detection was found to be 39 ng $L^{-1}$ Se using 11 consecutive measurements of 0.10 ng $mL^{-1}$ Se solution. The calibration plot was drawn by using peak height values; the equation for the best line was A= 0.1781C + 0.0226 where unitless absorbance signal height for CF measurement and C was concentration in units of ng $mL^{-1}$; $R^2$ was 0.9976. In studies with trap, 27.0 mL of sample solution was collected in 4.0 minutes. Peak height values were used since the peaks were very sharp. The calibration plot was also drawn by using peak area values; the equation for the best line was A = 0.0801C + 0.0167, where A was peak area in units of seconds and C was concentration in units of ng $mL^{-1}$; $R^2$ was 0.9987. For conventional VCG-AAS experiments, the equation for the best line was A = 0.0094C + 0.0062, where A was unitless absorbance signal height for CF measurement and C was concentration in units of ng $mL^{-1}$; $R^2$ was 0.9966; calibration plot was linear from 1.0 to 15.0 ng $mL^{-1}$; the limit of detection was found to be 260 ng $L^{-1}$ using 11 consecutive measurements of 1.0 ng $mL^{-1}$ Se solution. Enhancement in sensitivity using the ratio of characteristic concentration values is 20.1 while this value is 436 ng $L^{-1}$ and 21.7 ng $L^{-1}$ for conventional VCG-AAS and trap techniques, respectively. Peak profile of the analytical signal from a trap measurement is shown in Figure 3.2; it can be noticed that the half width of the transient signal was less than 0.5 s.

**Table 3.1.** Analytical figures of merit for Se determination calculated by using peak height; sample solution flow rate was 6.75 mL $min^{-1}$ , 27.0 mL of sample were collected in 4.0 minutes.

| | **W-coil trap HGAAS** | **HGAAS** |
|---|---|---|
| Limit of detection (3s), ng $L^{-1}$ | 39 | 260 |
| Characteristic concentration, $C_0$, ng $L^{-1}$ | 21.7 | 436 |
| RSD % (n=11) | 3.9 | 8.5 |

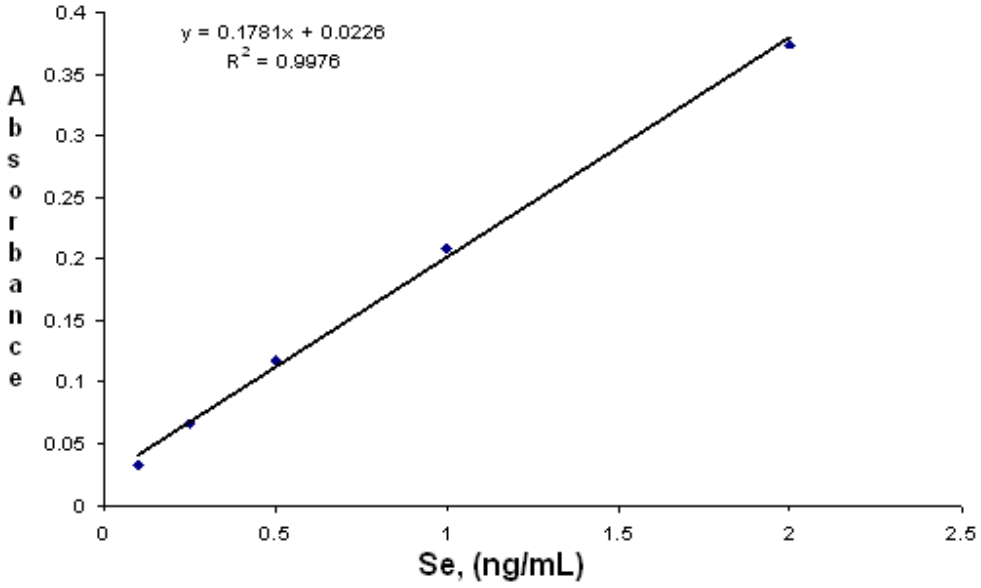


**Figure 3.1.** Calibration plot for gold coated W-coil trap VCG-AAS, sample solution flow rate was 6.75 mL $min^{-1}$; 27.0 mL of sample was collected in 4.0 minutes.

A comparison of LOD values is given in Table 3.2 for several recent studies on selenium determination. The works by Guo and Guo [142] and Barbosa group [122,188] can be compared with our study since trapping approaches are similar.

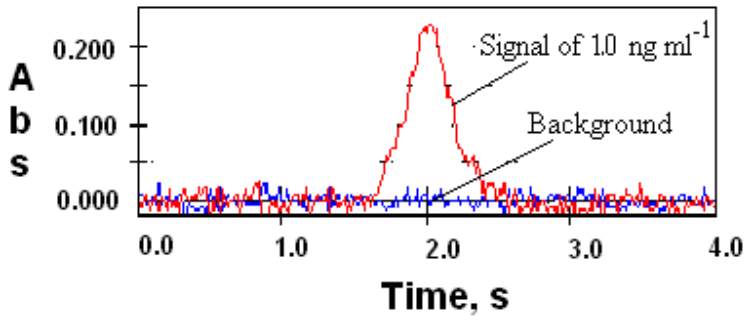


**Figure 3.2.** The analytical signal obtained by the gold coated W-coil trap VCG-AAS method for Se; 27.0 mL of sample solution of 1.0 ng $mL^{-1}$ Se were collected in 4.0 minutes.

In the study by Guo and Guo, revolatilization is rather slow since external heating of trap was used; the signal half width is about 5 seconds [142]. The main difference between our study and those by Barbosa group is that W-coil is an electrothermal vaporizer in the former, while it is an electrothermal atomizer in the latter cases [122,188]; the sensitivities are rather comparable. The report by Tyson's group shows that there are always powerful chemical preconcentration techniques as alternatives [189]. The sensitivity reported by Matusiewicz and Krawczyk should not be compared with other traps since the detection is by flame AAS [145] although it is included here as a related work. Another study using ICPMS is also given as a reference to the sensitivity of this technique [190].

**Table 3.2.** Comparison of some techniques for determination of Se.

| Technique | LOD, ng $L^{-1}$ | Sample size and time | Reference |
|---|---|---|---|
| HG and externally heated Au wire trap -AFS | 5 | 50 mL in 300 s | 142 |
| Preconcentration on anion column, FI-HG-ICP-OES | 6 | 16 mL in 120 s | 189 |
| HG and Rh coated W-coil-trap-ETA | 50 | 2.5 mL in 60 s | 122 |
| HG and Rh coated W-coil-trap-ETA | 35 | 1.5 mL in 30 s | 188 |
| HG and Pt treated WETA | 270 | 1.0 mL in 17.1 s | 126 |
| Integrated atom trap AAS | $3 \times 10^3$ | 10 mL (batch), 120 s | 145 |
| Isotope dilution ICPMS | $3.3 \times 10^3$ | Continous flow sampling | 190 |
| HG and Au coated W-coil-trap-QTA | 39 | 27 mL in 240 s | This study |

### 3.1.5 Accuracy Test

For the test of accuracy, the standard reference material from the National Institute of Standards and Technology (SRM 1640 Trace Elements in Natural Water) was analyzed using gold coated W-coil trap HGAAS and the optimized parameters mentioned. Result for SRM is in good agreement with the certified value as shown in Table 3.3.

**Table 3.3.** Results for the analysis of certified reference material for selenium using gold coated W-coil trap VCG-AAS.

| **Standart Reference Material** | **Certified Value, ng $mL^{-1}$** | **This study, ng $mL^{-1}$** |
|---|---|---|
| Natural Water NIST-SRM 1640 | 21.96 ± 0.51 | 22.4 ± 0.4 (n=5) |

### 3.1.6 Characterization of Gold Nanoparticles on the W-coil Trap

In this study, among the several approaches to have a Au plating, a novel analytical technique has been developed. The principle of the analytical technique used includes formation of volatile Au species, on-line trapping of these species on a W-coil atom trap at optimized temperature. W-coil atom trap was inserted into the inlet arm of QTA. For this reason, a laboratory-made quartz female joint was attached to inlet arm of QTA explained in 2.1.2 section. This configuration shown in Figure 2.1 allows a very rapid and convenient change of W-coil atom trap when needed. The W-coil atom trap temperature was manually controlled by a variable potential power supply (Variac) and a 750 W transformer connected to mains electricity (220 V ac) through a

power switch. The input voltage of the variable potential power supply was 220 V. The temperature measurements were carried out with a Ni-Cr thermocouple. In suggested study, W-coil atom trap was coated by using 1.0 mg $L^{-1}$ Au standard solution and 1.2% (w/v) $NaBH_4$ solution. Au and $NaBH_4$ solutions were pumped at a constant flow rate by a peristaltic pump with 2.30 mL $min^{-1}$ and 2.86 mL $min^{-1}$, respectively. Au volatile species were generated and separated from the solution by a cylindrical GLS, and was finally directed to the W-coil atom trap. After collection of four minutes enough Au plating can be seen by naked eye. Flow rate of gold solution (2.30 mL $min^{-1}$), $NaBH_4$ (2.86 mL $min^{-1}$), Ar (206 mL $min^{-1}$), $H_2$ (155 mL $min^{-1}$), collection temperature (675 $^oC$) and collection time (4 min) were optimized to obtain better collection efficiency. During the coating of W-coil atom trap with Au, optimum mixture of Ar and $H_2$ carrier gases were sent to system so that the W-coil atom trap was not oxidized. $H_2$ gas creates a reducing environment around the W-coil atom trap.

Scanning electron micrograph of bare W-coil atom trap was taken and shown in Figure 3.3 (5000-fold magnified). Later, same bare W-coil atom trap was placed inside the inlet arm of QTA as explained above and by using optimum experimental parameters; Au was coated on this W-coil atom trap. The scanning electron migrograph of Au coated W-coil atom trap is shown in Figure 3.4 (5000-fold magnified).

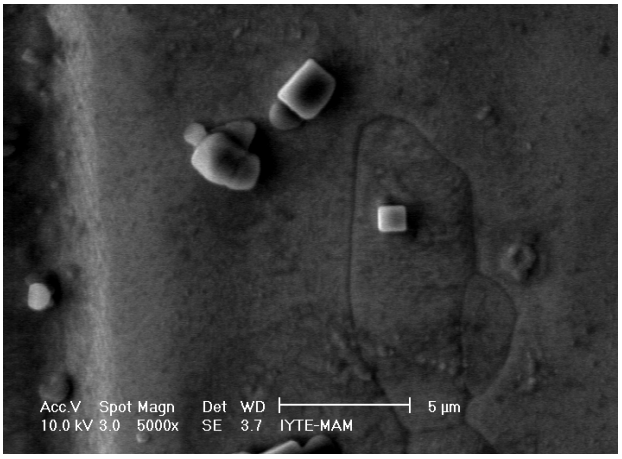


**Figure 3.3.** The scheme of scanning electron micrograph of bare W-coil atom trap magnified 5000-fold.

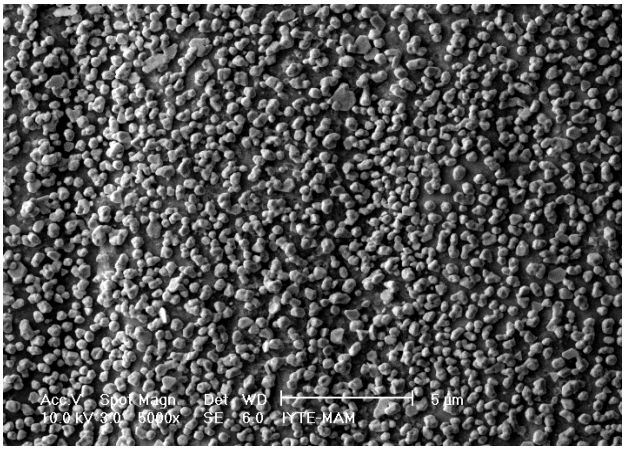


**Figure 3.4.** The scheme of scanning electron micrograph of 1.0 mg $mL^{-1}$ Au coated W-coil atom trap magnified 5000-fold.

The EDX photo of Au coated W-coil atom trap is shown in Figure 3.5. As seen, by using this suggested technique, coating of Au on W-coil atom trap was successfully realized.

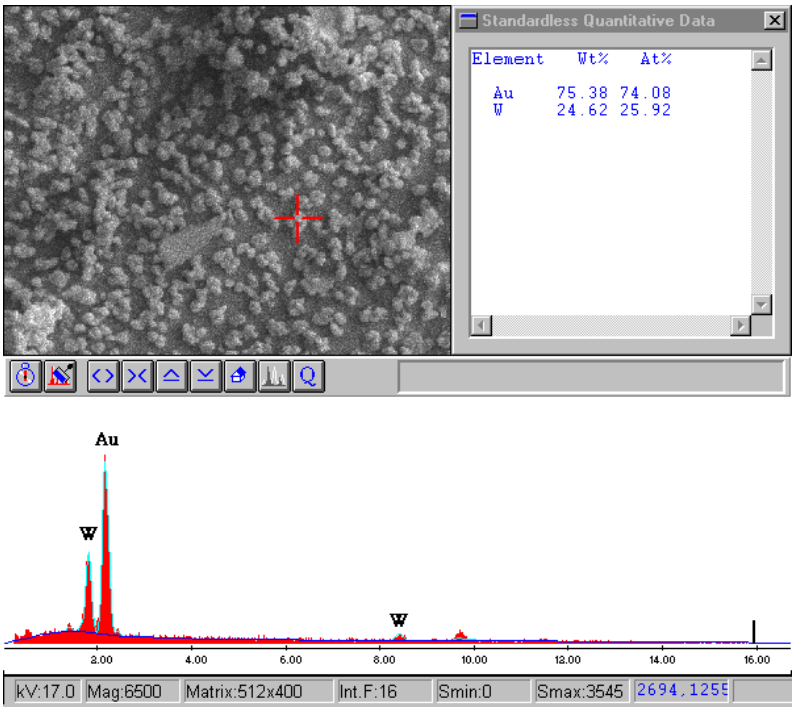


**Figure 3.5.** EDX image of gold coated W-coil atom trap (6500 fold magnified).

### 3.1.7 Conclusion

A novel analytical technique for the determination of Se has been developed by using trapping on a resistively heated gold coated W coil trap. When bare W-coil was used, Se signal could not be taken; gold coating provides a way of convenient trapping and releasing. The re-volatilized species are either molecular or short-lived atomic in nature, since no signal was observed when the QTA was not heated by flame. The

limit of detection achieved was comparable with other recently reported sensitive techniques for selenium determination. The technique is very simple, robust and economical. It can be applied in laboratories equipped with only with a flame AA spectrometer to provide sensitivity at ng $L^{-1}$ level. The sensitivity obtained is sufficient to handle many difficult analytical tasks in the fields of health, environment and food.

### 3.2 Gold Determination by VCG-AAS

In the preliminary phases of the our study, a classical VCG-AAS system with a U-shaped GLS was used to obtain a signal using the 10 mg $L^{-1}$ Au solution (Figure 3.6). In this experiment, different inner sizes of U-shaped GLS were used. Corresponding to the gas-liquid inner diameter of separation chamber, these sizes were 1, 2 and 4 cm. The best sensitivity was obtained when 2 cm inner size U-shaped GLS was used.

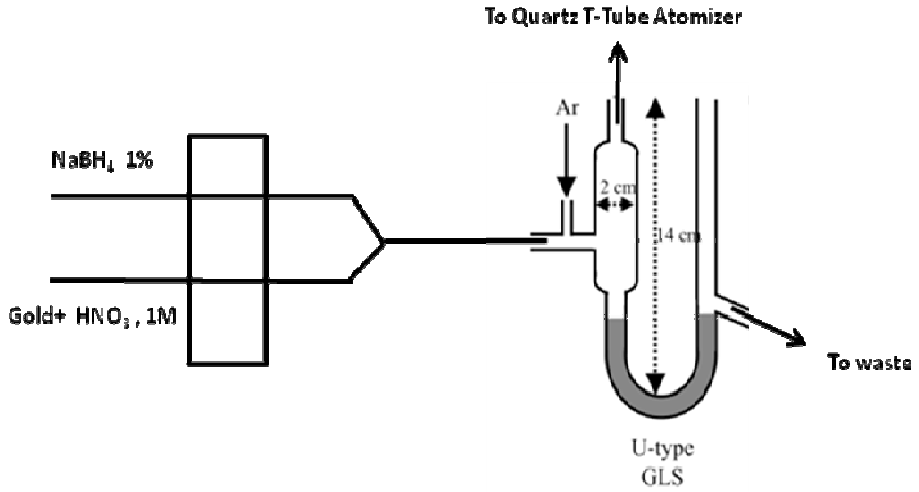


**Figure 3.6.** A classical U-shaped GLS and Volatile Compound Generation System.

It was recognized that when the Au and $NaBH_4$ solutions were sent to the U-shaped GLS by means of a peristaltic pump and Ar gas (376 mL $min^{-1}$) flowing continuously, no meaningful signal could be obtained.

In another experiment, after solutions were collected into a U-shaped GLS, the Ar gas flow and peristaltic pumps were stopped. After 2 minutes of waiting, Ar gas was sent with a flow rate of 376 mL $min^{-1}$. Then, generated volatile Au species were transported to the atomizer and a signal as shown in Figure 3.7 was obtained using 10 mg $L^{-1}$ Au solution.

In order to improve the analytical performance, a different GLS was designed, and it was called as high volume gas liquid separator (HVGLS); the design of this device was given in Figure 2.2.

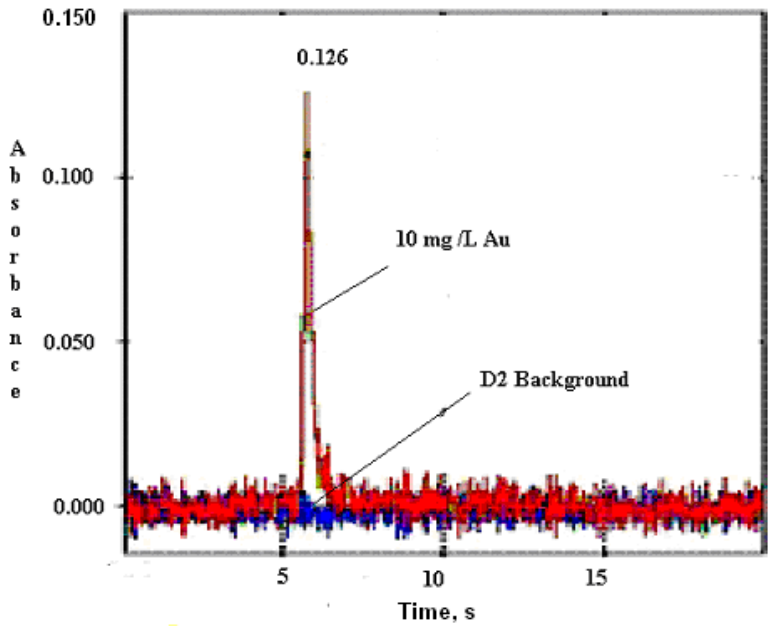


**Figure 3.7.** 10 mg $L^{-1}$ Au signal by using U-shaped GLS.

### 3.2.1 High Volume Gas Liquid Separator (HVGLS)

U-shape GLS experiment shows that waiting period after mixing the analyte and reductant solutions, is an important factor for the determination of Au in VCG system. The HVGLS consists of three two-way valves shown in Figure 2.2. The function of the valve 1 is to allow the Ar gas flow; that of the valve 2 is to send the mixed solutions of $NaBH_4$ and Au solution into the HVGLS. The valve 3 is used to send mixed solutions to waste after each experiment following the recording of signal.

### 3.2.2 Optimization of Experimental Parameters for Au Determination with HVGLS

In CF-VCG-AAS system using a HVGLS, when no W-coil trap was used, some experimental parameters were optimized. These parameters are *bubbling* and *waiting periods,* volume of Au and $NaBH_4$ solutions inside the HVGLS, flow rates of Au and $NaBH_4$ solutions, concentrations of $HNO_3$ and $NaBH_4$ solutions and the effects of different types of gases and their flow rates. During the optimizations, one parameter was varied while others were kept constant. Optimization cycles were repeated until a stable and repeatable signal was obtained. The optimum $HNO_3$ and $NaBH_4$ concentrations were found as 1.0 mol $L^{-1}$ and 1.0% (w/v) stabilized in 0.5% (w/v) NaOH, respectively by using 100.0 ng $mL^{-1}$ Au solutions. In the trap studies, different trapping materials, collection and revolatilization temperature of these materials, flow rates of argon and hydrogen gases and collection period of Au volatile species on W-coil trap were investigated using again HVGLS.

### 3.2.2.1. Effect of Bubbling Period

Owing to the low efficiency of U-shape GLS, HVGLS was used shown in Figure 2.2. Firstly, 20 mL Au with 100 ng $mL^{-1}$ concentration solution and 15 mL of reductant solution were sent through the valve 2 and collected in the HVGLS; then, valve 2 was closed. After waiting for 2 min, Ar gas was sent into the solution through valve 1. In this case, no signal was obtained. In another effort after collecting mixed solutions by using valve 2 in the HVGLS, Ar gas was sent through solutions again by valve 1 for different periods of time as 10, 20, 30 and 40 seconds in turn which are called *bubbling period* at the optimum flow rate of 76 mL $min^{-1}$. When each Ar gas flow was on, valve 2 was closed. After each *bubbling period*, a waiting period of 2 min was applied. Ar gas was sent again through the valve 1 immediately after the waiting period at its optimum flow rate of 376 mL $min^{-1}$. The signals obtained using the second procedure with 10, 20, 30 and 40 seconds *bubbling period* are shown in the Figure 3.8 a-d. 30 seconds *bubbling period* was chosen as optimum. The function of Ar gas during the *bubbling period* was not only to mix the solution but also to saturate the solution with Ar gas and to transport the generated volatile Au species into gas phase. In this case, it was observed that all of the signals obtained have tailing.

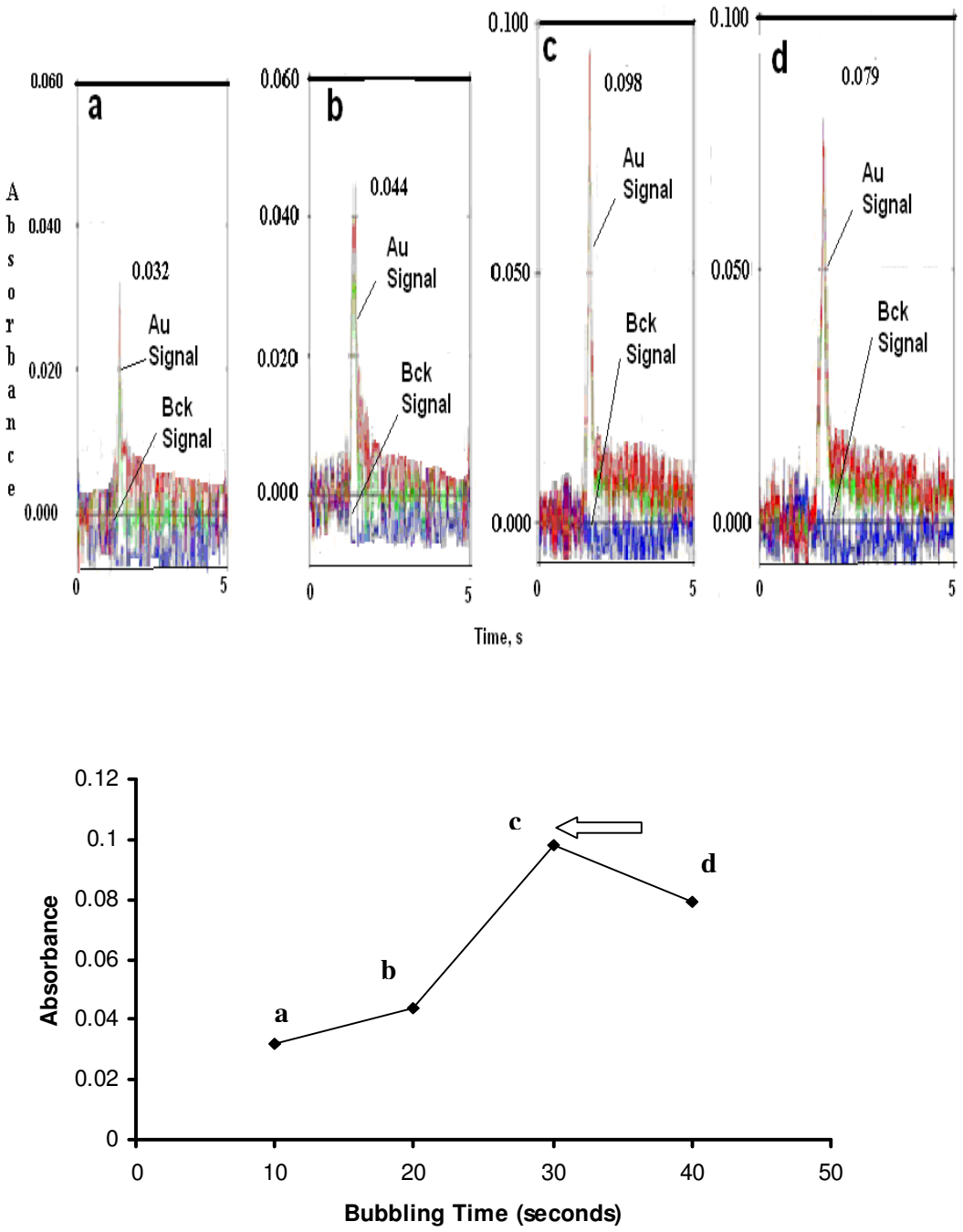


**Figure 3.8. a-d.** The signals obtained after 10, 20, 30 and 40 seconds *bubbling* and 2 *minutes waiting periods* by using 20 mL of 100 ng $mL^{-1}$ Au with VCG-AAS and HVGLS.

### 3.2.2.2 Effect of Waiting Period

Different amounts of *waiting period* such as 30, 60, 120 and 180 seconds were applied while the *bubbling period* was kept constant at its optimum value (30 s). When the *waiting period* is higher than 120 seconds, the sensitivity was not pronouncely changed for 100 ng $mL^{-1}$ Au solutions as shown in Figure 3.9 a-c. Owing to this reason, 120 seconds waiting period was chosen as optimum value. This experiment shows that the reaction between Au and $NaBH_4$ is slow. Because of this reason, for Au determination using HVGLS design, *bubbling* and *waiting periods* are important parameters in order to collect the volatile Au species which are slowly formed in a certain volume.

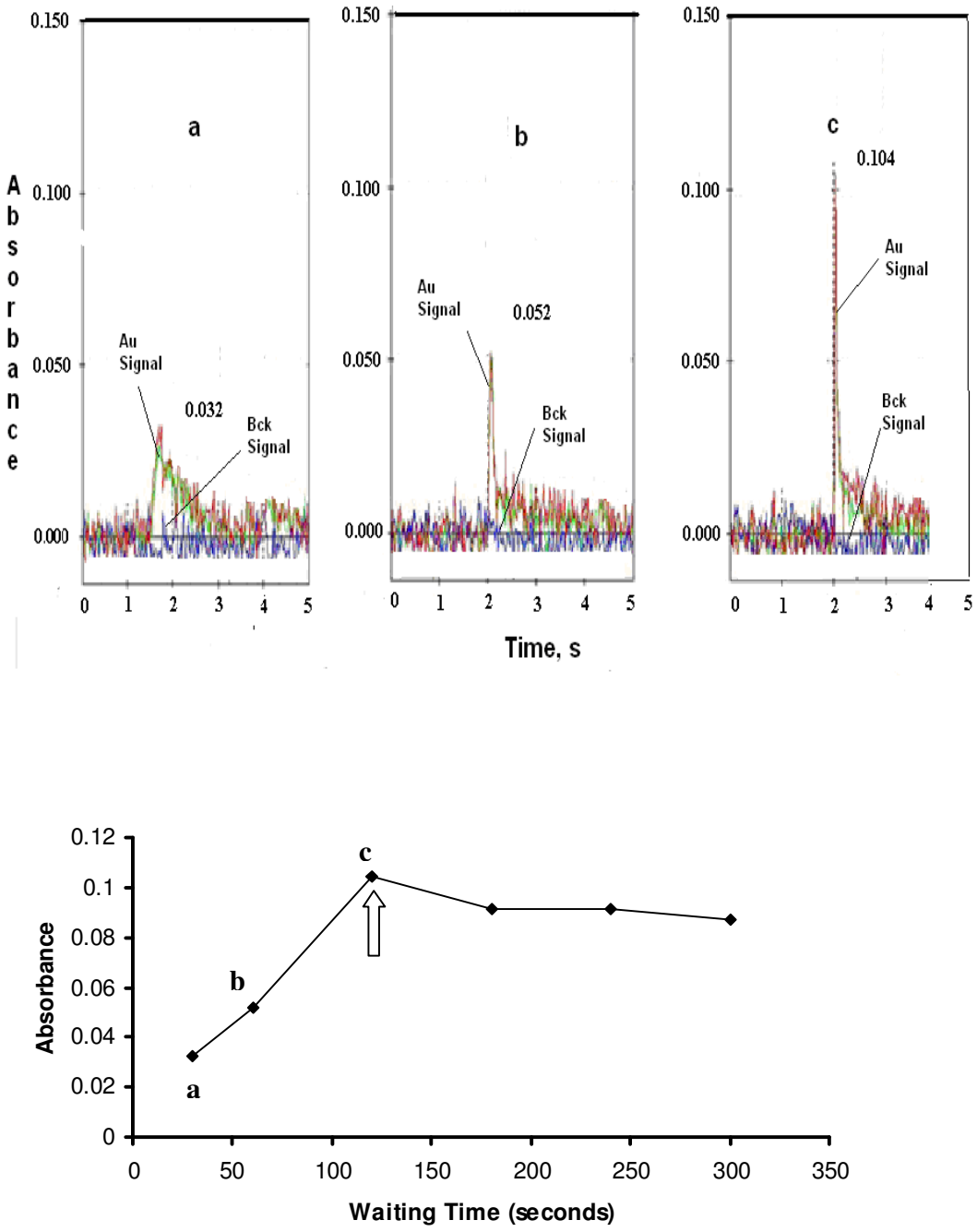





**Figure 3.9. a-c.** The signals obtained after applying a *bubbling period* of 30 s and *waiting periods* of 30 s, 60 s, 120 s, 180 s, 240 s and 300 s *bubbling* by using 20 mL of 100 ng $mL^{-1}$ Au with HVGLS.

### 3.2.2.3 Optimization of Volume of Au and $NaBH_4$ Solutions inside HVGLS

Total volumes of Au and $NaBH_4$ solutions inside the HVGLS were varied between 17.5 mL and 40 mL and optimum value was found as 35 mL. The signal increased as the volume of Au and $NaBH_4$ solutions increased till 35 mL and stayed almost the same afterwards as shown in Figure 3.10.

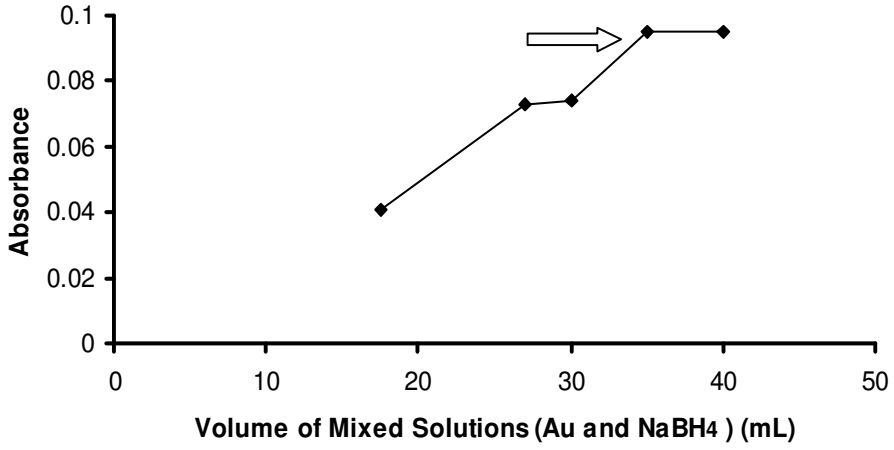


**Figure 3.10.** Optimization of total volume of Au and $NaBH_4$ solutions inside HVGLS (100.0 ng $mL^{-1}$ Au)

### 3.2.2.4 Optimization of Flow Rates of Au and $NaBH_4$ Solutions

After choosing optimized volume of Au and $NaBH_4$ solutions inside the HVGLS (35 mL), optimizations of flow rates of Au and $NaBH_4$ were carried out.

In principle, the production efficiency of Au volatile species is related to the flow rates of Au and $NaBH_4$ solutions. In this study, the flow rate of Au solution was

varied between 8.6 and 20.0 mL $min^{-1}$ and the optimum value was found to be 11.0 mL $min^{-1}$. As seen from Figure 3.11, the signal increased as the flow rate was increased until the value of 11.0 mL $min^{-1}$ and decreased afterwards. The flow rate of $NaBH_4$ solution was varied between 4.2 and 12.0 mL $min^{-1}$ and the optimum value was found as 8.3 mL $min^{-1}$. For the higher and lower flow rates of $NaBH_4$, Au signal was decreased as shown in Figure 3.12.

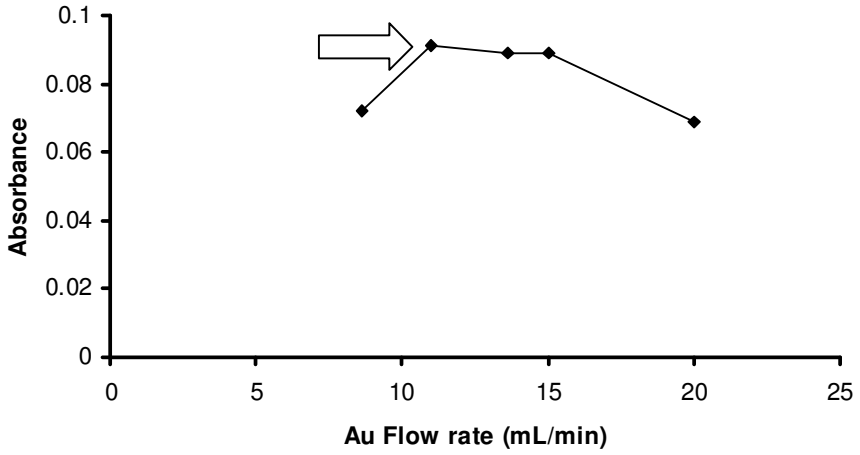


**Figure 3.11.** Optimization of flow rate of Au (100.0 ng $mL^{-1}$ Au)

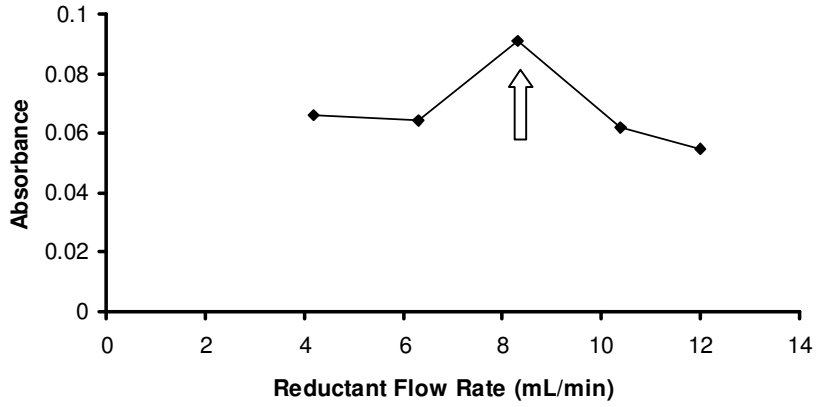


**Figure 3.12.** Optimization of flow rate of $NaBH_4$ (100.0 ng $mL^{-1}$ Au)

### 3.2.2.5. Optimization of $HNO_3$ and $NaBH_4$ Concentrations

In this study, $HNO_3$ was used as carrier solution in which the analyte solution was prepared. To find the optimum $HNO_3$ concentration, was varied between 0.1 mol $L^{-1}$ and 2.0 mol $L^{-1}$. The optimum value for $HNO_3$ was found as 1.0 mol $L^{-1}$, somewhat in the middle of the plateau. Higher and lower values resulted in a gradual decrease in the analytical signal. To produce Au volatile species, $NaBH_4$ was used as the reductant solution. Its concentration was varied between 0.5% (w/v) and 2.0 (w/v), 1.0% (w/v) $NaBH_4$ was found as the optimum value. During this optimization, it has been observed that when the $NaBH_4$ concentration was higher than 1.0% (w/v), analytical signal decreased because of the dilution effect since more hydrogen gas was evolved. In addition, NaOH was used to stabilize the $NaBH_4$. Concentration of NaOH was varied between 0.1% and 1.0% (w/v). The optimum concentration of NaOH was found to be 0.5% (w/v).

### 3.2.2.6 Optimization of Flow Rates of Ar during Bubbling and Releasing

Argon flow rate was varied between 25 mL $min^{-1}$ and 150 mL $min^{-1}$ during *bubbling period* while releasing argon flow rate was kept constant at 376 mL $min^{-1}$. The optimum *bubbling* argon flow rate was found to be 76 mL $min^{-1}$. After this experiment, flow rate of bubbling argon was kept constant as this optimum value. Releasing argon flow rate was varied between 25 mL $min^{-1}$ and 500 mL $min^{-1}$ and the optimum value was found to be 376 mL $min^{-1}$.

### 3.2.2.7 Effect of Different Gases

In order to compare sensitivity and memory effects, different types of the gases such as $H_2$, nitrogen ($N_2$) and air instead of Ar were used.

The signals obtained for blank and 100.0 ng $ml^{-1}$ Au solutions are shown in Figure 3.13, when $H_2$ gas was used at 30 s *bubbling period* and 2 min *waiting period*. As it is seem, the analyte signal is high, but the blank signal is also high in the case of using only $H_2$ gas. (*Bubbling* and releasing $H_2$ gas flow rate was 76.0 mL $min^{-1}$ and 376 mL $min^{-1}$, respectively).

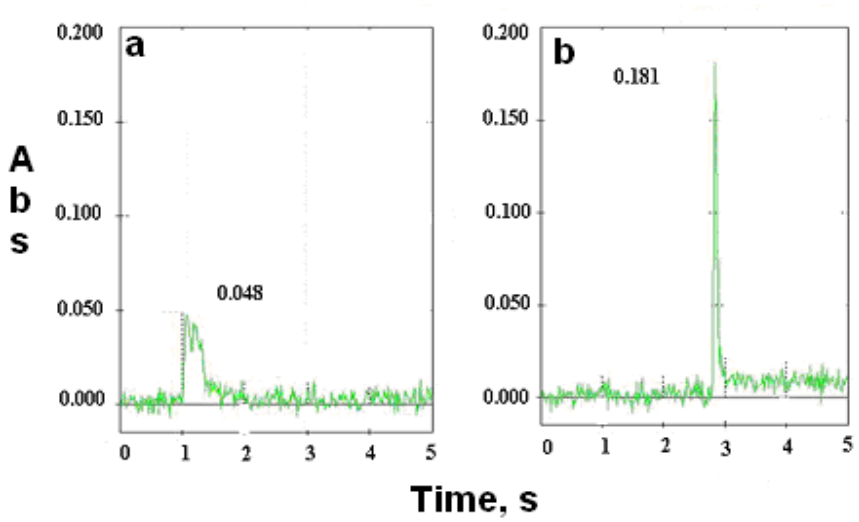


**Figure 3.13.** Signals for blank (a) and 100 ng $mL^{-1}$ Au (b) obtained using $H_2$ gas and HVGLS.

The signals for blank and 100.0 ng $ml^{-1}$ Au solutions are shown in Figure 3.14, when $N_2$ gas was used of 30 s *bubbling period* and 2 min *waiting period*. Bubbling and releasing $N_2$ gas flow rate was 76 mL $min^{-1}$ and 376 mL $min^{-1}$, respectively. It is clear that the sensitivity was much less than that in the cases of using $H_2$ and Ar gases.

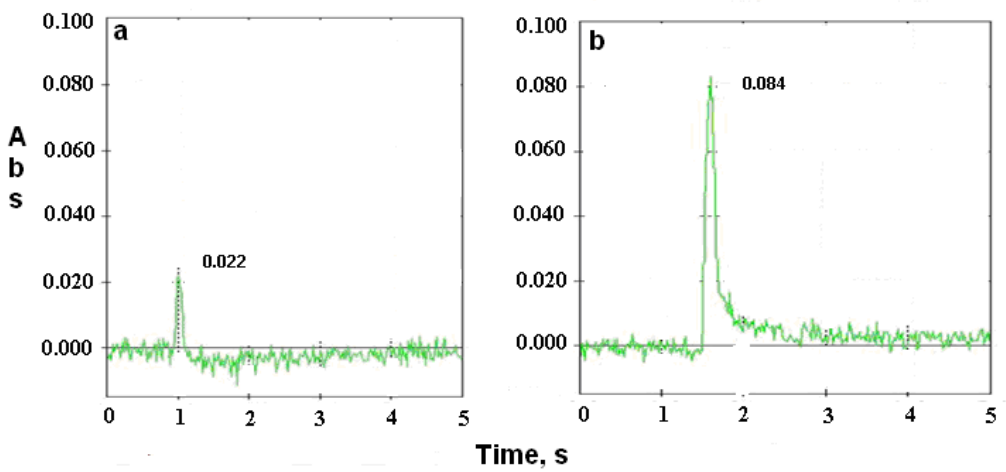


**Figure 3.14. a-b.** Signals for blank (a) and 100 ng $mL^{-1}$ Au (b) obtained using $N_2$ gas and HVGLS.

In the case of using air instead of Ar, no signal was obtained. Moreover, there was the danger of explosion as a result of reaction between $O_2$ gas in air used and $H_2$ gas which is evolved through the reaction between acidic Au and $NaBH_4$ solutions.

### 3.2.3 Calibration Plot for Au by Using HVGLS

Using optimum experimental parameters given in Table 2.2, linear calibration plot for Au with HVGLS was drawn between 10.0 and 100.0 ng $mL^{-1}$ shown in Figure 3.15. The best line equation and correlation coefficient were, A= 0.0006C + 0.009 and 0.9996, respectively, where A is absorbance and C is Au concentration in ng $mL^{-1}$.

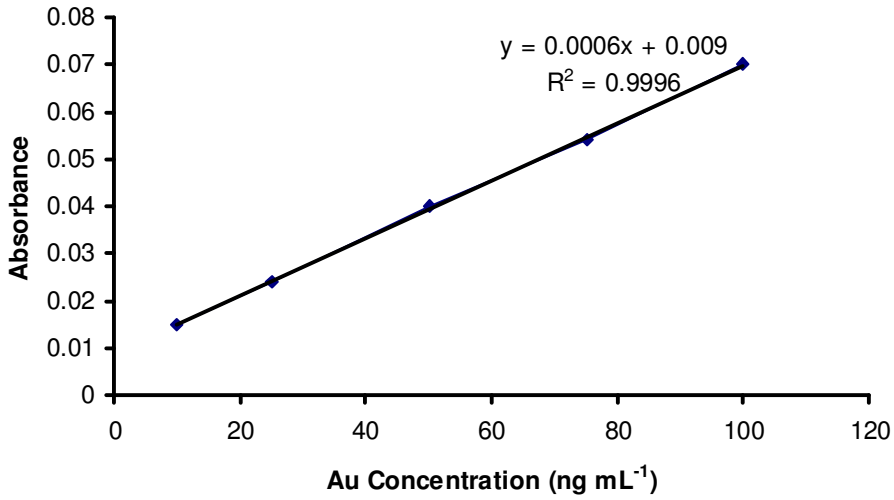


**Figure 3.15.** Calibration plot for Au by using HVGLS and the optimum conditions given in Table 2.2.

### 3.2.4 Investigation of Trapping Location in HVGLS

In order to understand the trapping location, two more valves valves 3 and 4, were connected to the downstream of HVGLS (i.e. after HVGLS) as shown in Figure 3.16. Distances between two valves varied as 18, 23 and 28 cm. After collection of 35 mL of mixed solutions including 20 mL of 100 ng $mL^{-1}$ Au solution, valve 2 was closed and Ar gas was bubbled into the solution through valve 1 for 30 seconds and then valve 1 was closed. After waiting for 2 minutes, Ar gas was sent to the system by using valve 3 instead of valve 1. When the distances between two valves were 23 cm, the sensitivity was higher than others as shown in Figure 3.17. The aim of this experiment was to understand the best trapping location of volatile Au species in the HVGLS. As seen from the Figure 3.14 a-b, the shape of the signals in HVGLS system was similar to usual trap signals. Therefore, it was obvious that in this HVGLS system, generated volatile Au species were trapped somewhere in some

locations in the system. The result of this experiment revealed that generated volatile Au species were trapped in the outlet of the HVGLS i.e. downstream of the HVGLS. It should be noted that the maximum signal obtained under these conditions was almost the same as in calibration plot given in Figure 3.15.

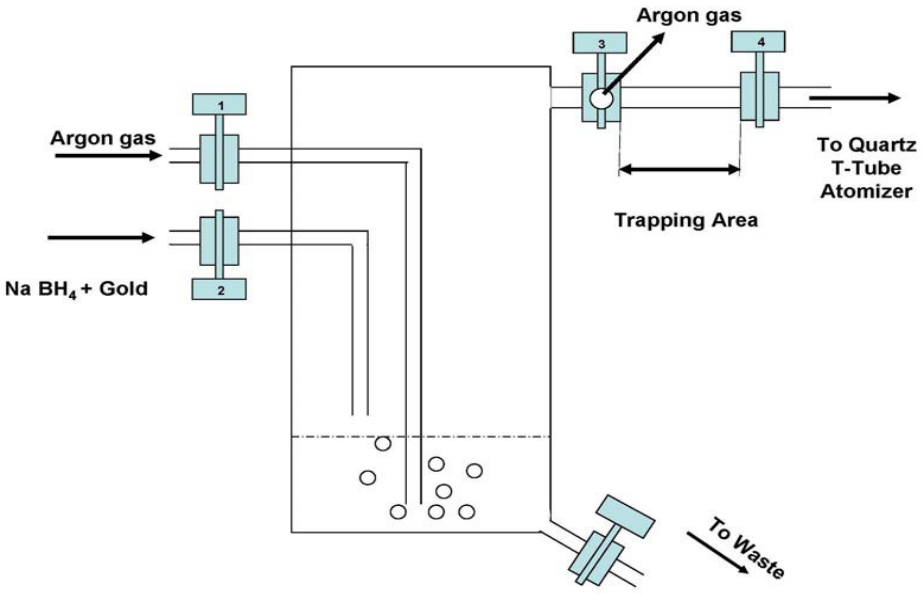


**Figure 3.16.** Modified HVGLS to understand trapping area

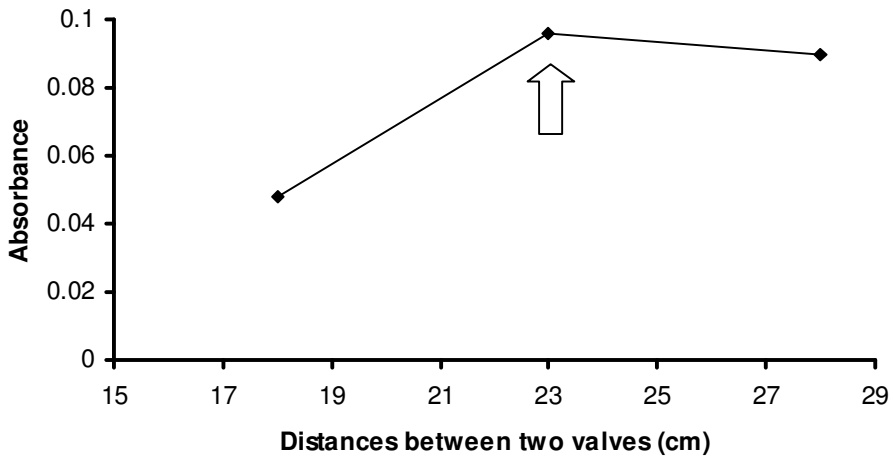


**Figure 3.17.** Investigation of the trapping location in the HVGLS showing the effect of distance between valve 3 and valve 4, for 100 ng $mL^{-1}$ Au and the optimum parameters given in Table 2.2.

### 3.2.5 Trapping of Volatile Au Species on Different Materials

#### 3.2.5.1 Copper Wire

In order to check the trapping ability, a piece of Cu wire was inserted inside the inlet arm of the atomizer 5 cm away from the junction point. It should be noted that this corresponds to the usual location of W-coil trap used in previous analyses. In order to control the trap temperature, outside of the inlet arm was surrounded by Ni-Cr wire that was resistively heated. After applying the procedure given in preceding sections and the parameters on Table 2.2 and Table 2.3, the Cu wire was heated under the flow of 376 mL $min^{-1}$ $H_2$ to obtain a signal. It was revealed that Au volatile species were trapped on the Cu wire when the temperature was around 750 $^{o}$C; however,

because of high affinity of Au to Cu element, it was not possible to release all of the collected Au species at lower temperatures and if temperature was increased too much, the Cu wire would be melt. The result of this experiment was shown in Figure 3.18.

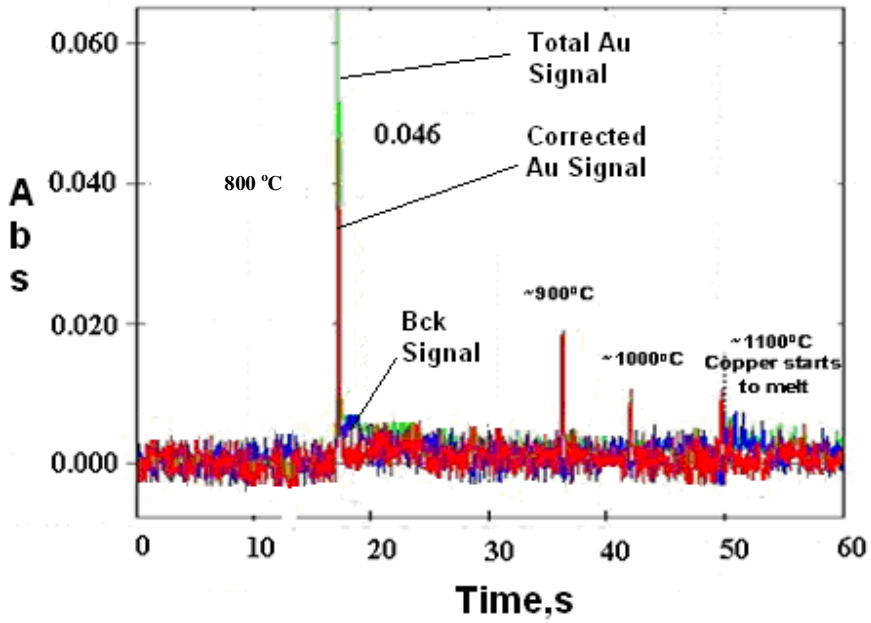


**Figure 3.18.** The trapping behavior of the 100 ng $mL^{-1}$ Au on the Cu wire as a result of the increasing the revolatilization temperature.

### 3.2.5.2. Platinum Gauze

Similar procedure and experimental set-up was applied using a small piece of Pt gauze instead of Cu wire. It was observed that Au volatile species were trapped on the surface of Pt gauze, however, again because of the high affinity of Au to Pt, even at high temperatures around 1100 $^{o}$C, a weak signal was obtained for 100 ng $mL^{-1}$ Au standard solution and it was not possible to increase the temperature more than

~1100°C because quartz tube would melt. The sample of signal is shown in the Figure 3.19.

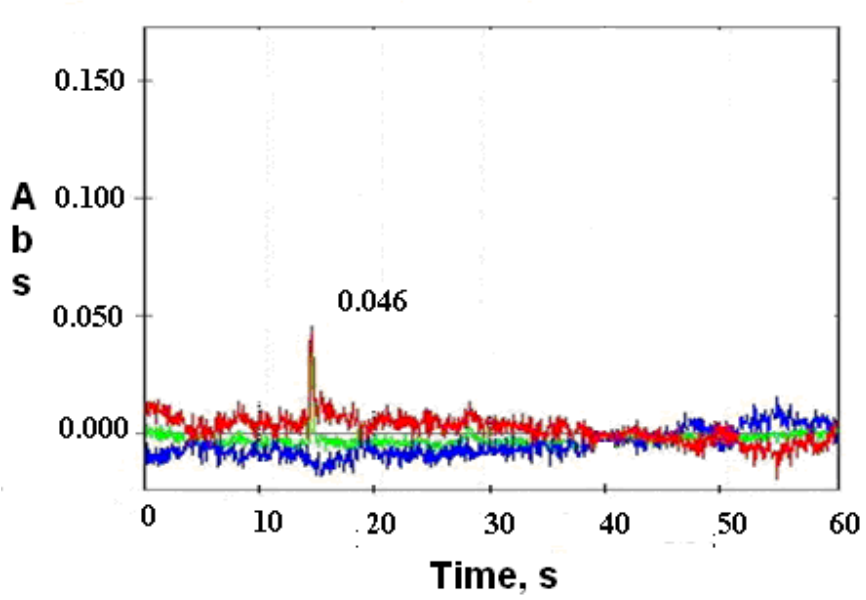


**Figure 3.19.** The trapping behavior of the 100 ng $mL^{-1}$ Au on the Pt gauze.

### 3.2.5.3 W-coil Trap

In this part of the experiment, W-coil was used as an atom trap. After positive results, an optimization study was carried out. For the collection period the parameters given in Table 2.2 were used; namely, carrier solution, reductant solution and reaction coil length.

### 3.2.6 W-coil Trap

#### 3.2.6.1 Optimization of Collection and Revolatilization Temperatures for W-coil Trap

To obtain higher trapping efficiency, collection temperature of W-coil trap should be optimized. During the optimizations, 10.0 ng $mL^{-1}$ Au standard solution was used. Collection temperature of W-coil atom trap was varied from 200 $^{o}$C to 1000 $^{o}$C. Sensitivity for Au increased sharply as the collection temperature of W-coil atom trap was increased up to 750 $^{o}$C. When the collection temperature of W-coil atom trap was increased further a decrease in the analytical signal was observed, owing to the partial release of the trapped Au species as shown in Figure 3.20. Hence, 750 $^{o}$C was found as the optimum W-coil trap collection temperature. Revolatilization W-coil trap temperature was varied from 1200 $^{o}$C to 1800 $^{o}$C while the collection W-coil trap temperature was kept constant as its optimized value of 750 $^{o}$C. The optimized W-coil trap temperature for revolatilization was 1400 $^{o}$C where the highest signal was obtained shown in Figure 3.21.

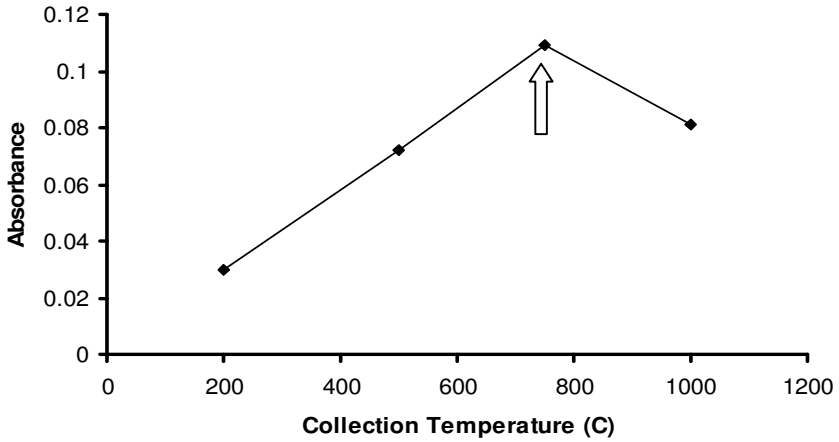


**Figure 3.20.** Optimization of collection temperature of W-coil atom trap by using 10.0 ng $mL^{-1}$ Au solution.

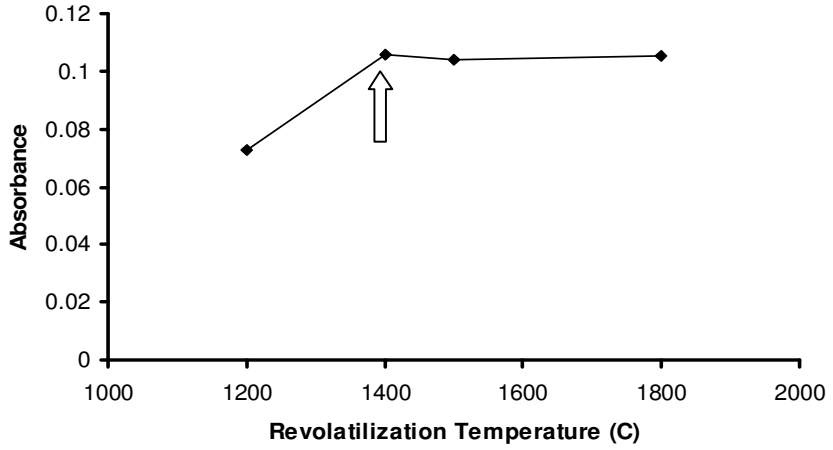


**Figure 3.21.** Optimization of revolatilization temperature of W-coil atom trap by using 10.0 ng $mL^{-1}$ Au solution.

### 3.2.6.2 Trapping of the Volatile Au Species on the W-coil Atom Trap Using HVGLS

As it was explained in the experimental part, a W-coil trap was used after the HVGLS, however, in this case some modifications have been done on the HVGLS design. As it is shown in Figure 2.3, a three-way valve was added to the outlet of the HVGLS to send $H_2$ gas. This HVGLS consists of three two-way valves plus one three-way valve shown as (1), (2), (4) and (3), respectively (Figure 2.3). Valve 1 is used for the Ar gas flow and the valve 2 is used for sending the mixed solutions of $NaBH_4$ and acidic Au solutions. The function of valve 3 is to introduce the $H_2$ gas in the W-coil trap study. Finally, valve 4 is used for discharging the waste solutions at the end of process.

The goal of using the $H_2$ gas flow was not only to eliminate the oxidation of the W-coil trap by high temperature but also to help the releasing of Au species during revolatilization that was trapped on the surface of W-coil.

In this HVGLS design, again univariate optimization has been applied in order to find the optimum conditions. First, W-coil trap was resistively heated to 750 $^{o}$C before turning the pumps on to deliver the Au and reductant solutions for subsequent trapping. After W-coil trap temperature was reached to 750 $^{o}$C, using valve 2, Au and $NaBH_4$ solutions were sent to the HVGLS in 120 seconds. During trapping, the carrier gases consisted of 76.0 mL $min^{-1}$ Ar and 146.0 mL $min^{-1}$ $H_2$ were bubbled continuously through the solutions inside of the HVGLS using valve 1. After the collection step for a chosen period of time which was 120 seconds, valve 2 was closed but gas flow was continued. When the collection time was increased more than 120 seconds, the magnitde of analytical signal was stayed constant. Therefore, optimum collection time of Au volatile species on W-coil trap was chosen as 120 seconds as shown Figure 3.22.

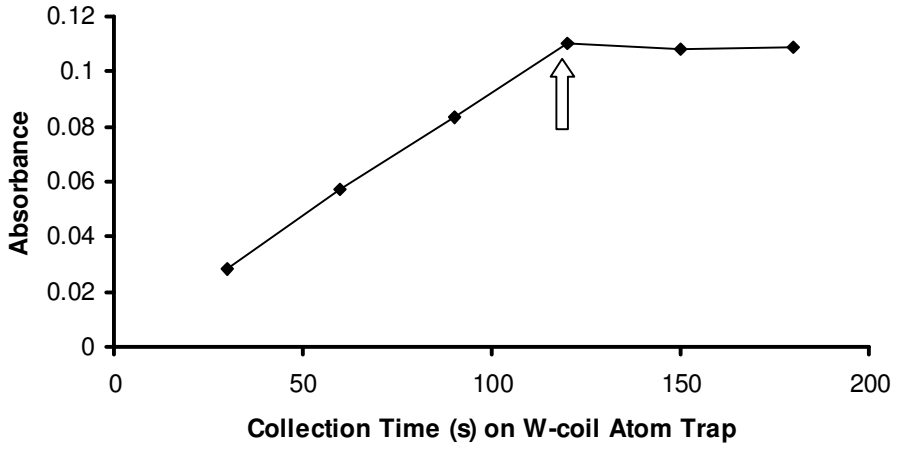


**Figure 3.22.** Optimization of collection period of Au volatile species on W-coil atom trap

The W-coil trap temperature was increased to 1400 $^{o}$C that needed about 1.0 s; and valve 1 was closed. Then, immediately valve 3 was opened while a flow of $H_2$ gas was allowed at 376.0 mL $min^{-1}$. The residence time of the analyte species on the light path is very short, about 1.0 s, and the half width of the transient signal is less than 0.5 s as shown in Figure 3.23. It was clear that in contrast to the other signals that were obtained previously by using only HVGLS itself without a W-coil trap, the signals had no tailing.

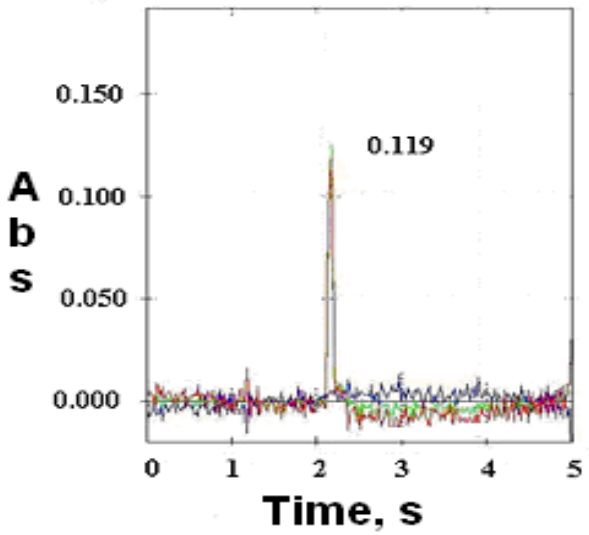


**Figure 3.23.** The signal of the 10 ng $mL^{-1}$ Au on the W-coil atom trap with HVGLS.

### 3.2.6.3 Calibration Plot of Au using HVGLS with W-coil Atom Trap

By using optimum analytical parameters, a linear calibration plot using HVGLS with W-coil atom trap system was obtained between 1.0 and 10.0 ng $mL^{-1}$ (Figure 3.24). The best line equation and correlation coefficient were, A= 0.0067C + 0.0126 and 0.9994, respectively, where C is the Au concentration in ng $mL^{-1}$. During the

construction of this plot, in addition to the parameters given in Table 2.2, collection and revolatilization trap temperatures were to be 750 $^{o}$C and 1400 $^{o}$C, respectively; collection period on trap was 120 s.

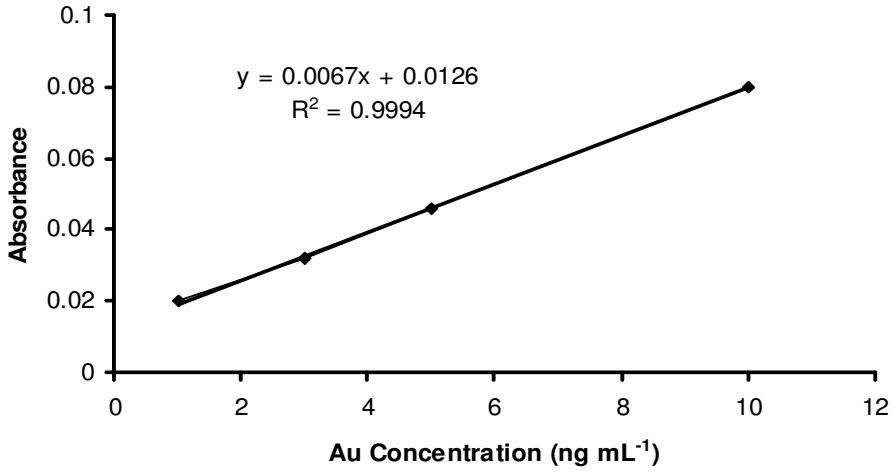


**Figure 3.24.** Calibration plot of Au using HVGLS with W-coil atom trap, parameters in Table 2.3, 750 $^{o}$C collection temperature, 1400 $^{o}$C revolatilization temperature and 120 s trapping period.

### 3.2.6.4 Analytical Figures of Merit for Au Determination by VCG-AAS

By using U-shape GLS, the detection limits and characteristic concentration were found as 250 ng mL$^{-1}$ and 174 ng mL$^{-1}$, respectively. On the other hand, by using HVGLS without W-coil trap, the calibration plot for 20 mL Au solution was linear between 10 and 100 ng mL$^{-1}$ Au. The limit of detection (3s) was found as 5.54 ng mL$^{-1}$ and the characteristic concentration value was found to be 5.45 ng mL$^{-1}$ by using HVGLS. Moreover, a W-coil trap was used to further decrease the detection limit and as a result to increase the sensitivity.

The calibration plot for 20 mL Au solution was linear from 1 to 10 ng $mL^{-1}$ Au. The enhancement factor for the characteristic concentration was found to be 10.7 when compared to HVGLS without W-coil trap by using peak height values. The figures of merit are shown in Table 3.4.

Table 3.5 reveals the limit of detection values of Au in some studies in literature.

**Table 3.4.** Analytical figures of merit calculated by using peak height; 20.0 mL of Au were collected.

| | **W-coil trap with a HVGLS** | **HVGLS** | **U type GLS [135]** |
|---|---|---|---|
| Limit of detection (3s) | 0.45 ng $mL^{-1}$ | 5.54 ng $mL^{-1}$ | 250 ng $mL^{-1}$ |
| Characteristic, concentration, $C_0$ | 0.51 ng $mL^{-1}$ | 5.45 ng $mL^{-1}$ | 174.0 ng $mL^{-1}$ |

**Table 3.5.** Comparison of Au LOD values.

| **Reference** | **[98]** | **[153]** | **[154]** | **[135]** | **[155]** | **This Study** |
|---|---|---|---|---|---|---|
| **Au, LOD, ng $mL^{-1}$** | 2300 | 24 | 2.8 | 2.6 | 0.8 | 0.45 |

### 3.2.6.5 Accuracy of the System

In order to check the accuracy of the method, a certified reference material, Canadian Certified Reference Material, Gold Ore, MA-1bg was analyzed; the certified and the found values were 17 mg $L^{-1}$ and 18.5 ± 1.5, mg $L^{-1}$ respectively for HVGLS. The

same certified reference material was used and found value was 17.4 ± 0.5 mg $L^{-1}$ for HVGLS with W-coil trap. Results are given in Table 3.6. As seen, there is a good correlation between the certified and the found values.

**Table 3.6. A**nalysis of certified reference material for Au using both only HVGLS itself and HVGLS with W-coil trap VCG-AAS.

| | **Certified Value, µg $mL^{-1}$ (Canadian Certified Reference Material, Gold Ore, MA-1bg)** | **This Study, µg $mL^{-1}$ (Canadian Certified Reference Material, Gold Ore, MA-1bg)** |
|---|---|---|
| **HVGLS** | 17.0 | 18.5 ± 1.5 |
| **HVGLS with W-coil Trap** | 17.0 | 17.4 ± 0.5 |

### 3.2.7 Conclusion

There have been some studies for determination of Au by VCG; however, in these studies, classical gas liquid separators which have low efficiency for Au determination were used. The low efficiency of classical gas liquid separators was the reason that limits the sensitivity of Au determination. In this study, a HVGLS was designed to improve the detection limit of gold down to the ng $mL^{-1}$ levels. In this apparatus, analyte and reductant solutions are collected in a limited volume and volatile species of the analyte are formed. After the separation of the volatile species from the liquid phase, the entire analyte vapor is sent to a quartz tube atomizer that is heated externally by a flame. A W-coil atom trap further helped to improve

sensitivity. The participation of active surface sites generally improves the efficiency of CVG compared with use of an inert surface. In this study, it was tried to use the participation of active surface area to improve the efficiency of volatile compound generation system by designing a HVGLS and the results that were obtained prove the success of this approach.

## 3.3 Gold Determination by Flow Injection Volatile Compound Generation Atomic Absorption Spectrometry (FI-VCG-AAS)

### 3.3.1 Optimization of Generation and on-line Atomization Using Multiatomizer

The formation of volatile compounds was performed in the FI generator (Figure 2.5) by the tetrahydroborate/acid reaction [184,186] in the presence of surfactants. The optimal conditions found for generation of VC of Ag [99,184] were taken as a base to optimize conditions for generation of VC of Au.

The optimized conditions are summarized in Table 3.7. Compositions of the reductant, the reaction modifier and the waste stabilizer were set as in experiments performed for Ag [99,184] and kept the same in all experiments. All the other reaction conditions (specified in Table 3.7) were optimized by AAS measurements on the basis of the univariate measurements. The optimum $HNO_3$ concentration (always kept the same in samples and in the carrier liquid) was the same as for Ag [184]. Besides $HNO_3$, HCl was also tested as acid medium in carrier liquid, sample and reaction modifier. In general, sensitivity did not differ significantly, however repeatibility observed with HCl was worse. Consequently, only $HNO_3$ was employed in further experiments.

**Table 3.7.** Optimized conditions for generation of volatile Au compounds and for its on-line atomization in multiatomizer.

| **Optimized Parameters** | **Optimum Values** |
|---|---|
| Carrier liquid composition/flow rate | 0.6 mol $L^{-1}$ $HNO_3$ / 0.5 mL $min^{-1}$ |
| Sample composition/injected volume | 0.01% (m/v) DDTC, 0.6 mol $L^{-1}$ $HNO_3$ / 0.5 mL $min^{-1}$ |
| Reaction modifier composition/flow rate | 20 µg $mL^{-1}$ Triton-X-100 in 0.1 mol $L^{-1}$ $HNO_3$ /0.5 mL $min^{-1}$ |
| Reductant composition/flow rate | 2.4% (m/v) $NaBH_4$, 0.1% (m/v) KOH, 132 µg $mL^{-1}$ Antifoam B / 0.5 mL $min^{-1}$ |
| Waste stabilizer composition/flow rate | 0.5 mol $L^{-1}$ NaOH / 0.5 mL $min^{-1}$ |
| Carrier Ar flow rate | 240 mL $min^{-1}$ |
| Atomizer temperature | 900 $^{o}C$ |
| Outer air flow rate for multiatomizer | 30 mL $min^{-1}$ |

The effect of the concentration of DDTC on the relative peak area of Au (related to the signal in the absence of DDTC normalized to 1) is shown in Figure 3.25. A concentration of 0.01% (m/v) DDTC yields the maximum signal, which is three times higher than that of obtained in the absence of DDTC. Therefore, It was employed in further experiments. The signal enhancement, even though substantial, is much lower than that reported by other authors, namely 20 to 30 times. This indicates that the VCG efficiency of Au in the absence of DDTC yielded by our procedure is much better than under conditions employed by the other authors [153-155,191] who were not using surfactants as additional reaction modifiers.

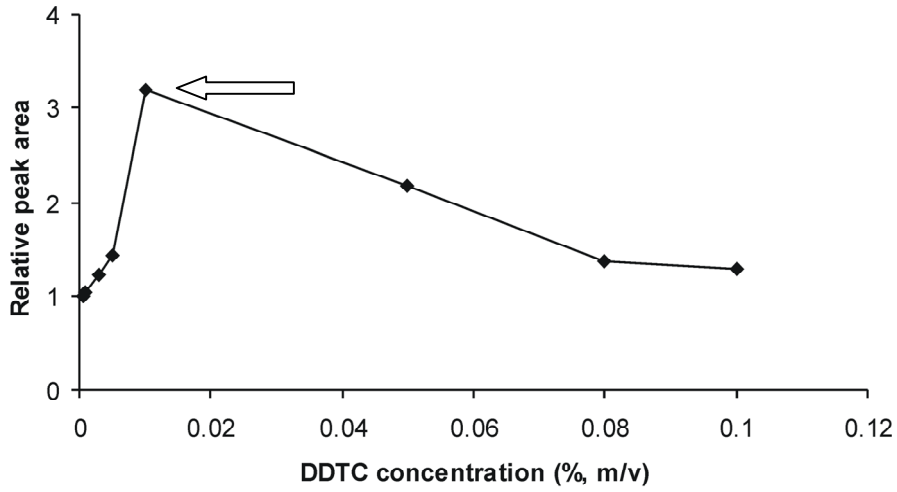


**Figure 3.25.** Influence of DDTC concentration in sample solution; see Table 3.7 for the other experimental conditions; 0.5 ml of 1.0 mg $L^{-1}$ Au; the peak area is normalized to that obtained in the absence of DDTC.

The typical peak shape is illustrated in Figure 3.26. It should be highlighted that 0.5 mL sample loop was chosen as a compromise between signal intensity (expressed as the peak area) and peak width: higher volumes produced broader signals. The rates of all four liquid reagents flows were kept the same. In accordance with our previous experience with generation of VC of Ag [184], the flow rates of 0.5 mL $min^{-1}$ were chosen as a compromise between peak area and peak width: lower flow rates produced higher peak areas but broader and lower peaks [184].

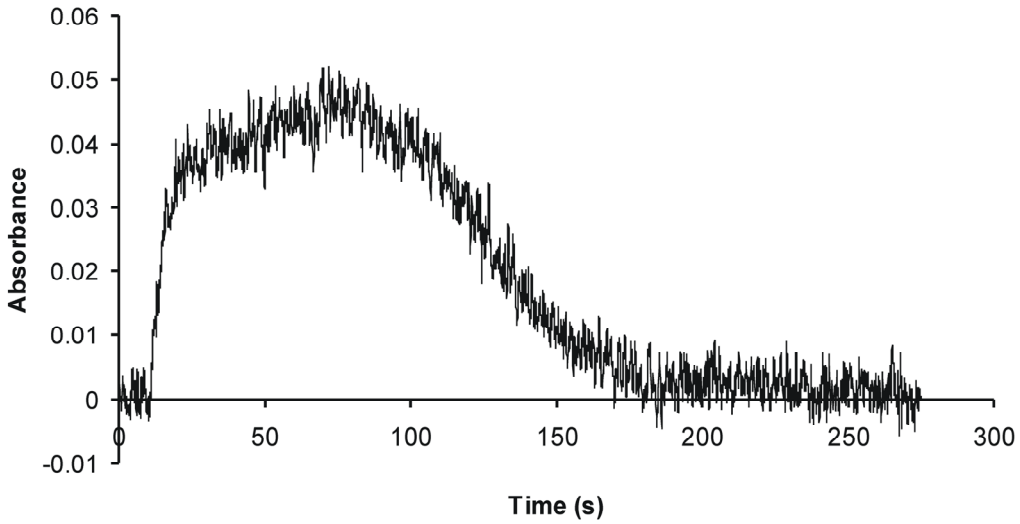


**Figure 3.26.** Typical signal with multiatomizer, time zero corresponds to the sample injection into the flow of carrier; see Table 3.7 for the experimental conditions; 0.5 mL of 1 mg $L^{-1}$ Au.

The peak width, expressed as full width at half maximum (FWHM), which is around 110 s (Figure 3.26), is almost twice longer than time required to deliver the sample plug of the loop volume to the generator. It takes about 170 s from the injection before the peak reaches the baseline. This is also similar to the case of the generation of VC of Ag [184]. In experiments designed to understand the peak broadening, GLS was bypassed by flow of carrier gas in times 60 and 90 s, i.e. in time coordinates corresponding to peak maximum (Figure 3.26). The signal of Au then decreased immediately to baseline level. This reveals that the observed broadening cannot be accounted to a memory downstream GLS, either in connective tubings or in the atomizer. The source of memory effect is therefore solely within GLS. It is worth noting that analyte dispersion in the dead volume of the GLS cannot be accounted for the observed broadening: since GLS volume and the total gas flow rate through it, respectively, are 3 mL and 240 mL $min^{-1}$, the dispersion broadening should be even

less than 1 s. However, the slow removal of reaction mixture from GLS can be accounted for the broadening since; taking into consideration the reaction mixture volume of 1 mL (see Section 2.3.3) and the total rate of liquid removal of 1.5 mL $min^{-1}$, the estimated liquid residence time in GLS is around 40 s. The processes proceeding in the pool of reaction mixture for VCG of silver in identical GLS were studied in detail in Ref [99]. Substantial part of Ag VC production as well as long washout times were ascribed to reaction of Ag present in this pool with freshly supplied reaction mixture [99].

The effect of outer oxygen/air flow rate was rather significant as shown in Figure 3.27. The optimum outer air flow rate, 30 mL $min^{-1}$, corresponding to 6 mL $min^{-1}$ $O_2$, was employed in all other experiments. It should be underlined that, in contrast to Ag atomization where outer oxygen flow rate below 10 mL $min^{-1}$ did not influence significantly the observed sensitivity, [184] suboptimum oxygen supply was reflected in a pronounced reduction of the observed peak area. The difference between Au and Ag cases suggests a different atomization mechanism. The gradual suppressing effect of oxygen flow rates above the optimum (Figure 3.27) corresponds to that observed for Ag [184].

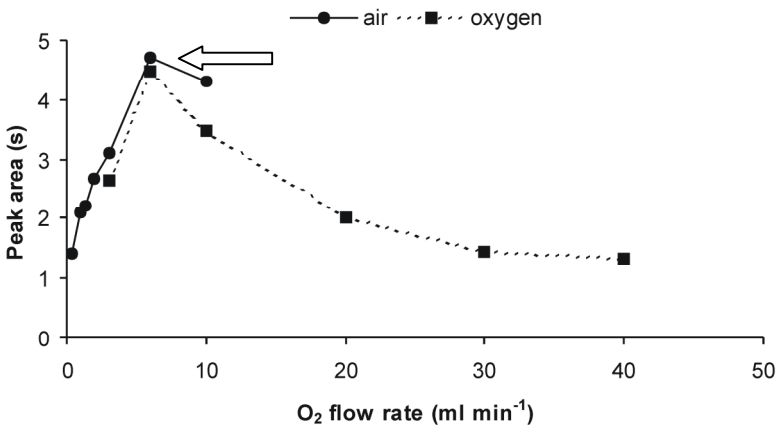


**Figure 3.27.** Influence of outer air (recalculated to oxygen flow rate) or oxygen flow rate to the multiatomizer; see Table 3.7 for the other experimental conditions; 0.5 mL of 1 mg $L^{-1}$ Au.

Regarding the dependence of the Au peak area on multiatomizer temperature, the maximum of 5.1 ± 0.2 s was observed at 900 $^{o}$C, which was approximately the double as compared to the peak area at the temperature of 700 $^{o}$C. The signal decrease with increasing temperature above the optimum was even more step - by 28% for 50$^{o}$C increase. It should be compared with the influence of quartz atomizer temperature in the case of silver atomization where sensitivity increases steadily 2.5 times between 750 and 950 $^{o}$C [184]. This supports the above mentioned difference in atomization mechanisms. The observed influence of atomizer temperature on Au signal is markedly different also from the case of hydride forming elements, where signals do not markedly change in the usual range of temperatures between 700 and 950 $^{o}$C [192,193]. The optimum temperature of 900 $^{o}$C, was employed in all other experiments.

As illustrated by curve A in Figure 3.28, the optimum carrier Ar flow rate found (and employed in all other experiments) was 240 mL $min^{-1}$. Higher Ar flow rate slightly reduced the observed peak area. Different measurements were performed, within a long time interval of several months in different pieces of multiatomizer of the same design, to compare sensitivity at a much higher Ar flow rate of 600 mL $min^{-1}$ with that obtained for the optimum flow rate of 240 mL $min^{-1}$. It has been found that the increase of Ar flow rate from 240 mL $min^{-1}$ to 600 mL $min^{-1}$ reduced sensitivity only slightly to 85 ± 7 % of the previous performance. However, the repeatability (typically around 3% at the optimum gas flow rate) was impaired at the high gas flow rate to 6 - 8%.

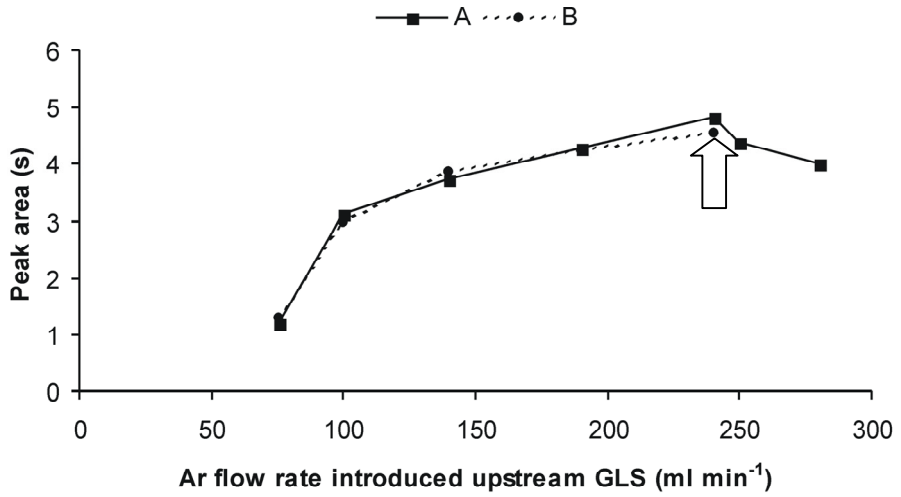


**Figure 3.28.** Influence of carrier Ar flow rate; A: Ar introduced exclusively upstream GLS (see Figure 2.5) - carrier Ar flow rate shown in x-axis is the total Ar flow rate; B: Ar introduced via two channels, carrier Ar flow upstream GLS and additional Ar flow downstream GLS, total Ar flow rate kept constant at 240 mL $min^{-1}$; see Table 3.7 for the other experimental conditions; 0.5 mL of 1 mg $L^{-1}$ Au.

The extent of the gas flow rate can influence observed signals mainly through processes in: (i) GLS, i.e. VCG efficiency and (ii) atomizer, i.e. atomization efficiency and removal of free atoms from the observation path. To decide between these two possibilities, a Y-connection was introduced downstream of the GLS. Ar was introduced via two channels. 1st channel: the carrier Ar flows upstream GLS, "normally" - as depicted in Figure 2.5. 2nd channel: an additional Ar flows downstream GLS via the Y-connection. The total Ar flow rate (both channels together) to the atomizer was kept constant at 240 mL $min^{-1}$ so that the processes in atomizer were not influenced. Curve B in Figure 3.28 shows the influence of Ar flow rate via "normal" channel upstream GLS (as shown in Figure 2.5) on the observed signal. The striking feature of curve B is that it is virtually identical with curve A in the whole range of the carrier Ar flow rate. This means that the processes in atomizer, i.e. atomization efficiency and removal of free atoms from the observation path, are not influenced by the extent of Ar flow rate at least in the range between 75 mL $min^{-1}$ and 240 mL $min^{-1}$. Since the Ar flow rate in this range does not affect processes in atomizer the observed influence of the Ar flow rate on the peak area indicates that the Ar flow rate affects processes in GLS, i.e. VCG efficiency. Consequently, the curve B in Figure 3.28 actually reflects the influence of Ar flow rate through GLS on the VCG efficiency of Au.

The curve A in Figure 3.28 shows a sensitivity decrease at flow rates over 240 mL $min^{-1}$. Since there is no conceivable reason for an efficiency drop with increasing Ar flow rate, the decrease must be attributed to processes in the atomizer. In other words, the dependence of $m_0$ of the employed multiatomizer exhibits a plateau for Ar flow rates from 75 mL $min^{-1}$ up to 240 mL $min^{-1}$ followed by a decrease at Ar flow rates above 240 mL $min^{-1}$.

As discussed above, the generation efficiency monotonously increases between 75 mL $min^{-1}$ and 240 mL $min^{-1}$ - curve B in Figure 3.28. The AAS measurements

presented do not make possible to determine optimum carrier Ar flow rate but the slope of B in Figure 3.28 which is significant even at flow rate approaching 240 mL $min^{-1}$ suggests that the optimum gas flow rate for the generation is well above the optimized value of 240 mL $min^{-1}$.

The optimized carrier Ar flow rate is much higher than the optimum of 50 mL $min^{-1}$ found in this atomizer for generation and atomization of classical hydride forming elements [106,107]. Gas flow rates of 50 mL $min^{-1}$ or higher were compatible with the optimum generation. Higher flow rates caused signal decrease due to processes in the atomizer, i.e. dilution and increased convection losses of free atoms [107]. This indicates a substantial difference in the generation of the VC of Au compared to the classical hydride forming elements.

The first line in Table 3.8 shows the summary of analytical figures of merit for peak area measurements under the optimized conditions. LOD for peak height measurements was determined as 17 ng $mL^{-1}$. These LOD values can be compared with LODs of 4200 ng $mL^{-1}$, 24 ng $mL^{-1}$ and 2.8 ng $mL^{-1}$, respectively, reported for on-line atomization in conventional quartz tube atomizers by Luna *et al.* [98], Du and Xu [153] and Xu and Sturgeon [154]. The LOD values reported in the present study are controlled by the relatively broad signals (see Figure 3.26). It should be highlighted that the target of the on-line atomization AAS measurements was to assess the relevance of individual conditions of the VCG. Therefore, no attempt was undertaken to optimize LOD of the analytical procedure. The peak area sensitivity between 9 and 12 s $\mu g^{-1}$ was registered under the optimized conditions within a time interval as long as several months. It should be underlined that the sensitivity is two orders of magnitude higher compared with that of around 0.1 s $\mu g^{-1}$ reported previously [98,153]. The peak area sensitivity decreased by around 19% at the concentration of 10 mg $L^{-1}$.

**Table 3.8.** Analytical figures of merit based on peak area measurements.

| | **LOD (3σ) (ng mL$^{-1}$)** | **Repeatability (%RSD)** | **Sensitivity (s µg$^{-1}$)** | **Linear range up to (µg mL$^{-1}$)** |
|---|---|---|---|---|
| VCG/on-line atomization | 28 | 3[a] | 9 to 12 | 5 |
| VCG/in-situ trapping in GF | 6.4 | 2[b] | 1.73 ± 0.04 | > 0.4 |
| Liquid sampling GF[c] | 1.5 | 1.1[d] | 156 ± 2 | > 0.15 |

[a]For 1 mg L$^{-1}$ Au. [b]For 50 ng mL$^{-1}$ Au. [c]15 µL sample injections. [d]For 100 ng mL$^{-1}$ Au.

### 3.3.2 Radiotracer Examination of VCG

The Au radiotracer was employed to track analyte transfer within the apparatus and to quantify VCG efficiency of Au. The only difference compared to spectrometric experiments was that the outlet from GLS was connected to a quartz tube via a transport PTFE tubing instead of atomizer. The reason using the quartz tube was to model the inlet arm of the atomizer and thus to monitor potential transport losses of the analyte. The analyte passing the quartz tube was removed from the gas stream in a trapping block formed by four units arranged in the following sequence: two columns packed with activated charcoal followed by two disc filters. The activated charcoal columns were used since they were proved to effectively trap classical hydrides (i.e. selenium hydride [194,195], stibine [196] and bismuthine) as well as to prevent blocking the subsequent filters by aerosol and/or condensing water experienced in the absence of columns at longer collection times. However, VC of Au had to be trapped on the disc filters since it was not efficiently trapped on the charcoal columns alone [184]. This was the reason for employing also the filters in the trapping block. Table 3.9 shows results for optimized generation conditions (see Table 3.7).

**Table 3.9.** Distribution of analyte expressed as analyte fraction (in %)[a] determined by radiotracer counting for the optimized generation conditions (see Table 3.7). 1 mg $L^{-1}$ Au

| | |
|---|---|
| Generator[b] and waste liquid | 88.1 ± 0.5 |
| Transport PTFE tubing[c] | 0.7 |
| Quartz tube[d] | 0.3 |
| 1st column[e] | 5.6 ± 0.1 |
| 2nd column | 1.5 |
| 1st filter | 4.8 ± 0.1 |
| 2nd filter | 0.0 |
| Total radiotracer recovery | 101.0 ± 0.5 |
| Release efficiency[f] | 12.9 ± 0.1 |
| Transport losses[g] | 1.0 |
| Generation efficiency[h] | 11.9 ± 0.1 |

[a]Three replicates, uncertainties below 0.05 % are not shown. [b]All generator components (GLS, capillaries, connections, tubings) downstream peristaltic pump tubing. [c]The connective tubing between GLS and the quartz tube including the PP junction downstream the tubing. [d]The imitation of the inlet arm of the atomizer. [e]Including the PP junction between the quartz tube and the 1. column. [f]Total analyte fraction found downstream GLS - it approximates the analyte fraction released from the sample. [g]Total analyte fraction retained on the way from GLS to the optical arm of the multiatomizer. [h]Total analyte fraction found downstream the quartz tube - it corresponds to the fraction transported the optical arm of the multiatomizer.

### 3.3.3 Estimate of VCG Efficiency by AAS Measurements

Even though the most reliable method to find the generation efficiency is to use radiotracers, AAS based approaches were tested for a comparison and also in order to assess their potential in the case when the extremely sophisticated radiotracer technique is not available.

As discussed, one of the employed ways to simply estimate the generation efficiency is to determine the analyte concentration in the waste solution. Since the determination can be, in principle, made by any method, this seems to be a very convenient way. However, the radiotracer investigation treated above proved that, at least in the case of Au, the result cannot be accurate. It was confirmed by Au determination using the liquid sample introduction GF AAS in the waste solution collected in the generation of 1 mg $L^{-1}$ Au solution under optimized conditions. The fraction of Au found in the waste ranged between 36% and 41%. This is more than the range between 10% and 30% determined by radiotracers (Section 3.3.2) but it is consistent with the above discussed poor reproducibility of the interaction between the surfaces and Au species in the waste. There was no attempt to determine the fraction of analyte retained on the surface of individual generator components since, in contrast to radiotracer measurements, a complete leaching (principally impossible) of the analyte from all surfaces would have to be made. The accuracy of the Au determination in the waste was verified by a full recovery of Au in the waste (100 ± 7%) found after a simulation of the generation experiment which differed from the above described procedure only in the way of mixing of all reactants: all of them were introduced directly into a glass container. Consequently, Au species resulting in the reaction with THB could be neither released from the reaction mixture nor retained at the surfaces since all the plastic components were removed and the probability of the Au species interaction with the glass surface was substantially reduced.

Since the determination of analyte concentration in the waste solution cannot yield meaningful estimate of the VCG efficiency, the alternative way the determination of the volatilized species after their collection on the filter, was tested. The experiments were done in the FI generator described above under optimized conditions. The only difference compared to Figure 2.5 was that the same filter as described above in the case of radiotracer experiments was inserted between the outlet from GLS and the atomizer inlet. VCG was thus performed from Au standards of concentrations between 2 and 50 μg $mL^{-1}$. This resulted in a complete suppression of the AAS signal. To quantify Au collected on the filter in the course of VCG from individual standard aliquots, the filter was leached into a volume of 1 mL of aqua regia. See Section 2.3.4 for the procedure of Au determination in leaches. The estimated efficiencies for Au standard concentrations 2, 5, 10 and 20 mg $L^{-1}$ did not differ significantly ranging between 8.3 and 9.6% (average: 8.8%, SD: 0.6%). However, in the case of the highest Au standard concentration of 50 mg $L^{-1}$, the efficiency decreased markedly down to 6.6 ± 0.2%. Even the values for the Au concentrations up to 20 mg $L^{-1}$ are lower than the efficiency of 12.1 ± 0.2 % found using the radiotracer for Au standard concentration of 1 mg $L^{-1}$ (see above) but taking into account all the possible sources of error involved in both approaches, the difference is not critical.

### 3.3.4 In-situ Trapping in GF

The procedure consists of two steps: (1) trapping and (2) volatilization/atomization. In the first step, VC carried from a generator by a flow of carrier gas via a quartz capillary is trapped in the GF until its evolution is completed. The trapping efficiency is defined as the fraction of generated VC which is trapped. The overall efficiency of generation and trapping is thus the fraction of the total analyte amount in the analyzed sample trapped in the GF. The trapping efficiency, which is a critical parameter for

the method performance, is controlled by the design of the interface between generator, i.e. by the inner diameter of the quartz introduction capillary, by the geometry and quality of inner graphite surface, by the trapping temperature and by the flow rate of the carrier gas [197].

The optimized conditions for the generation step (Table 3.7) were employed with the only exception of the carrier Ar flow rate which had to be optimized with regard to the trapping efficiency. The optimized parameters for in-situ trapping measurements are summarized in Table 3.10. The permanent Ir modifier was chosen because of its convenience [106]. The atomization temperature of 2200 $^{o}$C was chosen as the maximum one compatible with the stability of the Ir coating. The inner diameter of the capillary, the trapping temperature and the carrier Ar flow rate were optimized by AAS measurements on the basis of the univariate measurements.

**Table 3.10.** Optimized conditions for in-situ trapping in GF[a]

| **Optimized Parameters** | **Optimum Values** |
|---|---|
| Carrier Ar flow rate in the trapping step | 115 mL $min^{-1}$ |
| I.d. of the quartz introduction capillary | 0.7 mm |
| GF temperature in the trapping step | 500 $^{o}$C |
| Graphite modification | permanent Ir |
| Atomization temperature | 2200 $^{o}$C |

[a]Experimental conditions given in Table 3.7 were employed with the only exception of the carrier Ar flow rate.

Figure 3.29 exhibits a sharp dependence of the observed sensitivity on the carrier Ar flow rate. The sharp dependence of an analytical signal on an experimental parameter is generally troublesome for analytical practice since even a small difference in the value of the experimental parameter seriously influences the signal impairing precision and accuracy. Besides, such a sharp dependence indicates that the independently varied parameter affects the signal via at least by two opposed mechanisms. The influence of the carrier Ar flow rate on the AAS signal shown in Figure 3.29 suggests that the first mechanism, increasing sensitivity with the flow rate, is the above discussed positive influence of increasing the flow rate on the VCG efficiency (see also Figure 3.28). The second, opposite, mechanism is thus obviously the adverse influence of increasing of the flow rate on the trapping efficiency. The sharp maxima shown in Figure 3.29 indicate together with the character of the dependence of VCG efficiency on the Ar flow rate (Figure 3.28) that the trapping efficiency is dramatically reduced at the compromise Ar flow rate of 115 mL $min^{-1}$

optimized for the in-situ trapping signal.

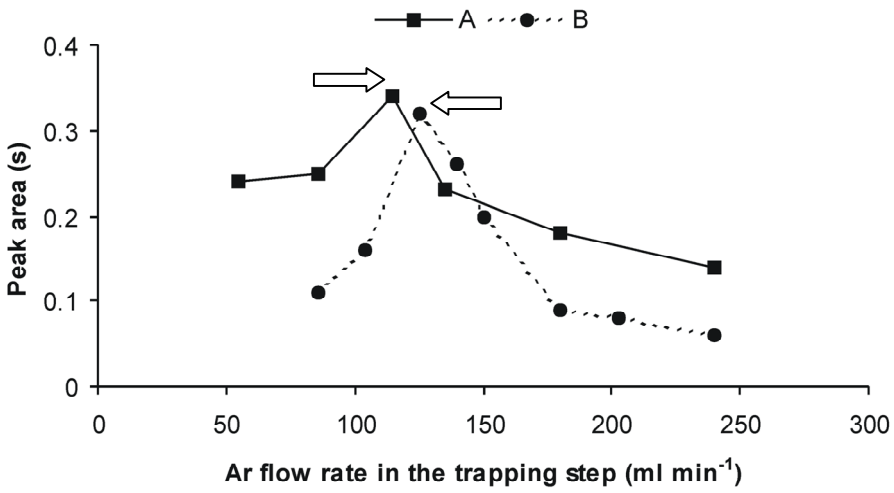


**Figure 3.29.** Influence of the carrier Ar flow rate on the in-situ signal for capillary i.d. of 0.7 mm (A) and of 0.87 mm (B); see Table 3.10 for the other experimental conditions; 0.5 mL of 1 mg $L^{-1}$ Au.

Figure 3.29 also proves that even the relatively small difference in the inner diameter of the quartz introduction capillary has a substantial impact on the performance of the analytical procedure. The beneficial effect of the lower capillary diameter for in-situ trapping in GF is well known [106]. Increasing i.d. from the optimized value of 0.7 mm to 0.87 mm (corresponding to an increase of the capillary inner cross section by 50%) results into slightly lower signal but mainly in a much sharper dependence of sensitivity on the carrier Ar flow rate. A narrower, well proven [106], capillary with i.d. of 0.53 mm could not be employed because of causing an unacceptable overpressure in the generator.

As shown in Figure 3.30, trapping temperature influences the observed signal markedly also even though the dependence is not as sharp as in the above case. A 100 $^{o}$C decrease from the optimum value of 500 $^{o}$C or a 200 $^{o}$C increase significantly reduces the observed sensitivity. The step sensitivity improvement with the trapping temperature below 500 $^{o}$C is compatible with an increase of the strength of the interaction between the surface and the VC of Au. The sensitivity decline above 500 $^{o}$C can be attributed to analyte losses from the surface and/or to the analyte capture in the capillary [106] at elevated temperatures - analogously as observed in the case of arsine [144].

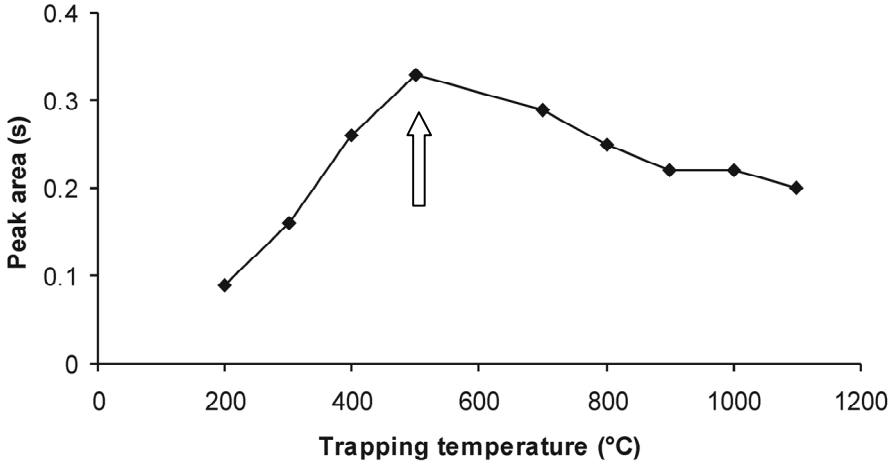


**Figure 3.30.** Influence of temperature in the trapping step on the in-situ signal; see Table 3.10 for the other experimental conditions; 1 mgL$^{-1}$ Au.

The second line in Table 3.8 shows the summary of analytical figures of merit for peak area measurements under the optimized conditions. LOD for peak height measurements was determined as 3.0 ng mL$^{-1}$. These LOD values can be compared with LODs of 0.8 ng mL$^{-1}$ and 2.6 ng mL$^{-1}$, respectively, reported for in-situ trapping

in GF by Ma *et al.* [155], and Ertas and Ataman [135]. It should be underlined that these two literature values were achieved for sample volume of 5 mL, i.e. ten times higher compared with that used in the present study. The peak area sensitivity observed under the optimized conditions was 1.73 ± 0.04 s $\mu g^{-1}$.

The above figures of merit could be compared with those for the conventional liquid sampling listed in the last row of Table 3.8. Sensitivity corresponds to $m_0$ of 28.2 ± 0.4 pg. Since all the atomization parameters for in-situ trapping are identical to those for conventional liquid sampling, the ratio sensitivity for in-situ trapping to the sensitivity determined by the liquid sampling yields the overall efficiency of generation and trapping: 1.11 ± 0.03%. This should be compared with the value of 0.14% corresponding to the peak area sensitivity found by Ma *et al.* [155], 0.4% reported by Ertas and Ataman [135] and either 0.1% (with sole THB reductant) or 0.8% (with tetraethylborate added to the THB reductant) found by Xu and Sturgeon [154]. It should be highlighted that all the three sources [135,154,155] employed optimized DDTC concentration for VCG. Considering the generation efficiency of 12.1 ± 0.2 % at the Ar flow rate of 240 mL $min^{-1}$ (Table 3.9) and the influence of the Ar flow rate on the generation efficiency (Figure 3.29), the generation efficiency at the Ar flow rate of 115 mL $min^{-1}$ can be estimated as 8.0 ± 0.4 %. Since the overall efficiency is defined as the product of the generation efficiency with the trapping efficiency [106], the resulting value of the trapping efficiency is 13.9 ± 0.8 %.

### 3.3.5 Search for the Nature of VC of Au

In analogy to the recent finding that Ag is generated in the form of nanoparticles [184], we employed TEM to test an assumption that Au is volatilized as nanoparticles as well. The glow discharge activated copper grid was situated just downstream of the GLS to collect (presumed) particles generated under optimized VCG conditions

(Table). TEM investigation revealed the presence of nanoparticles on the grids. See Figure 3.31 for an illustration. The detected nanoparticles, with minimum and maximum diameters of less than 3 nm and 24 nm, respectively, were associated in isolated clusters of few to few tens of particles. The mean value ± standard deviation of the nanoparticle size was 10 ± 6 nm (25 particles measured); the most abundant are particles of sizes 2 - 5 nm and 9 - 16 nm; smaller particles could not be counted due to insufficient image resolution. It should be compared with the recently found more uniform distribution of generated Ag nanoparticles: [184] 8 ± 2 nm. However, Ag nanoparticles were associated [184] in a similar manner as found here. The proof that it is Au that forms the nanoparticles detected is presented in Figure 3.31 showing EDS spectra of two particle positions and of a background: there are peaks corresponding to Au in the spectra which are not present in background spectrum. The intensive Cu peak comes from the grid material.

Even though the TEM/EDS experiments prove the presence of Au containing nanoparticles, it remains unclear what their fraction is in the volatilized analyte since these experiments can detect only particles of the size above 1 nm.

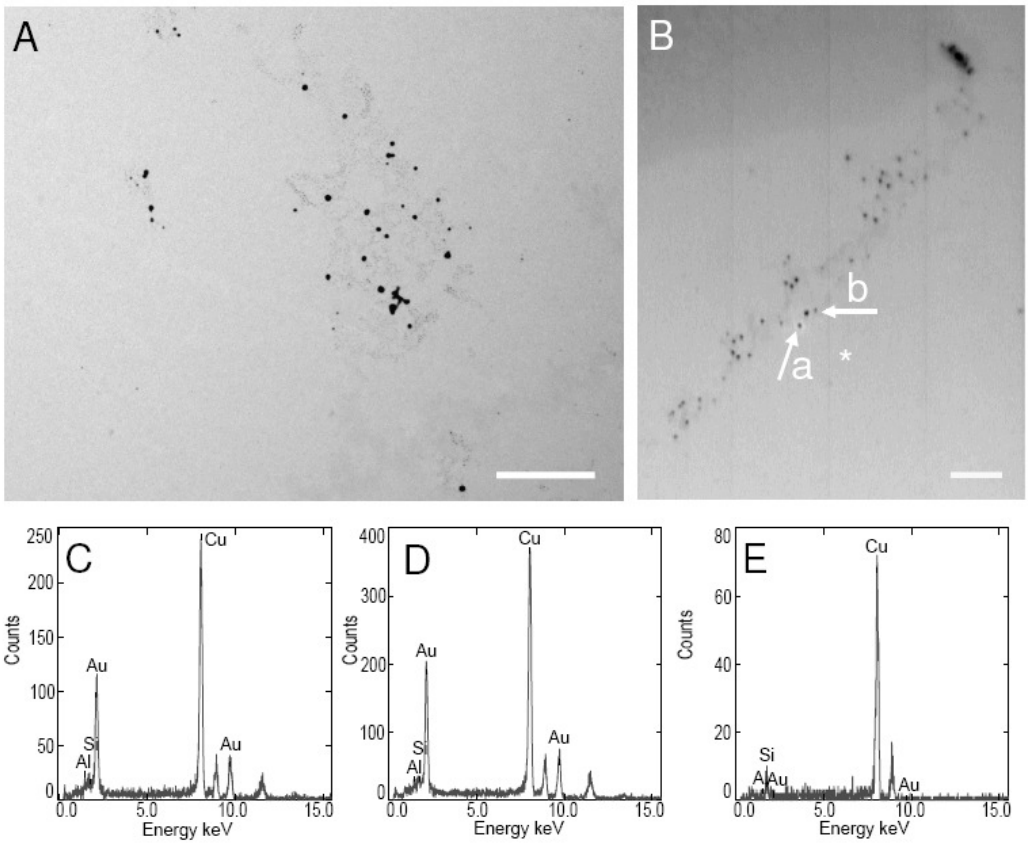


**Figure 3.31.** A – TEM image of gold particles adsorbed onto carbon coated formvar film; scale bar = 200 nm. B – Image of the gold particles from scanning electron microscope used for x-ray microanalysis of particles; the same sample as in A; scale bar = 140 nm. C – EDS spectrum from particle marked with 'a' arrow in panel B. D - EDS spectrum from particle marked with 'b' arrow in panel B. E - Background spectrum recorded from region marked with an asterisk in panel B. Cu peaks in all spectra originate from copper grid used for sample preparation.

### 3.3.6. Conclusions

The optimization of the VCG of Au using the multiatomizer/AAS atomization/detection combination resulted in an analytical procedure yielding satisfactory figures of merit, notably a very good long range (several months) reproducibility of the analytical signal. The concentration LOD is one order of magnitude higher compared to that for the conventional liquid sampling GF but the advantage of the VCG approach for practical analysis is the use of very simple and low cost equipment and a potential to avoid matrix interferences inherent to conventional liquid sampling GF technique [1]. However, the main benefit of the presented results is the assessment of the influence of individual conditions of generation and atomization on the observed AAS signal. This knowledge, together with the detailed insight into the transfer of analyte in the course of generation and transport to the atomizer produced with the help of radiotracers (including the direct determination of the release and transport efficiencies), can be used for predictive purposes and applied for improved performance.

The major significance should be attributed to the understanding of the influence of the carrier gas flow rate on the generation efficiency and of the nature of the peak broadening. This can serve as a basis to an ample improvement of the performance of the analytical procedure based on VCG of Au. However, such a procedure cannot employ the on-line atomization of the generated Au compound for AAS because of the two reasons: (i) a slow kinetics of the generation resulting in inconveniently broad signals, and (ii) a high flow rate of the carrier gas required for the efficient generation resulting in an unacceptable dilution of the analyte and, consequently, in an unacceptable increase of the peak area characteristic mass which deteriorates the observed sensitivity. Both the factors, (i) and (ii), inevitably impair the observed LOD. An evident way to eliminate the adverse influence of the slow kinetics is to employ some of the in-atomizer trapping approaches [106]. However, the most

popular approach, in-situ trapping in GF as it is typically performed [106], is completely unsuitable in this case since the trapping efficiency is poor at the high flow rate of the carrier gas required for the efficient generation. It is a subject of further investigations whether an alternative in-atomizer collection method [106] can yield good performance even under the high gas flow rates required.

Regarding the characterization of the nature of the generated VC of Au, TEM/EDS experiments brought a decisive proof that the VC of Au generated by the reaction with THB contains nanoparticles. The presence of a different form of the volatilized analyte besides nanoparticles (e.g. Au hydride [98,153,155]) cannot be ruled out on the basis of these experiments.

### 3. 4. Silver Determination by VCG-AAS

In the preliminary parts of this study, U-shaped GLS was used for the optimization of system. By the effect of the peristaltic pumps, Ag and $NaBH_4$ solutions were mixed into the reaction coil whose lenght was 30 cm. Reaction coil consists of the tubing between the merging point of analyte and reductant solutions and point where Ar and/or $H_2$ is introduced as the purge gas; as the continuation of the flow system, stripping coil is the tubing between the Ar introduction point and the GLS as shown in Figure 2.5 (a). After mixing the solutions in reaction coil, generated Ag species were sent to the U-shaped GLS by the effect of 76.0 mL $min^{-1}$Ar gas shown in Figure 2.5 (b). After volatile Ag species are separated from the liquid phase in the U-shaped GLS, they were transferred to QTA which was externally heated by air/acetylene flame. Under these circumstances, no meaningful signal could be obtained.

After this experiment, the optimization of Ar flow rate was carried out. Its flow rate was varied from 0 to 200 mL $min^{-1}$. This experiment revealed that when the flow rate

of Ar was decreased, the Ag signal increased. It has been concluded that if there was no Ar gas in the system, the Ag signal was best by considering both peak height and signal to noise ratio (S/N). Hence, after solutions were mixed in the reaction coil, they were sent to the U-shaped GLS by the effect of only the $H_2$ gas which was evolved from the reaction between $NaBH_4$ and acid content that was used in all the standard solutions. Thus, additional carrier gas was not used to transport generated Ag species to QTA as shown in Figure 2.5 (d). By the effect of the additional carrier gas flow, most probably generated volatile Ag species are diluted. As a result, the sensitivity of the Ag decreased.

### 3.4.1 Silver Determination by CF-VCG-AAS Using U-shaped GLS

The experimental parameters were optimized by both CF-VCG-AAS and W-coil trap VCG-AAS. All the reaction conditions were optimized on the basis of the univariate measurements. Optimization cycles were repeated until stable and repeatable signal was obtained. Optimizations of flow rates of analyte and reductant solutions, concentrations of $HNO_3$ which was prepared in analyte solution and reductant solutions were common in both CF-VCG-AAS and W-coil trap VCG-AAS systems. The optimum $HNO_3$ and $NaBH_4$ concentrations were determined in without W-coil trap studies in CF mode by using 250 ng $mL^{-1}$ Ag standard solutions.

#### 3.4.1.1 Optimization of Flow Rates of Reactants

The efficiency of the production of Ag volatile species is directly related with the flow rates of analyte and reductant solutions. In this study, the flow rate of analyte solution was varied between 10.0 mL $min^{-1}$ and 40.0 mL $min^{-1}$ and the optimum value was found to be 30.0 mL $min^{-1}$. The signal increased as the flow rate was

increased until the value of 30.0 mL $min^{-1}$ and decreased afterwards as shown in Figure 3.32. The flow rate of $NaBH_4$ solution was varied between 3.0 mL $min^{-1}$ and 7.0 mL $min^{-1}$ and the optimum value was found as 4.2 mL $min^{-1}$. For the higher and lower flow rates of $NaBH_4$, Ag signal decreased as shown in Figure 3.33. Optimization of concentrations and flow rates for $HNO_3$ and reductant solutions were carried out by keeping all parameters constant as given in Table 2.4 while only the tested parameter was varied. In this study, the suction rate of the waste flow rate optimization was also carried out. The suction rate of the waste affected the Ag signal efficiently. If the suction rate of the waste was increased, Ag signal decreased. In this study, suction rate of the waste was chosen as 20 mL $min^{-1}$. As an example, if suction rate of the waste is selected as 25 mL $min^{-1}$ instead of 20 mL $min^{-1}$, Ag signal is decreased around 30%. Therefore, the waste flow rate should be optimized. If the suction rate of waste was very low, there would be excessive accumulation of solution in GLS. This relatively large volume of liquid phase may be absorbing the volatile species causing a lower signal.

At the beginning of study, 250 ng $mL^{-1}$ Ag and 1.0% (w/v) $NaBH_4$ were used to optimize the flow rates of analyte and reductant solutions using U-shaped GLS system by CF mode and the results are shown in Figure 3.32 and Figure 3.33, respectively.

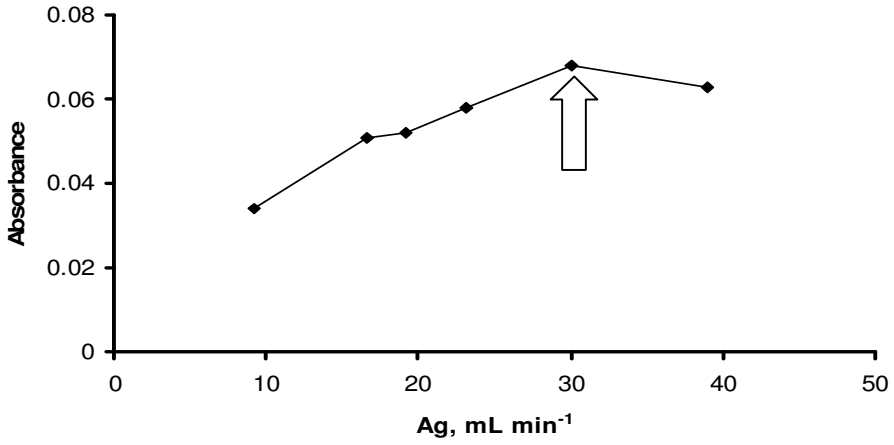


**Figure 3.32.** Optimization of the Ag flow rate with U-shaped GLS in CF mode (250 ng $mL^{-1}$ Ag, 1.0% (w/v) $NaBH_4$ with a flow rate of 4.2 mL $min^{-1}$).

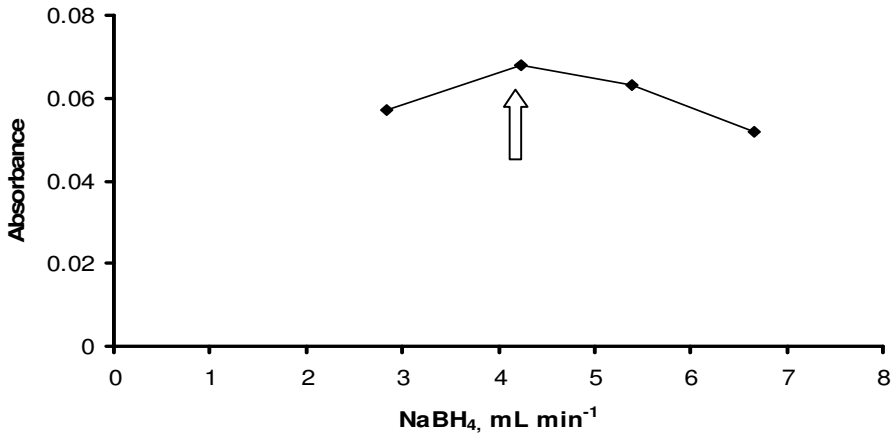


**Figure 3.33.** Optimization of the $NaBH_4$ flow rate with U-shaped GLS in CF mode (30.0 mL $min^{-1}$ for 250 ng $mL^{-1}$ Ag, 1.0% (w/v) $NaBH_4$).

### 3.4.1.2 Optimization of $HNO_3$ Concentration

In this study, $HNO_3$ was used in preparation of analyte solution. In order to find the optimum $HNO_3$ concentration, its concentration in the analyte solution was varied between 0.5 mol $L^{-1}$ and 2.0 mol $L^{-1}$. The optimum value for $HNO_3$ was found as 1.0 mol $L^{-1}$, somewhat in the middle of the plateau. Higher and lower values resulted in a gradual decrease in the analytical signal as shown in Figure 3.34. The effect of sample acidity was also checked in W-coil trap VCG-AAS system and found to be as same as in without W-coil trap system.

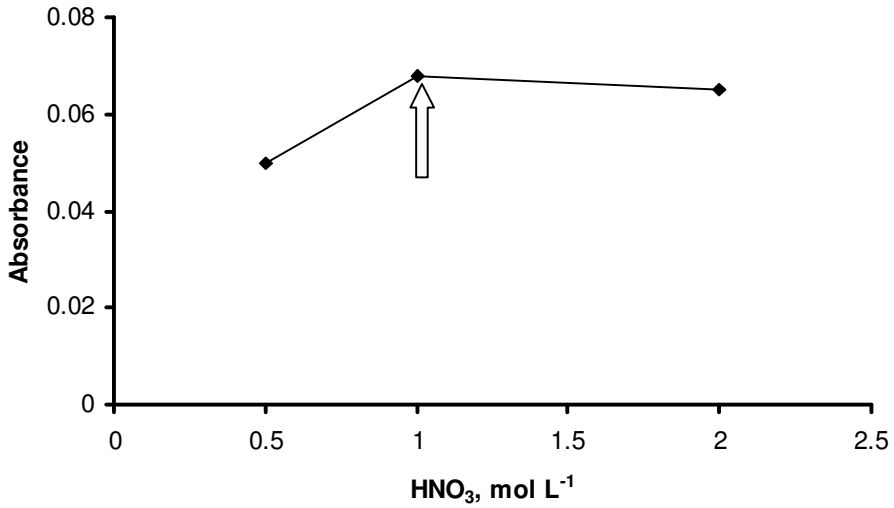


**Figure 3.34.** Optimization of the $HNO_3$ concentration with U-shaped GLS in CF mode (250 ng $mL^{-1}$ Ag, 30 mL $min^{-1}$ and 1.0% (w/v) $NaBH_4$, 4.2 mL $min^{-1}$).

### 3.4.1.3 Optimization of Reaction Coil Length

In the optimization study, length of reaction coil was varied between 20.0 cm and 100.0 cm. The optimum length for reaction coil was found as 30.0 cm. The analyte signal decreased with the values both lower and higher than the optimum value shown in Figure 3.35.

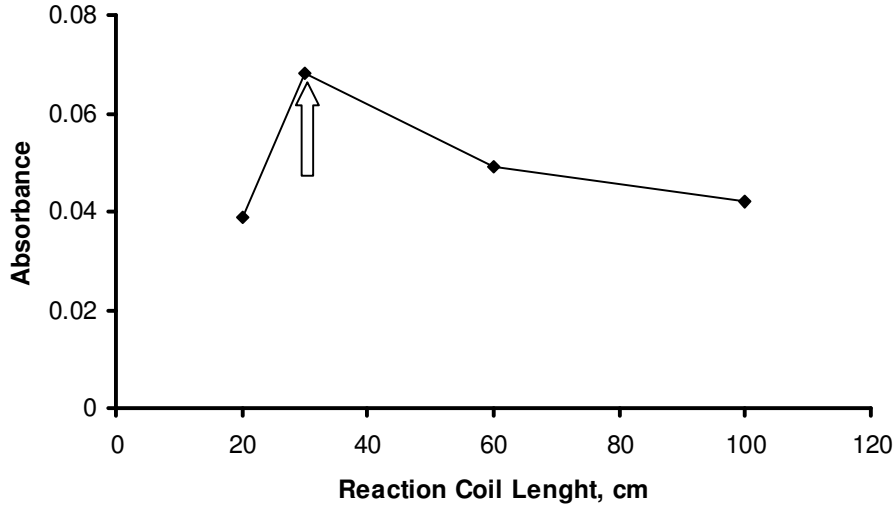


**Figure 3.35.** Optimization of the length of reaction coil with U-shaped GLS in CF mode (250 ng $mL^{-1}$, Ag, 30 mL $min^{-1}$ and 1.0% (w/v) $NaBH_4$, 4.2 mL $min^{-1}$, 1.0 mol $L^{-1}$ $HNO_3$).

### 3.4.1.4 Optimization of $NaBH_4$ Concentration

For the production of Ag volatile species, $NaBH_4$ was used as the reductant solution. The effect of $NaBH_4$ concentration on formation of volatile Ag species was investigated by using CF mode. In order to find the optimum $NaBH_4$ concentration,

its concentration was varied between 0.5% and 1.5% (w/v) and 1.0% (w/v) $NaBH_4$ was found as the optimum reductant solution concentration in without W-coil trap system. In this optimization, it was observed that the Ag signal increased until 1.0% (w/v) and then decreased for higher values as shown in Figure 3.36. The decrease can be explained by the dilution effect, since more $H_2$ was evolved at higher concentrations of reductant. In addition, NaOH was used for the stabilization of $NaBH_4$. Concentration of NaOH was varied between 0.1% and 1.0% (w/v). The highest signal for Ag was obtained using the reductant solution containing 0.5% (w/v) of NaOH while the other parameters were kept at their optimum values.

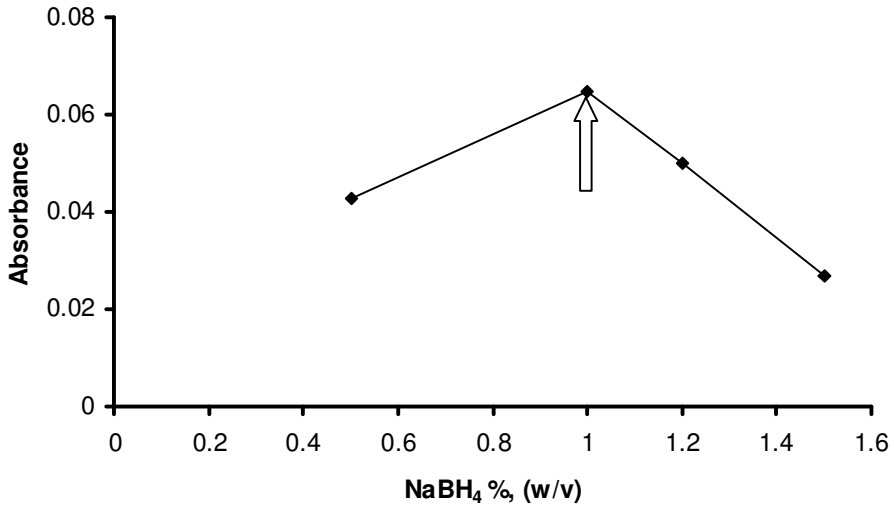


**Figure 3.36.** Optimization of the $NaBH_4$ % with U-shaped GLS in CF mode (250 ng $mL^{-1}$ Ag, 30 mL $min^{-1}$ and $NaBH_4$, 4.2 mL $min^{-1}$, 1.0 mol $L^{-1}$ $HNO_3$, 30 cm reaction coil length).

### 3.4.1.5 Calibration Plot of Ag by using U-Shaped GLS

A calibration plot of Ag was drawn by using the U-shaped GLS. It is necessary to mention that to eliminate the memory effect, GLS and glass part in the system were silanized using the procedure given in section 2.4.2 [135,181]. Silanization significantly lowered the memory effects and improved reproducibility. A linear calibration plot starting from 50 to 500 ng $mL^{-1}$ was obtained by using U-shaped GLS system as shown in Figure 3.37. The best line equation and correlation coefficient were, A= 0.0003C + 0.0014 and 0.9997, respectively. In this equation, C is the Ag concentration in ng $mL^{-1}$, and A is the absorbance. All the statistical calculations are based on the average of triplicate readings for each standard solution.

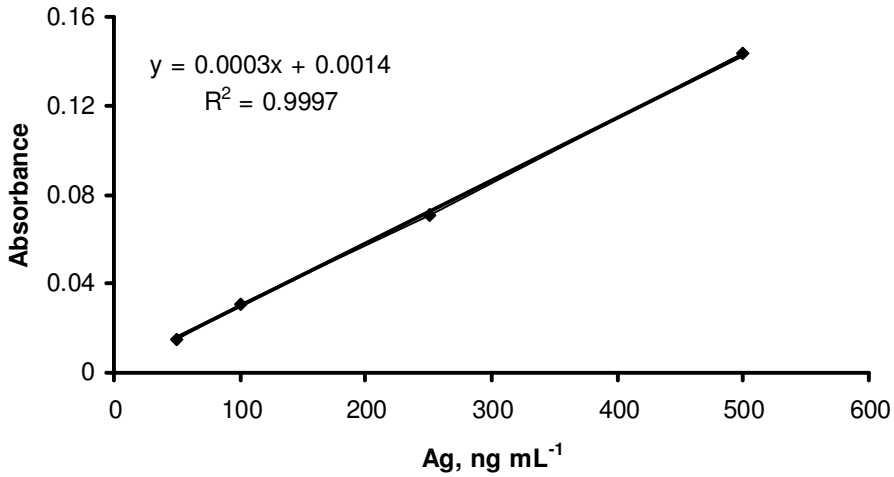


**Figure 3.37.** Calibration plot of Ag using U-shaped GLS (Ag, 30 mL $min^{-1}$ and 1.0% (w/v) $NaBH_4$, 4.2 mL $min^{-1}$, 1.0 mol $L^{-1}$ $HNO_3$, 30 cm reaction coil length).

Sensitivity enhancement limit of detection (LOD) and characteristic concentration

($C_0$) were found as 29 and 15 ng $mL^{-1}$, respectively as shown in Table 3.11. In order to determine LOD, 11 measurements of blank solution were used.

**Table 3.11.** Analytical performance of Ag with U-shaped GLS, cylindrical GLS and HVGLS

| GLS types | LOD (ng $mL^{-1}$) | $C_0$ (ng $mL^{-1}$) | E (w.r.to US) | E (w.r.to C) | E (w.r.to C with W-coil) |
|---|---|---|---|---|---|
| US | 29 | 15 | 1.0 | - | - |
| C | 2.14 | 3.03 | 5.0 | 1.0 | - |
| C with W-coil | 0.43 | 0.48 | 31.3 | 6.3 | 1.0 |
| HVGLS with W-coil | 0.05 | 0.05 | 300 | 60 | 9.6 |

US= U-shaped; C= Cylindrical; w.r.to= with respect to; E= Sensitivity enhancement; when W-coil was used 15.0 mL of analyte solution was collected in 30 s.

### 3.4.2 Silver Determination by CF-VCG-AAS Using Cylindrical GLS

In this part of experiment, cylindrical GLS was used instead of U-shaped GLS as shown in Figure 2.5 (a). In this GLS design, firstly optimization was carried out again for the flow rate of Ar gas. It has been found that when there was no Ar gas in the system, Ag signal was the highest. Hence, in further experiments with cylindrical GLS system, Ar gas was not used. Therefore, stripping coil from the system was removed and dilution of analyte species was minimized as shown in Figure 2.5 (c). Using this design, the flow rates of reductant and analyte solutions were optimized by using 10 ng $mL^{-1}$ Ag solution and the flow rates of analyte and reductant solutions were found as 30 mL $min^{-1}$and 4.2 mL $min^{-1}$ respectively. It seems that the flow rates of the solutions are the same as those with U-shaped GLS. The length of the reaction

coil was optimized and found as 30 cm. When the length of the reaction coil was higher or lower than that value, the Ag signal was decreased.

### 3.4.2.1 Calibration Plot for Ag by Using Cylindrical GLS

Using above optimum experimental parameters, linear calibration plot with cylindrical GLS system for Ag was drawn between 5.0 and 50.0 ng $mL^{-1}$ as shown in Figure 3.38. The best line equation and correlation coefficient were, A= 0.0011C + 0.0089 and 0.9999, respectively, where A is absorbance and C is Ag concentration in ng $mL^{-1}$. LOD and $C_0$ values are shown in Table 3.11. Sensitivity enhancement of cylindrical GLS systems with respect to U shaped GLS was around 5.0 fold when $C_0$ values were compared.

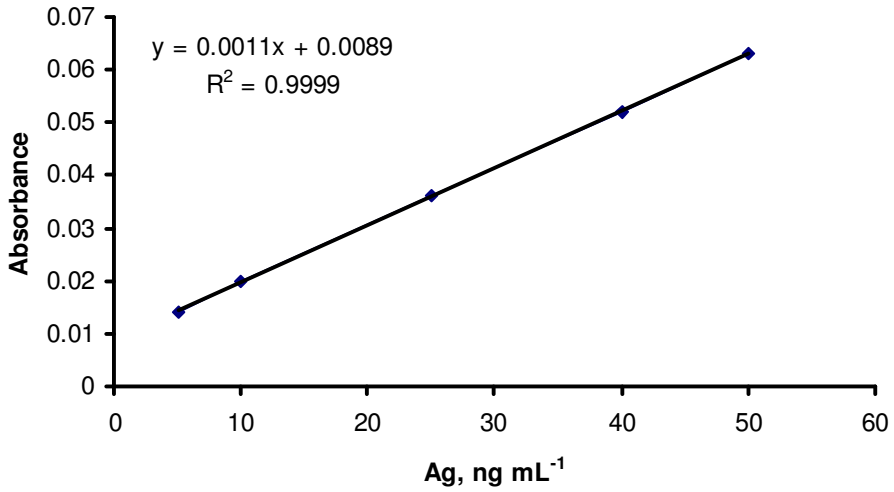


**Figure 3.38.** Calibration plot of Ag using cylindrical GLS (Ag, 30 mL $min^{-1}$ and 1.0% (w/v) $NaBH_4$, 4.2 mL $min^{-1}$, 1.0 mol $L^{-1}$ $HNO_3$, 30 cm reaction coil length).

### 3.4.3 Silver Determination by VCG-AAS Using Cylindrical GLS and W-coil Trap

To increase the sensitivity of Ag, a resistively heated W-coil trap was used in this study. Each W-coil can be used for at least 100 firings under optimum parameters. $H_2$ flow in the system directly affects the lifetime of W-coil trap. Sensitivity of the system decreased as some oxidation of W-coil trap takes place by extended usage. As an example, if W-coil trap was not replaced after some usage, sensitivity of system decreased by around 25%. If the flow rate of the $H_2$ is lower than 37.5 mL $min^{-1}$ in collection and revolatilization steps, the lifetime of W-coil trap becomes shorter. The presence of $H_2$ gas is necessary for both effecting a more efficient revolatilization and protecting the W-coil trap against oxidation. The coil should be heated as fast as possible at the revolatilization stage to obtain relatively sharp signals. For this purpose, a power switch was connected in front of the variable potential power supply, the switch was turned of prior to rapid heating, voltage was selected and then the switch was turned on to assure the highest heating rate.

#### 3.4.3.1 Optimization of Collection and Revolatilization W-coil Trap Temperature

In order to obtain a high trapping efficiency, W-coil trap temperature should be optimized. For this goal, 10 ng $mL^{-1}$ Ag standard solutions were used. In this study, collection trap temperature was varied from 200 $^{o}$C to 1000 $^{o}$C. The efficiency of W-coil trap increases sharply as the temperature increases up to approximately 750 $^{o}$C. Increasing the W-coil trap temperature further resulted in a decrease in the analytical signal due to the partial release of the trapped Ag species and lowered trapping efficiency as shown in Figure 3.39. Hence, 750 $^{o}$C was found as the optimum W-coil trap temperature for efficient collection of Ag species on W-coil trap.

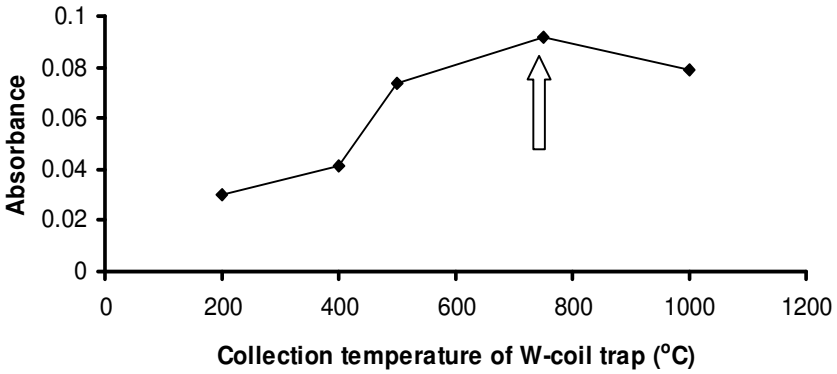


**Figure 3.39.** Optimization of collection temperature of W-coil trap with cylindrical GLS (Revolatilization at 1800 °C; 10.0 ng $ml^{-1}$ Ag, 30 mL $min^{-1}$ and 1.0 % (w/v) $NaBH_4$, 4.2 mL $min^{-1}$, 1.0 mol $L^{-1}$ $HNO_3$, 30 cm reaction coil length).

W-coil trap temperature for revolatilization was varied from 1250 °C to 2000 °C while the collection W-coil trap temperature was kept constant at its optimized value, 750°C. The optimum W-coil trap temperature for revolatilization was 1800 °C as shown in Figure 3.40. There is no need for waiting to cool the W-coil trap after revolatilization step or heat for the activation of W-coil trap before each collection cycle because the W-coil trap cools down very rapidly in only few seconds due to the continued gas flow once the electrical power was turned off. In order to protect the W-coil trap, hydrogen flow should be on throuhout the experiment.

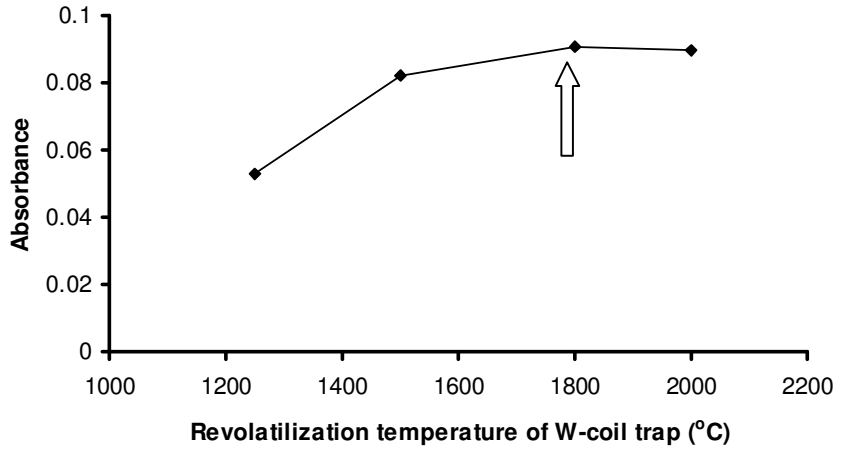


**Figure 3.40.** Optimization of revolatilization temperature of W-coil trap with cylindrical GLS (Collection at 750 °C; 10.0 ng $ml^{-1}$ Ag, 30 mL $min^{-1}$ and 1.0 % (w/v) $NaBH_4$, 4.2 mL $min^{-1}$, 1.0 mol $L^{-1}$ $HNO_3$, 30 cm reaction coil length).

### 3.4.3.2 Optimization of Flow Rates and Composition of Gases in the Collection and Revolatilization Stages

In this experiment, during the optimization of both gas flow rates and compositions, 10 ng $mL^{-1}$ Ag standard solutions were used. In VCG system, different carrier gases introduced before or after the reaction coil are used to separate the volatile Ag species from the liquid phase and furthermore transport these species from GLS to externally heated QTA. In this study, $H_2$ gas was applied not only in the collection but also in the revolatilization steps. In general, the flow rate of $H_2$ gas was kept constant at an optimized value so that the oxidation of the W-coil trap was minimized or eliminated. $H_2$ gas was used not only to prevent oxidation of the W-coil trap by creating a reducing environment around the W-coil trap but also to improve the revolatilization efficiency of Ag species from the W-coil trap. If flow rate of $H_2$ gas higher than optimized value during the collection stage especially, excess $H_2$ causes W-coil trap

temparature decrease around the W-coil. This situation negatively affects the sensitivity in Ag determination. In this experiment, when W-coil was not used, gas was not used and the dilution of volatile Ag species was eliminated. On the other hand, in W-coil trap experiment with cylindrical GLS, a T connection was placed downstream of the GLS to send $H_2$ gas through the system as shown in Figure 3.41. In the collection and revolatilization steps, $H_2$ flow rates were optimized using CF mode in W-coil trap studies. In both collection and revolatilization steps, Ar gas was not used so as to eliminate the dilution of volatile Ag species. The flow rate of $H_2$ was varied between 40 mL $min^{-1}$ and 200 mL $min^{-1}$ during the collection stage. The optimum value was found to be 146.0 mL $min^{-1}$; signal decreased for lower and higher values. In the revolatilization step, the flow rate of $H_2$ was increased from 146.0 ml $min^{-1}$ to 376.0 ml $min^{-1}$. Although Ag signal was obtained with some other carrier gases compositions, this change in composition provided an increase in sensitivity by a factor of almost 2.0 fold and sharper peaks were obtained.

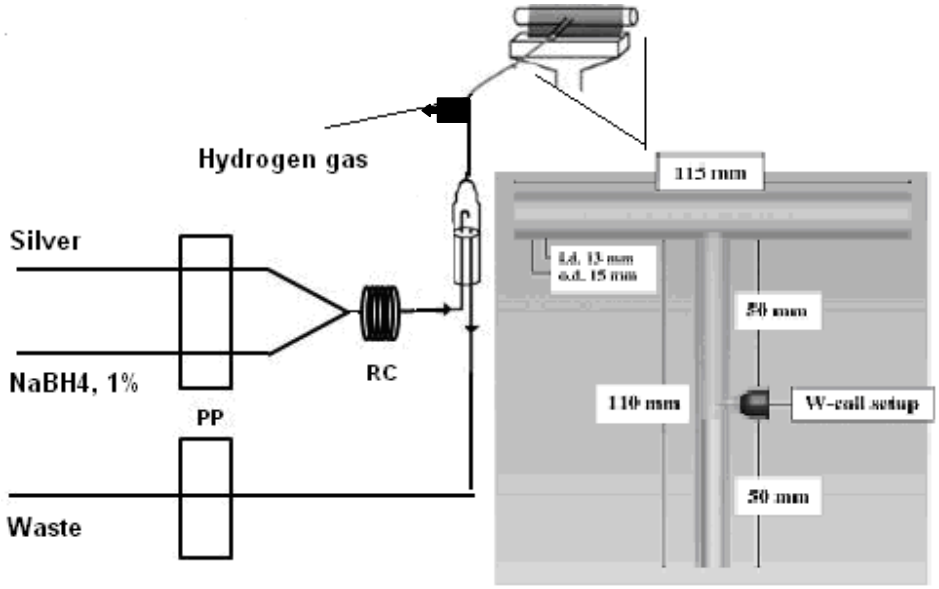


**Figure 3.41.** VCG system without SC for cylindrical GLS with W-coil trap.

### 3.4.3.3 Calibration Plot for Ag by using Cylindrical GLS with W-coil Trap

For linear calibration plot using cylindrical GLS with W-coil trap, Ag standards between 1.0 and 10.0 ng $ml^{-1}$ were used as shown in Figure 3.42. The best line equation and correlation coefficient were, A= 0.0084C + 0.0054 and 9996, respectively. A was absorbance and C was concentration in ng $mL^{-1}$. LOD and $C_0$ values of this system are shown in Table 3.11. When compared using the $C_0$ values, 31.3 and 6.3 fold sensitivity enhancements were obtained with respect to U shaped GLS without W-coil trap and cylindrical GLS without W-coil trap systems, respectively. Optimization of collection time was carried out and found as 30 seconds for 10 ng $mL^{-1}$. For collection times longer than 30 seconds, the peak height of the Ag signal did not significantly increase. This may be due excess analyte accumulation on trap, diminishing the sites available for analyte trapping. Therefore, collection time was chosen as 30 seconds afterwards.

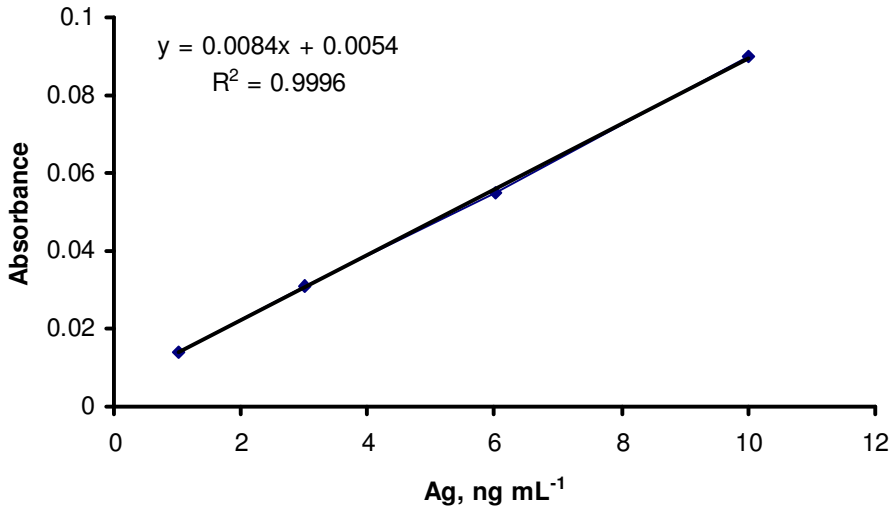


**Figure 3.42.** Calibration plot for Ag by using cylindrical GLS with W-coil trap.

### 3.4.4 Silver Determination by VCG-AAS Using HVGLS and W-coil Trap

The design of HVGLS is shown in Figure 3.43 with the W-coil trap system. Main body of HVGLS is a cylinder with a height of 180 mm and a diameter of 50 mm. This HVGLS consists of three two-way valves plus one three-way valve shown as (1), (2), (4) and (3) in Figure 3.43, respectively. The valve 1 is used to send the Ar gas flow rate and the valve 2 is used for sending the mixed solutions of $NaBH_4$ and analyte solutions. The function of valve 3 is to introduce the $H_2$ gas in the W-coil trap study. Finally, the valve 4 is used to send solutions to the waste at the end of process.

In this part of experiment, W-coil trap was located between the HVGLS and QTA. $H_2$ gas through valve 3 was used for releasing the Ag species that was trapped on the surface of W-coil trap after applying revolatilization temperature. For this HVGLS design, again univariate optimization has been applied to find the optimum conditions. At first, W-coil trap was resistively heated to 750 $^{o}$C. After W-coil trap

temperature reached to 750 °C, using valve 2, Ag and $NaBH_4$ solutions were sent into the HVGLS. Simultaneously, the carrier gas consisted of 76.0 mL $min^{-1}$ Ar with 146.0 mL $min^{-1}$ $H_2$ was bubbled continuously through the contents of HVGLS using valve 1. After the collection step for a chosen period of time which was 30 seconds, the valve 2 was closed but the carrier gas flow was continued. The W-coil trap temperature was increased to 1800 °C that needed about 1.0 s; and valve 1 was closed and then immediately using valve 3, the $H_2$ gas was introduced at a flow rate of 376.0 mL $min^{-1}$.

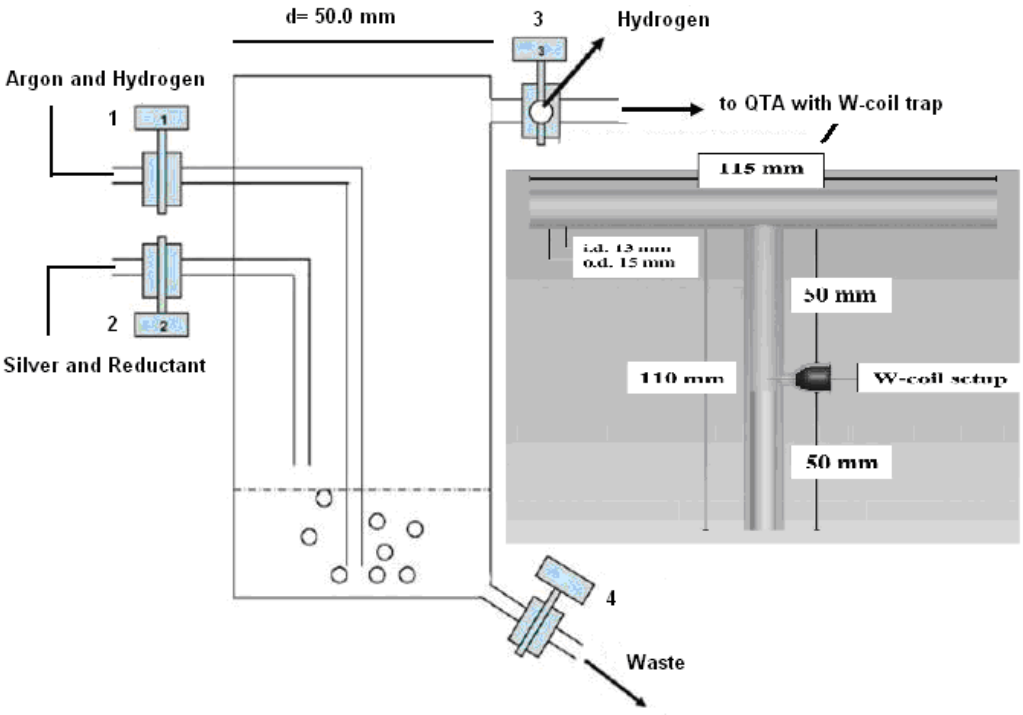


**Figure 3.43.** High Volume Gas Liquid Separator (HVGLS) for Ag determination.

The residence time of the analyte species on the light path is very short, about 1.0 s, and the half width of the transient signal is less than 0.5 s shown in Figure 3.44. In

this study, it was tried to improve the efficiency of VCG by designing a HVGLS and the results that were obtained prove the success of this study

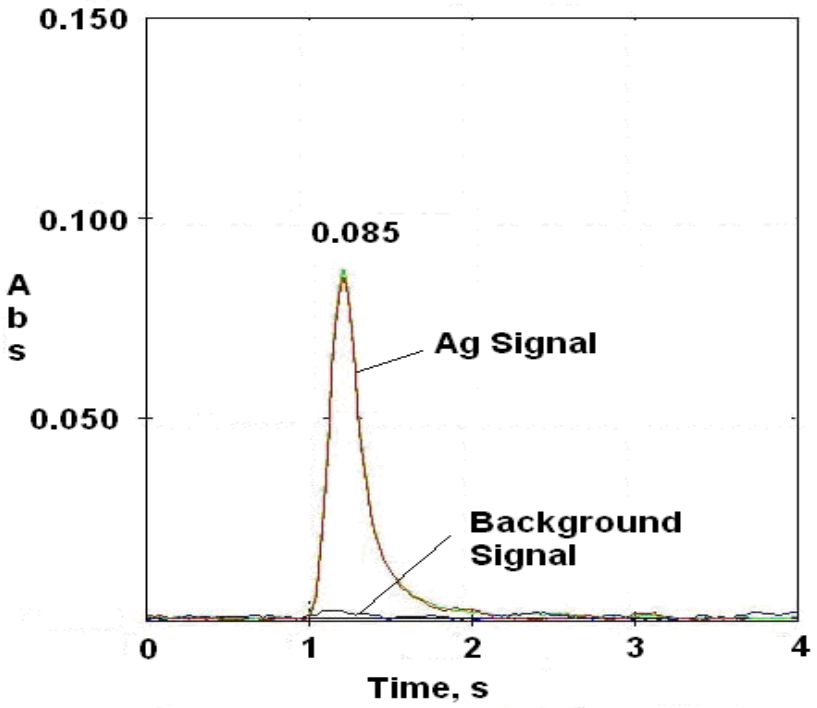


**Figure 3.44.** Signal obtained for 0.75 ng $mL^{-1}$ Ag using W-coil trap with HVGLS without blank correction (Mean Absorbance Value of Blank Ag: 0.021) (Volume of Ag: 15 mL).

### 3.4.4.1 Calibration Plot for Ag by using HVGLS with W-coil Trap

By using optimum analytical parameters, a linear calibration plot using HVGLS with W-coil trap system was obtained between 0.1 and 1.0 ng $mL^{-1}$ as shown in Figure 3.45. The best line equation and correlation coefficient were, A= 0.0822C + 0.0024 and 9992, respectively. A is the absorbance and C is the concentration of Ag in ng

$mL^{-1}$. LOD and $C_0$ values of this system are shown in Table 3.11. When compared the $C_0$ values, 300, 60.6 and 9.6 fold sensitivity enhancements were obtained with respect to U shaped GLS without W-coil trap, cylindrical GLS without W-coil trap and cylindrical GLS with W-coil trap systems, respectively.

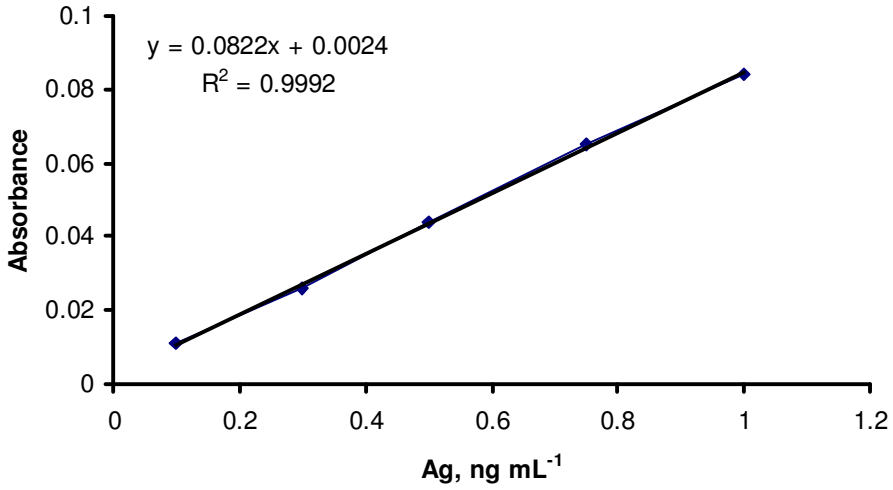


**Figure 3.45.** Calibration plot for Ag by using HVGLS with W-coil trap.

### 3.4.4.2 Evaluation of System Performance

In principle, when the $C_0$ values of two systems are compared, sensitivity enhancement (E) can be found. E also means the ratio of calibration sensitivities (slopes). Ataman [62] introduced two new terms, enhancement factors in term of unit time, $E_t$, and unit volume, $E_v$. $E_t$ is obtained by dividing E value by total time spent in terms of minutes, and $E_v$ is obtained by dividing E value by total volume consumed in terms of milliliters. Therefore, it would be possible to make a fair comparison of two methods using the terms of the trapping period and the total amount trapped. For HVGLS with W-coil trap system, $E_t$ and $E_v$ values are shown in Table 3.12 with

respect to U-shaped GLS and cylindrical GLS for Ag determination.

**Table 3.12.** Comparison of HVGLS with W-coil trap system in terms of $E_t$ and $E_v$ values with US and C gas liquid separators

| | With respect to US | | With respect to C | |
|---|---|---|---|---|
| Sensitivity Enhancement | Et | Ev | Et | Ev |
| Normalized to time or volume | 600 | 20 | 120.0 | 4.0 |

US= U-shaped; C= Cylindrical ; collection time= 30 s, collected Ag volume= 15 mL.

### 3.4.5 Conclusions

This study revealed that when the Ar gas was used with both U-shaped and cylindrical GLS systems without W-coil trap, meaningful Ag signal could not be obtained. However, when the Ar carrier gas was removed from the system, Ag signal was obtained. It is believed that this is due to dilution of volatile Ag species with the carrier gas. It was observed that the sensitivity of cylindrical GLS is 5-fold higher than U-shaped GLS by comparing $C_0$ values. Moreover, W-coil trap was employed with cylindrical GLS system. For this reason, in order to eliminate the oxidation of W-coil trap, a three way valve was placed after the GLS which introduces $H_2$ gas. In this case, the sensitivity of Ag is 6.3-fold higher than cylindrical GLS without W-coil trap by comparing the $C_0$ values.

Furthermore, a HVGLS was designed to improve the detection limit of Ag down to the sub ng $mL^{-1}$ levels. In this apparatus, volatile Ag species are collected in a limited volume and after separation of the volatile Ag species from liquid phase, the entire analyte vapor is sent to QTA that was heated externally by an air/acetylene flame.

The sensitivity of the HVGLS with W-coil trap is 9.6-fold higher than cylindrical GLS with W-coil trap by comparing the $C_0$ values.

## 3.5 Indium Determination by VCG-AAS

### 3.5.1 Indium determination by CF-VCG-AAS Using Cylindrical GLS

In the preliminary experiments of this study, a cylindrical GLS without W-coil trap was used for the optimization of VCG-AAS system. By using the peristaltic pumps, indium and $NaBH_4$ solutions were mixed in the reaction coil whose length was 23 cm. The position of reaction coil and stripping coil were explained previosly in Ag study in section 3.4.1.3. After mixing the solutions in reaction coil, generated indium species were sent to the cylindrical GLS by means of 76.0 mL $min^{-1}$Ar carrier gas. After volatile indium species are separated from the liquid phase in the cylindrical GLS, they were transferred to QTA which was externally heated by air/acetylene flame. However, using this set-up, no meaningful signal could be obtained.

After this experiment, the optimization of Ar flow rate was carried out. Its flow rate was varied from 0 to 150 mL $min^{-1}$. This experiment revealed that when the flow rate of Ar was decreased, the indium signal increased. This behaviour was the same as that in Ag study by using U-shaped and cylindrical GLS. It has been concluded that if there was no Ar carrier gas in the system, the indium signal was the highest by considering both peak height and signal to noise ratio (S/N). Hence, after solutions were mixed in the reaction coil, they were sent to the cylindrical GLS via $H_2$ gas only which was evolved from the reaction between $NaBH_4$ and acid content of standard solutions. Thus, additional carrier gas was not used to transport the generated indium species to QTA as shown in Figure 2.5 (c). It is believed that by the effect of the carrier gas, generated volatile indium species are diluted and as a result, the

sensitivity of the indium decreased. This behavior was similar to that observed during Ag determinations.

#### 3.5.1.1 Optimization of Experimental Parameters

The optimization of the experimental parameters for indium determination was carried out using both CF-VCG-AAS and W-coil trap-VCG-AAS. All the experimental conditions were optimized on the basis of the univariate measurements. Optimizations of flow rates of indium and reductant solutions, concentration of HCl which was used in analyte solution and concentration of reductant solution were common in both CF-VCG-AAS and W-coil trap VCG-AAS systems. The optimum HCl and $NaBH_4$ concentrations were determined without using W-coil trap and in CF mode by using 4.0 mg $L^{-1}$ indium standard solution.

#### 3.5.1.2 Optimization of Flow Rates of Indium and $NaBH_4$ Solutions

In principle, generation of indium volatile species is directly related with the flow rates of analyte and reductant solutions. In this study, the flow rate of indium solution was varied between 5.0 mL $min^{-1}$ and 25.0 mL $min^{-1}$ and the optimum value was found to be 15.0 mL $min^{-1}$. The signal increased as the flow rate was increased until the value of 15.0 mL $min^{-1}$ and decreased afterwards as shown in Figure 3.46. The flow rate of $NaBH_4$ solution was varied between 4.0 mL $min^{-1}$ and 16.0 mL $min^{-1}$ and the optimum value was found as 10.0 mL $min^{-1}$. For the higher and lower flow rates of $NaBH_4$, indium signal decreased as shown in Figure 3.47. Optimization of concentrations and flow rates for HCl and reductant solutions were also carried out by keeping all parameters constant while only the test parameter was varied.

At the beginning of this study, by using 4.0 mg $L^{-1}$ indium standard solution, both HCl and $HNO_3$ were tried to obtain maximum sensitivity. In the case of $HNO_3$, sensitivity of indium was about 2 times lower when compared to HCl. Therefore, in further studies, HCl was used to acidify the indium standard solutions. For the optimization of flow rates of indium and reductant solutions, HCl concentration was chosen as 3.0 mol $L^{-1}$.

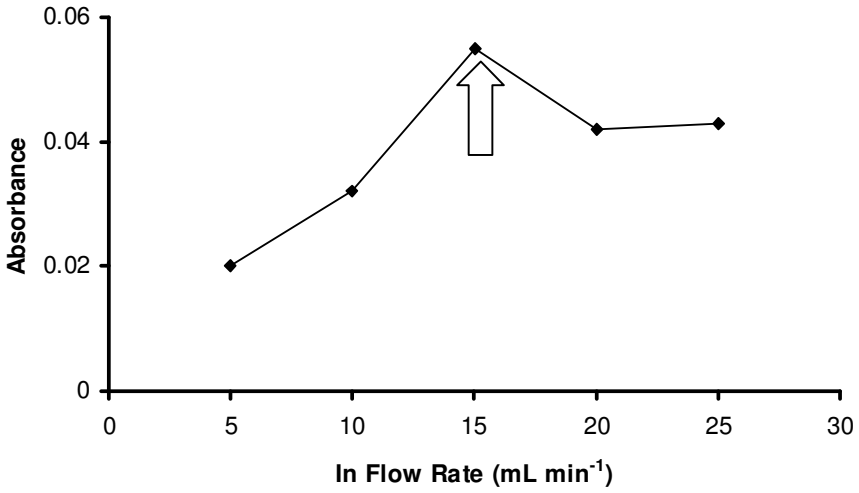


**Figure 3.46.** Optimization of flow rate of indium (1.0% $NaBH_4$, 10 mL $min^{-1}$; 3.0 mol $L^{-1}$ HCl; reaction coil length: 23 cm; 4.0 mg $L^{-1}$ In).

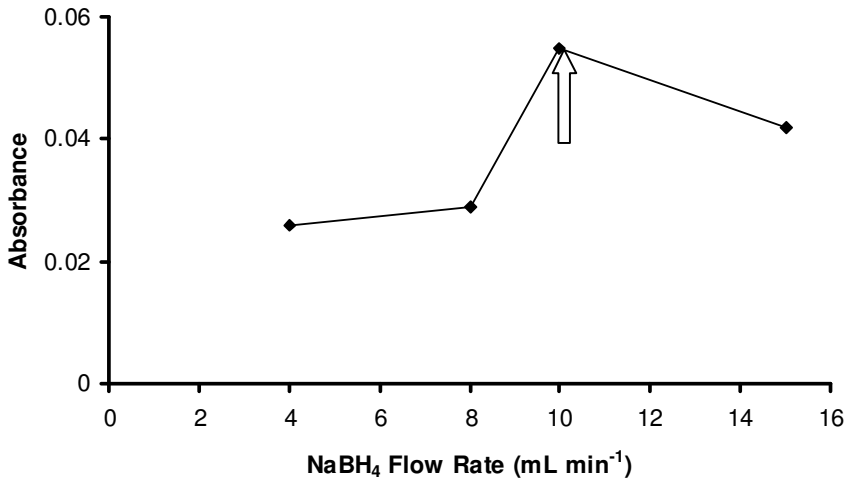


**Figure 3.47.** Optimization of flow rate of $NaBH_4$ (1.0% $NaBH_4$, 3.0 mol $L^{-1}$ HCl; reaction coil length: 23 cm; 4.0 mg $L^{-1}$ In, 15 mL $min^{-1}$).

### 3.5.1.3 Optimization of HCl Concentration

In this study, analyte solutions were prepared in agueous HCl. To find the optimum HCl concentration, its concentration in the analyte solution was varied between 0 and 5.0 mol $L^{-1}$. The optimum value for HCl was found as 3.0 mol $L^{-1}$, somewhat in the middle of the plateau. Higher and lower values resulted in a gradual decrease in the analytical signal as shown in Figure 3.48. When the concentration of HCl exceeds 3.0 mol $L^{-1}$, decrease in indium signal was observed. The effect of sample acidity was also checked in W-coil trap VCG-AAS system and found to be the same as that of without W-coil trap system.

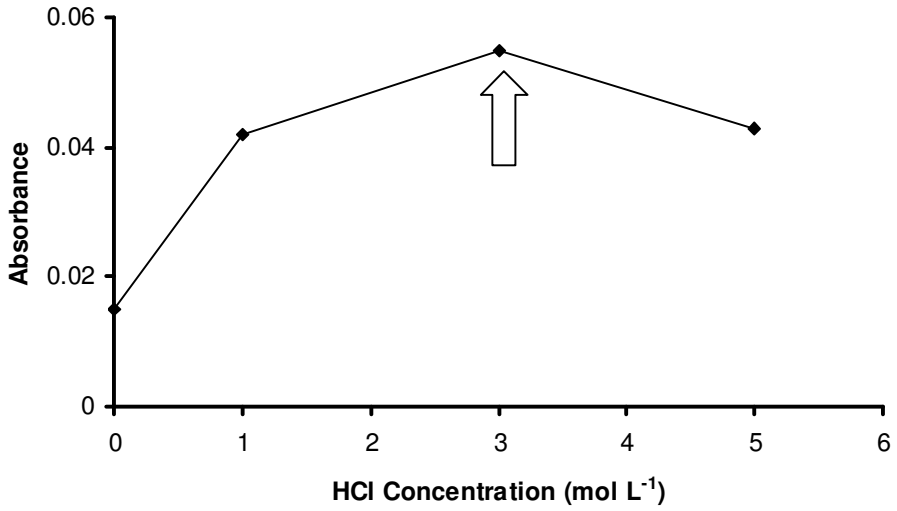


**Figure 3.48.** Optimization of concentration of HCl (mol $L^{-1}$)(1.0% $NaBH_4$, 10 mL $min^{-1}$; reaction coil length: 23 cm; 4.0 mg $L^{-1}$ In, 15 mL $min^{-1}$).

### 3.5.1.4 Optimization of Concentration of $NaBH_4$

To produce indium volatile species, $NaBH_4$ was used as a reductant solution. The effect of $NaBH_4$ concentration on volatile indium species production was investigated by using CF mode. To find the optimum $NaBH_4$ concentration, its concentration was varied between 0.5% and 3.0% (w/v) and 1.0% (w/v) $NaBH_4$ was found as the optimum reductant solution concentration. In this optimization, it was observed that the indium signal increased until 1.0% (w/v) and then decreased for higher values as shown in Figure 3.49. The decrease can be explained by the dilution effect, since more $H_2$ was evolved at higher concentrations of reductant. In addition, NaOH was used for the stabilization of $NaBH_4$. Concentration of NaOH was varied between 0.1% and 1.0% (w/v). The highest signal for the indium was obtained using the reductant solution containing 0.5% (w/v) of NaOH while the other parameters were kept at their optimum found values.

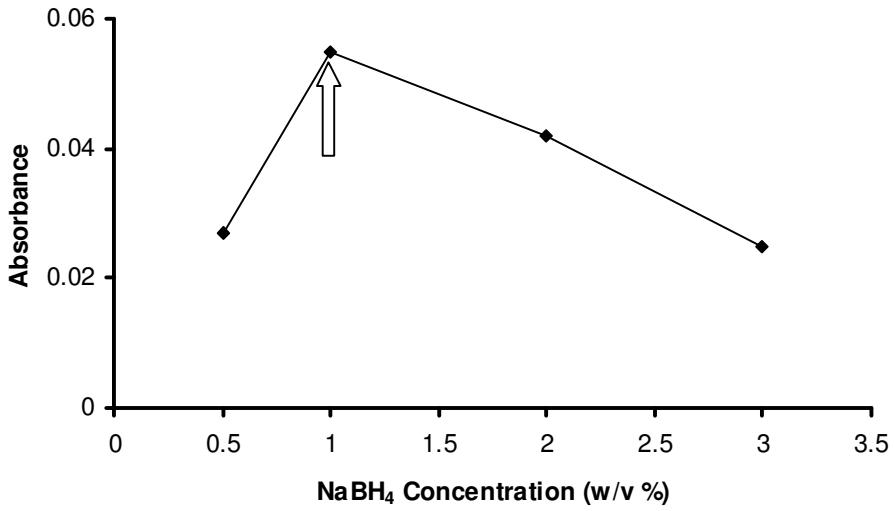


**Figure 3.49.** Optimization of concentration of $NaBH_4$ (w/v, %) ($NaBH_4$, 10 mL $min^{-1}$; reaction coil length: 23 cm; 4.0 mg $L^{-1}$ In, 15 mL $min^{-1}$; 3.0 mol $L^{-1}$ HCl).

### 3.5.1.5 Optimization of Reaction Coil Length

In this part of study, length of reaction coil was varied between 5.0 cm and 30.0 cm. The optimum length for reaction coil was found as 23.0 cm. The analyte signal decreased with the values both lower and higher than the optimum values as shown in Figure 3.50. In this study, as explained before, stripping coil was not used because carrier gas was not used in the system in CF mode.

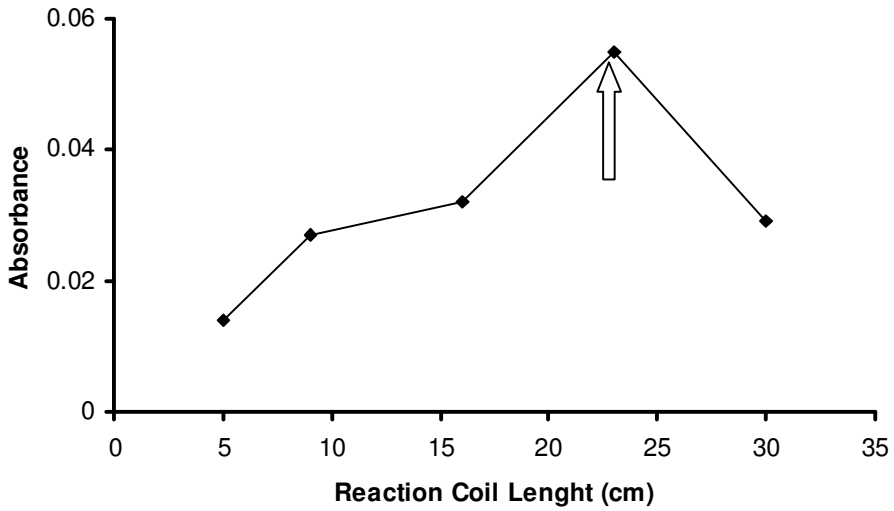


**Figure 3.50.** Optimization of lenght of reaction coil (1.0% $NaBH_4$, 10 mL $min^{-1}$; 4.0 mg $L^{-1}$ In, 15 mL $min^{-1}$; 3.0 mol $L^{-1}$ HCl).

### 3.5.1.6 Calibration plot for Indium by using Cylindrical GLS

Calibration plot for indium was drawn by using cylindrical GLS. As mentioned in the Ag determination study, to eliminate the memory effect, GLS and glass parts in the system were silanized. A linear calibration plot starting from 1.0 to 6.0 mg $L^{-1}$ was obtained by using cylindrical GLS system as shown in Figure 3.51. The best line equation and correlation coefficient were, A= 0.0123C + 0.0068 and 0.9993, respectively. In this equation, C is the indium concentration in mg $L^{-1}$, and A is the absorbance. All the statistical calculations are based on the average of triplicate readings for each standard solution.

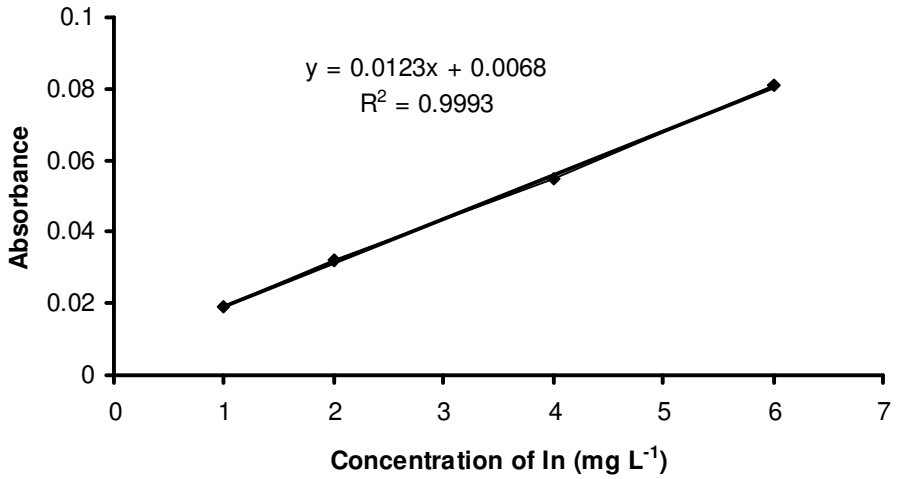


**Figure 3.51.** Calibration plot of indium using cylindrical GLS.

Sensitivity enhancement LOD and $C_0$ were found as 148 and 317 ng $mL^{-1}$, respectively as shown in Table 3.13. To determine LOD, 11 measurements of blank solution were used.

As shown in Table 3.13, in the case of cylindrical gas liquid separator, the sensitivity of the system is not very high for indium determination. HVGLS with W-coil trap was used to increase the sensitivity of indium determination by VCG-AAS.

**Table 3.13.** Analytical figures of merit for indium determination

| | **LOD (3s), ng $mL^{-1}$** | **Co, ng $mL^{-1}$** | **Enhancement w.r.to C-GLS** | **Enhancement w.r.to-HVGLS withW-coil trap** |
|---|---|---|---|---|
| Cylindrical GLS | 148 | 317 | 1.00 | - |
| HVGLS with W-coil trap | 0.46 | 0.98 | 323.5 | 1.00 |
| HVGLS with W-coil trap in the case of using $Ru(acac)_3$ | 0.13 | 0.23 | 1378 | 4.3 |

C-GLS: Cylindrical gas liquid separator

### 3.5.2 Indium Determination by VCG-AAS Using HVGLS and W-coil Trap

The design of HVGLS is shown before in Figure 3.43 with the W-coil trap system. In this part of the experiment, W-coil trap was used after the HVGLS. As it is shown in Figure 3.43, a three-way valve was placed downstream of HVGLS to introduce $H_2$ gas. $H_2$ gas was used for releasing the indium species that was trapped on the surface of W-coil trap after applying revolatilization temperature. In this HVGLS design, univariate optimization has been applied to find the optimum conditions for indium determination. To obtain better sensitivity for indium determination, some of the experimental parameters such as collection and revolatilization temperature of W-coil trap and flow rates and composition of gases in the collection and revolatilization stages were optimized.

### 3.5.2.1 Optimization of Collection and Revolatilization W-coil Trap Temperature for Indium

To obtain a high trapping efficiency, W-coil trap temperature should be carefully optimized. For this aim, 10 ng $mL^{-1}$ indium standard solutions were used. In this study, collection trap temperature was varied from 300 $^{o}$C to 1000 $^{o}$C. The efficiency of W-coil trap increases sharply as the temperature increases up to approximately 750 $^{o}$C. In this stage, revolatilization W-coil trap temperature was kept at 1800 $^{o}$C. Increasing the W-coil trap temperature further resulted in a decrease in the analytical signal due to the partial release of the trapped indium species and lowered trapping efficiency as shown in Figure 3.52.

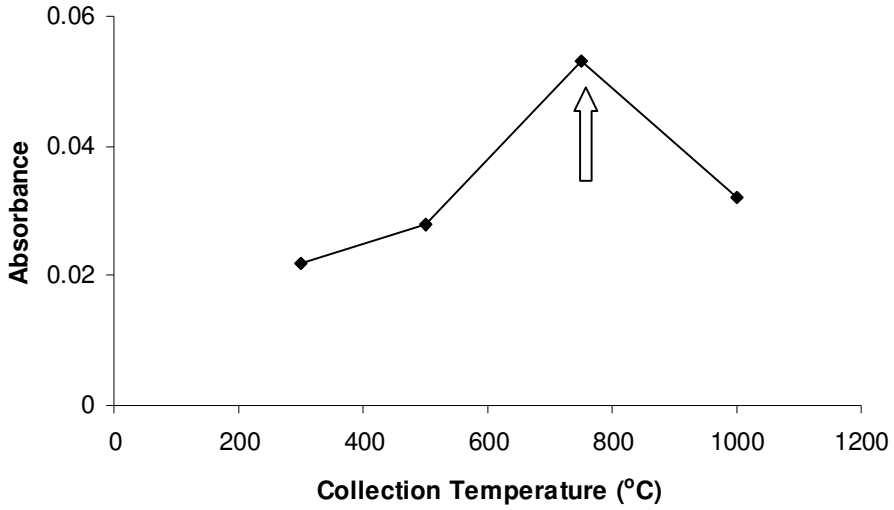


**Figure 3.52.** Optimization of collection temperature of W-coil trap.

Hence, 750 $^{o}$C was found as the optimum W-coil trap temperature for efficient collection of indium species on W-coil trap. Revolatilization W-coil trap temperature

was varied from 1200 °C to 2000 °C while the collection W-coil trap temperature was kept constant at its optimized value. The optimum W-coil trap temperature for revolatilization was 1800 °C at which the highest signal was obtained as shown in Figure 3.53. For the next sampling, there is no need for waiting to cool the W-coil trap or heat for the activation of W-coil trap before each collection cycle because the W-coil trap cools down very rapidly in only few seconds due to the continued gas flow once the electrical power is turned off. In addition, the system was free of memory; therefore there was no need for any extra heating step to clean W-coil trap. In order to protect the W-coil trap, hydrogen flow should be on throughout the experiment.

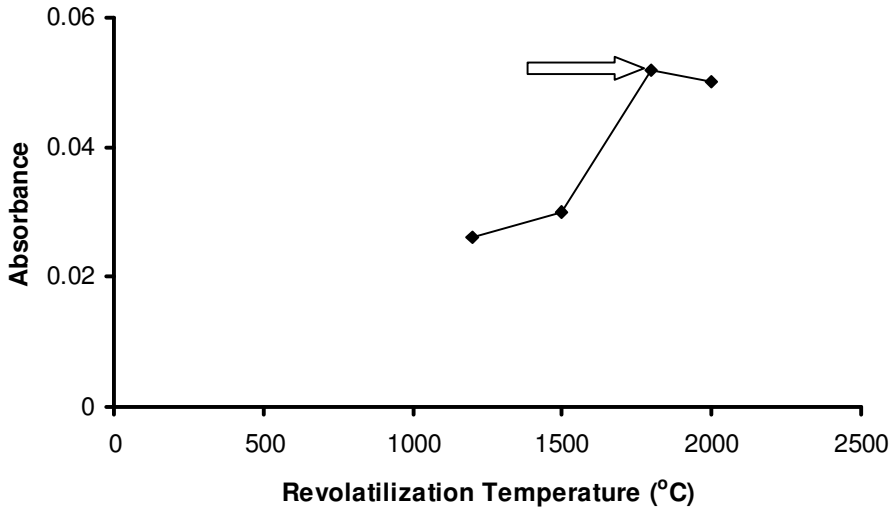


**Figure 3.53.** Optimization of revolatilization temperature of W-coil trap.

### 3.5.2.2 Optimization of Flow Rates and Composition of Gases in the Collection and Revolatilization Stages

For the optimization of gases flow rates and compositions, 10 ng $mL^{-1}$ indium standard solution was used. In this study, $H_2$ gas was applied not only in the collection but also in the revolatilization steps. In general, the flow rate of $H_2$ gas was kept constant at an optimized value so that the oxidation of the W-coil trap was minimized or eliminated. If the flow rate of $H_2$ gas higher than the optimized value during the collection stage, excess $H_2$ causes a decrease in the W-coil trap temperature. In this experiment, in without W-coil trap study, no carrier gas was used as similar to Ag study. In the optimum collection and revolatilization steps, $H_2$ flow rates were determined in CF mode in W-coil trap studies using HVGLS. During the collection stage, Ar gas was varied from 50 mL $min^{-1}$ to 200 mL $min^{-1}$ and 76 mL $min^{-1}$ was found to be optimum Ar flow rate for indium determination. The flow rate of $H_2$ was varied between 30 mL $min^{-1}$ and 200 mL $min^{-1}$ during the collection stage. The optimum value was found to be 146.0 mL $min^{-1}$; signal decreased for lower and higher values. In the revolatilization step, Ar gas was not used so as to eliminate the dilution of indium species. The flow rate of $H_2$ was increased from 146.0 ml $min^{-1}$ to 376.0 ml $min^{-1}$. Although indium signal was obtained with other carrier gases compositions, this change in composition provided an increase in sensitivity by a factor of almost 1.5 fold and sharper peaks were obtained.

### 3.5.2.3 Operation of HVGLS System with W-coil Trap for Indium Determination by VCG-AAS

As it is shown in Figure 3.43, a three-way valve was placed the downstream of HVGLS to introduce $H_2$ gas. $H_2$ gas was used for releasing the indium species that was trapped on the surface of W-coil trap after applying revolatilization temperature.

At first, W-coil trap was resistively heated to 750 $^{o}$C. After W-coil trap temperature reached to 750 $^{o}$C, using valve 2, indium and $NaBH_4$ solutions were sent to the HVGLS. During trapping, the carrier gases consisted of 76.0 mL $min^{-1}$ Ar with 146.0 mL $min^{-1}$ $H_2$ were bubbled continuously through the solution inside HVGLS using valve 1. After the collection step for a chosen period of time which was 60 seconds as shown in Figure 3.54, the valve 2 was closed but gas flow was continued. The W-coil trap temperature was increased to 1800 $^{o}$C that needed about 1.0 s; and valve 1 was closed and then immediately using the valve 3, $H_2$ gas was introduced with a flow rate of 376.0 mL $min^{-1}$. The residence time of the analyte species on the light path is very short, about 1.0 s, and the half width of the transient signal is less than 0.5 s shown in Figure 3.55.

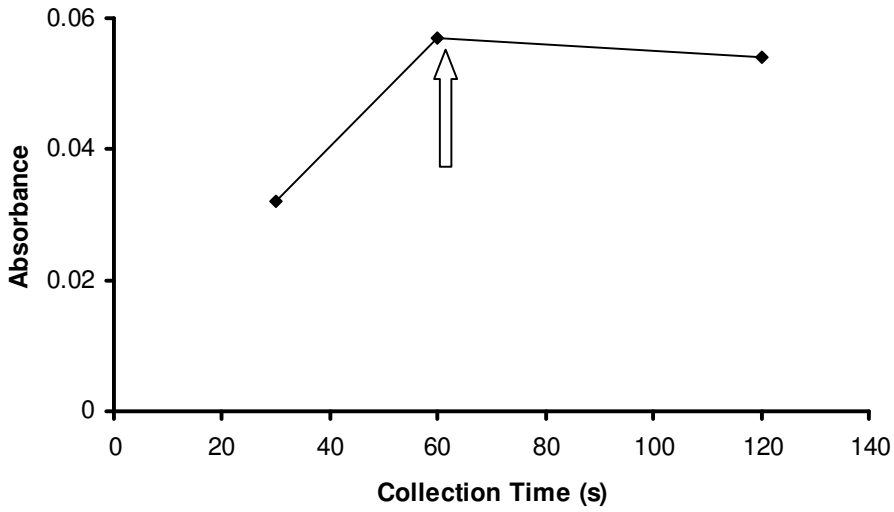


**Figure 3.54.** Optimization of collection time of indium species on the W-coil trap using HVGLS.

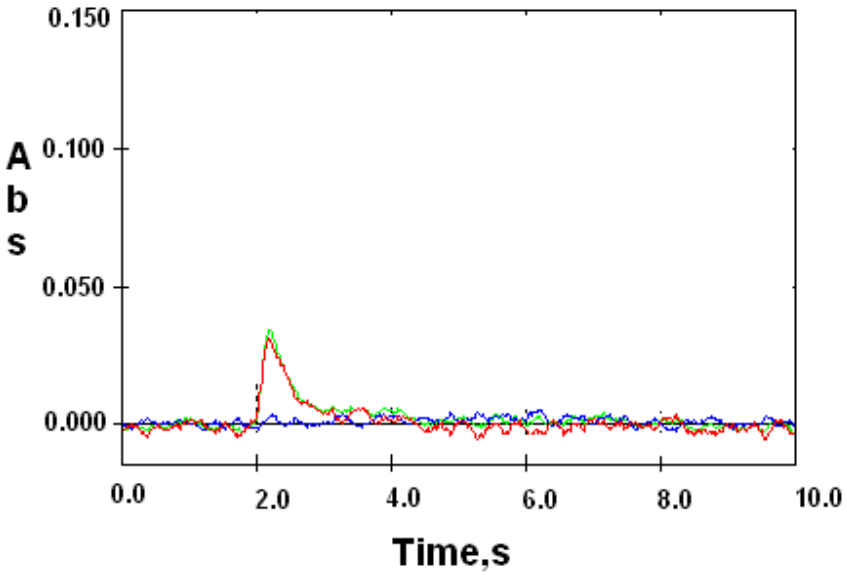


**Figure 3.55.** The signal of 5.0 ng $mL^{-1}$ indium using W-coil trap with HVGLS and VCG-AAS.

### 3.5.2.4 Calibration Plot for Indium by HVGLS with W-coil Trap and VCG-AAS

By using optimum analytical parameters shown in Table 2.5, a linear calibration plot using HVGLS with W-coil trap system was obtained between 1.0 and 10.0 ng $mL^{-1}$ as shown in Figure 3.56. The best line equation and correlation coefficient were, A= 0.0037C + 0.0044 and 9968, respectively where a is the absorbance and C is the concentration of In in ng $mL^{-1}$. LOD and $C_0$ values of this system were shown in Table 3.13. When compared the $C_0$ values, 324 fold sensitivity enhancements was obtained with respect to cylindrical GLS without W-coil trap.

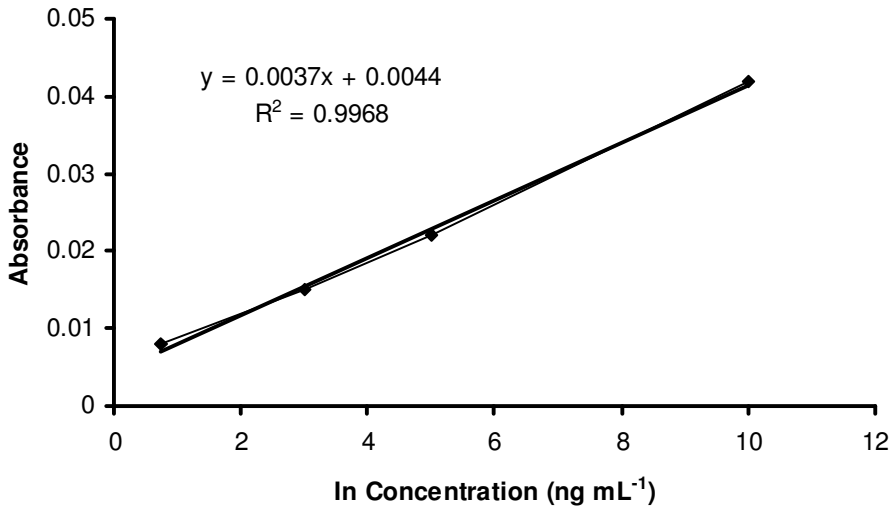


**Figure 3.56.** Calibration plot of indium using HVGLS with W-coil trap.

### 3.5.3 Determination of Indium by HVGLS with W-coil Trap and VCG-AAS with Ruthenium (III) Acetylacetonate [$Ru(acac)_3$] Catalyst

In this part of experiment, to reach the lower LOD values and increase the sensitivity of system, 0.5 g $Ru(acac)_3$ catalyst was placed inside the reaction coil and mixed indium and reductant solutions passed through this catalyst. The aim of this study is to increase the reactivity between indium and reductant solutions and to form indium volatile species more efficiently. To insert the catalyst inside the reaction coil, the catalyst was placed inside plastic gauze produced using a nylon stocking which was then placed inside a 5 cm glass tubing. Both ends of this glass tubing was connected to reaction coil by tygon tubings. The signal from 5.0 ng $mL^{-1}$ indium standard solution obtained using this set-up is shown in Figure 3.57.

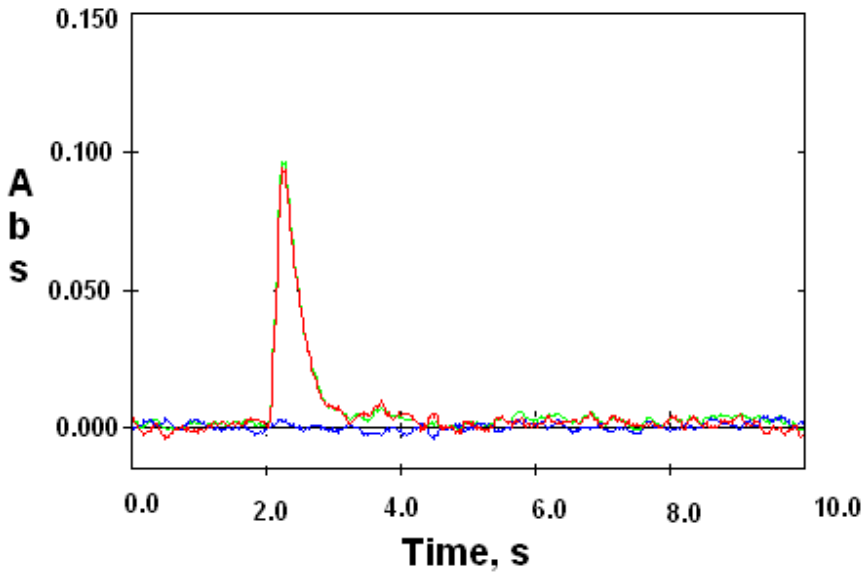


**Figure 3.57.** The signal of 5.0 ng $mL^{-1}$ indium by W-coil trap with HVGLS in the case of using $Ru(acac)_3$ catalyst.

### 3.5.3.1 Calibration Plot of Indium by HVGLS with W-coil Trap and VCG-AAS using Ruthenium (III) Acetylacetonate [$Ru(acac)_3$] Catalyst

A linear calibration plot using HVGLS with W-coil trap system in the case of using $Ru(acac)_3$ catalyst was obtained between 0.75 and 10.0 ng $mL^{-1}$ as shown in Figure 3.58. The best line equation and correlation coefficient were, A= 0.0191C - 0.0014 and 9990, respectively, A is the unitless absorbance and C is the concentration of In in ng $mL^{-1}$. LOD and $C_0$ values of this system were found to be in turn 0.13 ng $mL^{-1}$ and 0.23 ng $mL^{-1}$ shown in Table 3.13**.** When compared the $C_0$ value of this technique with other techniques, 4.3 and 1378 fold sensitivity enhancements were obtained with respect to W-coil trap with HVGLS and cylindrical GLS without W-coil trap, respectively.

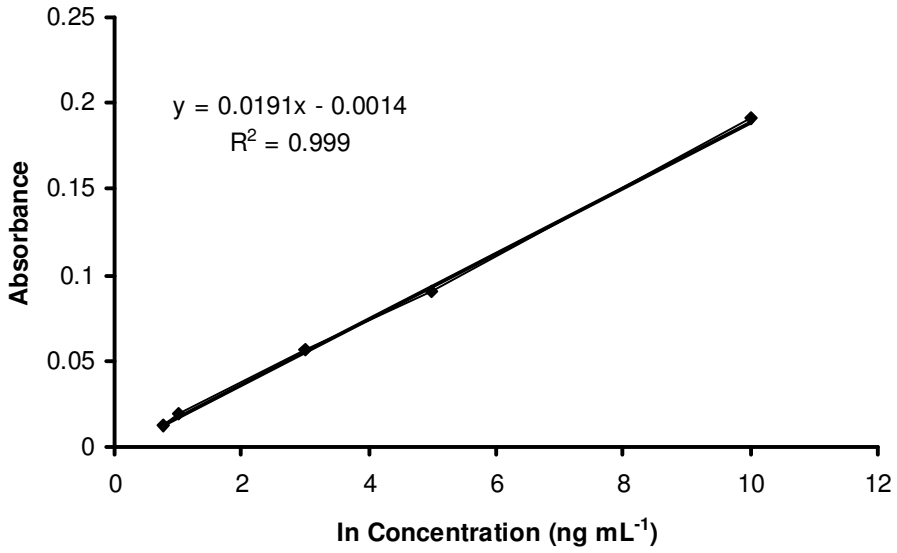


**Figure 3.58.** Calibration plot for indium by HVGLS with W-coil trap in the case of using $Ru(acac)_3$.

### 3.5.3.2 Evaluation of System Performance

In this part of experiment, $E_t$ (enhancement factor in term of unit time) and $E_v$ (enhancement factor in term of unit volume) values were calculated for indium determination shown in Table 3.14.

**Table 3.14.** Comparison of HVGLS with W-coil trap in the case of using $Ru(acac)_3$ system in terms of $E_t$ and $E_v$ values with C GLS and HVGLS with W-coil trap GLS for indium

| Sensitivity Enhancement | **w.r.to C GLS** | | **w.r.to HVGLS with W-coil** | |
|---|---|---|---|---|
| | $E_t$ | $E_v$ | $E_t$ | $E_v$ |
| Normalized to time or volume | 1378 | 91.9 | 4.3 | 0.29 |

C GLS= cylindrical gas liquid separator; w.r.to= with respect to; E= Sensitivity enhancement; collection time= 60 s, volume of indium= 15.0 mL

### 3.5.4. Conclusion

When the Ar gas was used with cylindrical GLS systems without W-coil trap study, indium signal was not obtained. However, when the Ar gas flow and the stripping coil were removed from the system, indium signal could be obtained. This is more probably due to the dilution of volatile indium species by carrier gas. It has beeen observed that when the cylindrical GLS was used, sensitivity of system was not very good. Because of this reason, to improve the sensitivity for indium detection, HVGLS was connected to the W-coil trap system. In this case, sensitivity of indium was improved around 324 times as compared to cylindrical GLS. Furthermore, Ruthenium (III) Acetylacetonate [$Ru(acac)_3$] catalyst was used to increase the reactivity between indium and $NaBH_4$ reductant solutions. For this reason, this catalyst was placed inside the reaction coil and mixed indium and reductant solutions were sent onto this catalyst. The function of this plastic gauze is to allow the mixed solutions passed through the catalyzer surface. When catalyst was used, the sensitivity of indium was increased 4.3 times with respect to W-coil trap with HVGLS.

# CHAPTER 4

# CONCLUSION

This thesis consists of determination selenium (Se), gold (Au), silver (Ag) and indium (In) by volatile compound generation atomic absorption spectrometry (VCG-AAS) technique.

*Selenium (Se):* A novel analytical technique for the determination of Se has been developed by using trapping on a resistively heated W coil coated with gold. "When bare W-coil was used, Se signal could not be taken; gold coating provides convenient trapping and releasing. The re-volatilized species are either molecular or short-lived atomic in nature, since no signal was observed when the QTA was not heated by flame." The limit of detection achieved was comparable with other recently reported sensitive techniques for selenium determination. The technique is very simple, robust and economical. It can be applied in laboratories equipped with only a flame AA spectrometer which provides a sensitivity at the level of ng $L^{-1}$. The sensitivity obtained is sufficient to handle many difficult analytical tasks in the fields of health, environment and food.

*Gold(Au):* There have been some studies for determination of Au using VCG-AAS; however, in these studies, classical gas liquid separators which have low efficiency for Au determination were used. In this study, a HVGLS was designed to improve the detection limit of gold down to the ng $mL^{-1}$ levels. In this apparatus, analyte and

reductant solutions are collected in a limited volume and volatile species of the analyte are formed. After the separation of the volatile species from liquid phase, the entire analyte vapor is sent to a heated QTA. In addition, the optimization of the VCG for Au using the multiatomizer/AAS atomization/detection combination resulted in an analytical procedure yielding satisfactory figures of merit, notably a very good long range (several months) of reproducibility of the analytical signal. The concentration LOD is one order of magnitude higher compared to that for the conventional liquid sampling GF but the advantage of the VCG approach for practical analysis is its very simple and low cost equipment and its potential to avoid matrix interferences inherent to conventional liquid sampling GF technique. However, the main benefit of the presented results is the assessment of the influence of individual conditions of generation and atomization on the observed AAS signal. "This knowledge, together with the detailed insight into the transfer of analyte in the course of generation and transport to the atomizer produced with the help of radiotracers (including the direct determination of the release and transport efficiencies), can be used for predictive purposes and applied for improved performance. The major significance should be attributed to the understanding of the influence of the carrier gas flow rate on the generation efficiency and of the nature of the peak broadening. This can serve as a basis to an ample improvement of the performance of the analytical procedure based on VCG of Au. However, such a procedure cannot employ the on-line atomization of the generated Au compound for AAS because of the two reasons: (i) a slow kinetics of the generation resulting in inconveniently broad signals, and (ii) a high flow rate of the carrier gas required for the efficient generation resulting in an unacceptable dilution of the analyte and, consequently, in an unacceptable increase of the peak area characteristic mass which deteriorates the observed sensitivity. Both the factors, (i) and (ii), inevitably impair the observed LOD. An evident way to eliminate the adverse influence of the slow kinetics is to employ some of the in-atomizer trapping approaches. However, the most popular approach, in-situ trapping in GF as it is typically performed is completely unsuitable

in this case since the trapping efficiency is poor at the high flow rate of the carrier gas required for the efficient generation. It is a subject of further investigations whether an alternative in-atomizer collection method can yield good performance even under the high gas flow rates required. Regarding the characterization of the nature of the generated VC of Au, TEM/EDS experiments brought a decisive proof that the VC of Au generated by the reaction with THB contains nanoparticles. The presence of a different form of the volatilized analyte besides nanoparticles (e.g. Au hydride) cannot be ruled out on the basis of these experiments.

*Silver (Ag):* This study reveals that when the Ar gas was used with both U-shaped and cylindrical GLS systems without a W-coil trap, meaningful Ag signal was not obtained. However, when the carrier Ar gas flow was removed from the system, Ag signal was obtained. It is believed that the carrier gas causes dilution of volatile Ag species. It was observed that the sensitivity for cylindrical GLS is 5-fold higher than U-shaped GLS by comparing $C_0$ values. Moreover, W-coil trap was employed with cylindrical GLS system. For this reason, to eliminate the oxidation of W-coil trap, a three way tap was placed after the GLS to introduce $H_2$ gas. In this case, the sensitivity of Ag is 6.3-fold higher than cylindrical shape GLS without W-coil trap by comparing the $C_0$ values. Furthermore, a HVGLS was designed to improve the detection limit of Ag down to the sub ng $mL^{-1}$ levels. In this apparatus, volatile Ag species are collected in a limited volume and after separation the volatile Ag species from liquid phase, the entire analyte vapor is sent to a QTA that was heated externally by an air/acetylene flame. "The sensitivity of the HVGLS with W-coil trap is 9.6-fold higher than cylindrical shape GLS with W-coil trap by comparing the $C_0$ values."

*Indium (In):* When the Ar gas was used with cylindrical GLS systems without W-coil trap study, indium signal was not obtained. However, when the Ar gas flow and the stripping coil were removed from the system, indium signal was obtained. This is probably due to dilution of volatile indium species with carrier gas. It has beeen

observed that when the cylindrical GLS was used, sensitivity of system was not so good. Because of this reason, to improve the sensitivity for indium, HVGLS was connected to the W-coil trap system. In this case, sensitivity of indium was improved around 324 times compared to cylindrical GLS. Furthermore, Ruthenium (III) Acetylacetonate [$Ru(acac)_3$] catalyst was used to further increase the reactivity between indium and $NaBH_4$ reductant solutions. For this reason, this catalyst was placed inside the reaction coil and mixed indium and reductant solutions were sent through this catalyst. After catalyst was used, the sensitivity of indium was increased 4.3 times with respect to W-coil trap with HVGLS without catalyst.

As a conclusion, several novel and sensitive techniques have been proposed for determination of Se, Au, Ag and In by VCG-AAS. However, particularly for analytes of Au, Ag and In VCG-AAS applications need improvement. It was also shown that the analyte gaseous stream for Au contains nanoparticles of this metal. Furthermore, future research should be carried out in order to elucidate the signal formation procedures with HVGLS.

## REFERENCES


[1]. Welz, B., and Sperling, M. (1984) *Atomic Absorption Spectrometry*. Wiley-VCH, Weinheim.

[2]. Crouch, S.R., and Ingle, J.D.J. (1988) *Spectrochemical Analysis*. Prentice-Hall Inc., Englewood Cliffs, New Jersey.

[3]. L'Vov, B.V. (2005) Fifty years of atomic absorption spectrometry. *Journal of Analytical Chemistry*,60: 382–382.

[4]. Walsh, A. (1955) The application of atomic absorption spectra to chemical analysis. *SpectrochimicaActa*, 7: 108–117.

[5]. Alkemade, C.T.J., Hollander, T., Snelleman, W., and Zeegers, P.J.T. (1982) *Metal Vapours in Flames*. Pergamon Press, Oxford.

[6]. L'Vov, B.V. (1997) Forty years of electrothermal atomic absorption spectrometry. Advancesand problems in theory. *Spectrochimica Acta Part B: Atomic Spectroscopy*, 52: 1239–1245.

[7]. Axner, O., and Meyers, R.A. (2000) *Encyclopedia of Analytical Chemistry*. JohnWiley & Sons,Inc, New York, 9506-9595.

[8]. A. Zybin, J. Koch, H.D. Wizemann, J. Franzke, K. Niemax, Diode laser atomic absorption spectrometry, Spectrochim. Acta Part B 60 (2005) 1-11.

[9]. Fuwa, K., and Vallee, B.L. (1963) Physical basis of analytical atomic absorption spectrometry—pertinence of beer-lambert law. *Analytical Chemistry*, 35: 942–946.

[10]. Delves, H.T. (1970) A micro-sampling method for rapid determination of lead in blood by atomic-absorption spectrophotometry. *Analyst*, 95: 431–438.

[11]. Lajunen, L.H.J., and Peramaki, P. (2004) *Spectrochemical Analysis by Atomic Absorption and Emission*. University of Oulu, Wakefield, Finland.

[12]. Tsujii, K., and Kuga, K. (1974) Determination of arsenic by non-dispersive atomic fluorescence spectrometry with a gas sampling technique. *Analytica Chimica Acta*, 72: 85–90.

[13]. Thompson, K.C. (1975) Atomic-fluorescence determination of antimony, arsenic, selenium and tellurium by using hydride generation technique. *Analyst*, 100: 307–310.

[14]. Corns, W.T., Stockwell, P.B., Ebdon, L., and Hill, S.J. (1993) Development of an atomic fluorescence spectrometer for the hydride-forming elements. *Journal of Analytical Atomic Spectrometry*, 8: 71–77.

[15]. Frank, J., Krachler, M., and Shotyk, W. (2006) Determination of arsenic in peat samples using HG-AFS and L-cysteine as pre-reductant. *Journal of Analytical Atomic Spectrometry*, 21: 204–207.

[16]. Chen, B., Krachler, M., Gonzalez, Z.I., and Shotyk, W. (2005) Improved determination of arsenic in environmental and geological specimens using HG-AFS. *Journal of Analytical Atomic Spectrometry*, 20: 95–102.

[17]. Cava-Montesinos, P., Cervera, P.L., Pastor, A., and de la Guardia, M. (2004) Determination of As, Sb, Se, Te and Bi in milk by slurry sampling hydride generation atomic fluorescence spectrometry. *Talanta*, 62: 175–184.

[18]. Mendez, H., Lavilla, I., and Bendicho, C. (2004) Mild sample pretreatment procedures based on photolysis and sonolysis-promoted redox reactions as a new approach for determination of Se(IV), Se(VI) and Se(-II) in model solutions by the hydride generation technique with atomic absorption and fluorescence detection. *Journal of Analytical Atomic Spectrometry*, 19: 1379–1385.

[19]. Cava-Montesinos, P., de la Guardia, A., Teutsch, C., Cervera, M.L., and de la Guardia, M. (2003) Non-chromatographic speciation analysis of arsenic and antimony in milk hydride generation atomic fluorescence spectrometry. *Analytica Chimica Acta*, 493: 195–203.

[20]. Cava-Montesinos, P., Cervera, M.L., Pastor, A., and de la Guardia, M. (2003) Determination of arsenic and antimony in milk by hydride generation atomic fluorescence spectrometry. *Talanta*, 60: 787–799.

[21]. El-Hadri, F., Morales-Rubio, A., and de la Guardia, M. (2000) Atomic fluorescence spectrometric determination of trace amounts of arsenic and antimony in drinking water by continuous hydride generation. *Talanta*, 52: 653–662.

[22]. D'Ulivo, A. (1989) In Harrison, R.M. and Rapsomanikis, S. (eds.), *Environmental Analysis using Chromatography Interfaced with Atomic Spectroscopy*. Ellis Horwood, Chichester.

[23]. D'Ulivo, A. (1997) Determination of selenium and tellurium in environmental samples. *Analyst*, 122, 117R–144R.

[24]. Stockwell, P.B., and Corns, W.T. (1994) Environmental sensors based on atomic fluorescence. *Analyst*, 119: 1641–1645.

[25]. Stockwell, P.B., and Corns, W.T. (1992) *Spectroscopy World*, 4: 14–18.

[26]. Burguera, J.L., and Burguera, M. (2002) On-line flow injection-atomic spectroscopic configurations: road to practical environmental analysis, *Quimica Analitica* 20: 255–273.

[27]. Nolte, J. (1994) ICP-OES analysis of wastewaters and sludges. *Atomic Spectroscopy*, 15: 223–228.

[28]. dos Santos, E.J., Herrmann, A.B., Frescura, V.L.A., Welz, B., and Curtius, A.J. (2007) Determination of lead in sediments and sewage sludge by on-line hydride-generation axial-view inductively-coupled plasma optical-emission spectrometry using slurry sampling. *Analytical and Bioanalytical Chemistry*, 388: 863–868.

[29]. Marrero, J., Arisnabarreta, S.P., and Smichowski, P. (2003) Comparison of effects of four acid oxidant mixtures in the determination of lead in foods and beverages by hydride generation- ICP-OES. *Atomic Spectroscopy*, 24: 133–142.

[30]. Elfering, H., Andersson, J.T., and Poll, K.G. (1998) Determination of organic lead in soils and waters by hydride generation inductively coupled plasma atomic emission spectrometry. *Analyst*, 123: 669–674

[31]. Brindle, I.D.,McLaughlin,R., and Tangtreamjitmun, N. (1998) Determination of lead in calcium carbonate by flow-injection hydride generation with dc plasma atomic emission detection. *Spectrochimica Acta Part B-Atomic Spectroscopy*, 53: 1121–1129.

[32]. Stripeikis, J., Tudino, M., Troccoli, O., Wuilloud, R., Olsina, R., and Martinez, L. (2001) Online copper and iron removal and selenium(VI) pre-reduction for the determination of total selenium by flow-injection hydride generation-inductively coupled plasma optical emission spectrometry. *Spectrochimica Acta Part B-Atomic Spectroscopy*, 56: 93–100.

[33]. Rubio, R., Padro, A., and Rauret, G. (1997) Photoreduction-hydride generation: a new on-line system for the determination of selenate and selenite. *Analytica Chimica Acta*, 353: 91–97.

[34]. Stec, K., Bobrowski, A., Kalcher, K., Moderegger, H., and Goessler, W. (2006) Determination of arsenic in dolomiteswith a simple field spectrometric device. *Microchimica Acta*, 153: 45–49.

[35]. Suarez, C.A., and Gine,M.F. (2005)Areactor/phase separator coupling capillary electrophoresis to hydride generation and inductively coupled plasma optical emission spectrometry (CE-HGICPOES) for arsenic speciation. *Journal of Analytical Atomic Spectrometry*, 20: 1395–1397.

[36]. Pena-Vazquez, E., Bermejo-Barrera, A., and Bermejo-Barrera, P. (2005) Use of lanthanum hydroxide as a trapping agent to determine of hydrides by HG-ICP-OES. *Journal of Analytical Atomic Spectrometry*, 20: 1344–1349.

[37]. Pena-Vazquez, E., Villanueva-Alonso, J., and Bermejo-Barrera, P. (2007) Optimization of a vapour generationmethod formetal determination using ICP-OES. *Journal of Analytical Atomic Spectrometry*, 22: 642–649

[38]. Thomas, R. (2003) *Practical Guide to ICP-MS (Practical Spectroscopy)* Marcel Dekker, New York.

[39]. Browner, R.F., and Boorn, A.W. (1984) Sample introduction—the achilles heel of atomic spectroscopy. *Analytical Chemistry*, 56: 786–798.

[40]. Linge, K.L., and Jarvis, K.E. (2007) *Geostandards and Geoanalytical Research*, 33: 445–467.

[41]. Mora, J., Maestre, S., Hernandis, V., and Todoli, J.L. (2003) Liquid-sample introduction in plasma spectrometry. *Trac-Trends in Analytical Chemistry*, 22: 123–132.

[42]. Bjorn, E., Jonsson, T., and Goitom, D. (2002) Noise characteristics and analytical precision of a direct injection high efficiency and micro concentric nebuliser for sample introduction in inductively coupled plasma mass spectrometry. *Journal of Analytical Atomic Spectrometry*, 17: 1257–1263.

[43]. Nam, S.H., Lim, J.S., and Montaser, A. (1994) High-efficiency nebulizer for argon inductivelycoupled plasma-mass spectrometry. *Journal of Analytical Atomic Spectrometry*, 9: 1357–1362.

[44]. Sharp, B.L. (1988) Pneumatic nebulizers and spray chambers for inductively coupled plasma spectrometry—a review.2. spray chambers. *Journal of Analytical Atomic Spectrometry*, 3: 939–963.

[45]. Linge, K.L., and Jarvin, K.E. (2010) *The essentials of ICP-MS*. Viridian Publishing, Berkshire, UK.

[46]. Hutton, R.C., and Eaton, A.N. (1987) Role of aerosolwater-vapor loading in inductively coupled plasma mass-spectrometry. *Journal of Analytical Atomic Spectrometry*, 2: 595–598.

[47]. Chang, Y.T., and Jiang, S.J. (2008) Determination of As, Cd and Hg in emulsified vegetable oil by flow injection chemical vapour generation inductively coupled plasma mass spectrometry. *Journal of Analytical Atomic Spectrometry*, 23: 140–144.

[48]. Chung, S.W.C., Kwong, K.P., Yau, J.C.W., and Wong, W.W.K. (2008) Dietary exposure to antimony, lead and mercury of secondary school students in Hong Kong. *Food Additives and Contaminants*, 25: 831–840.

[49]. Chandrasekaran, K., Ranjit, M., Karunasagar, D., and Arunachalam, J. (2008) Determination of selenium (IV) at ultratrace levels in natural water samples by UV-

assisted vapor generation—'Collect and punch'—inductively coupled plasma mass spectrometry. *Atomic Spectroscopy*, 29: 129–136.

[50]. Park, C.J., and Do, H. (2008) Determination of inorganic and total mercury in marine biological samples by cold vapor generation inductively coupled plasma mass spectrometry after tetramethylammonium hydroxide digestion. *Journal of Analytical Atomic Spectrometry*, 23: 997–1002.

[51]. Tsai,M.W., and Sun,Y.C. (2008) On-line coupling of an ultraviolet titanium dioxide film reactor with a liquid chromatography/hydride generation/inductively coupled plasma mass spectrometry system for continuous determination of dynamic variation of hydride- and nonhydrideforming arsenic species in very small microdialysate samples. *Rapid Communications in Mass Spectrometry*, 22: 211–216.

[52]. Palace, V.P., Halden, N.M., Yang, P., Evans, R.E., and Sterling, G. (2007) Determining residence patterns of rainbow trout using laser ablation inductively coupled plasma mass spectrometry (LA-ICP-MS) analysis of selenium in otoliths. *Environmental Science & Technology*, 41: 3679–3683.

[53]. Tseng, Y.J., Liu, C.C., and Jiang, S.J. (2007) Slurry sampling electrothermal vaporization inductively coupled plasma Mass spectrometry for the determination of As and Se in soil and sludge. *Analytica Chimica Acta*, 588: 173–178.

[54]. D. Vincent, N. Laurent, G. Thierry, Determination of chromium, iron and selenium in foodstuffs of animal origin by collision cell technology, inductively coupled plasma mass spectrometry (ICP-MS), after closed vessel microwave digestion. Anal. Chim. Acta 565 (2006) 214-221.

[55]. Gabel-Jensen, C., Gammelgaard, B., Bendahl, L., Sturup, S., and Jons, O. (2006) Separation and identification of selenotrisulfides in epithelial cell homogenates by LC-ICP-MS and LCESI- MS after incubation with selenite. *Analytical and Bioanalytical Chemistry*, 384: 697–702.

[56]. Kremer, D., Ilgen, G., and Feldmann, J. (2005) GC-ICP-MS determination of dimethylselenide in human breath after ingestion of Se-77-enriched selenite:

monitoring of in-vivo methylation of selenium. *Analytical and Bioanalytical Chemistry*, 383: 509–515.

[57]. Iserte, L.O., Roig-Navarro, A.F., and Hernandez, F. (2004) Simultaneous determination of arsenic and selenium species in phosphoric acid extracts of sediment samples by HPLC-ICPMS. *Analytica Chimica Acta*, 527: 97–104.

[58]. Paul, M.C., Toia, R.F., and von Nagy-Felsobuki, E.I. (2003) A novel method for the determination of mercury and selenium in shark tissue using high-resolution inductively coupled plasma-mass spectrometry. *Spectrochimica Acta Part B-Atomic Spectroscopy*, 58: 1687–1697.

[59]. Watling, R.J. (1977) Use of a slotted quartz tube for analysis of trace-metals in fresh-water. *Water S.A*, 3: 218–220.

[60]. Watling, R.J. (1977) Use of a slotted quartz tube for determination of arsenic, antimony, selenium and mercury. *Analytica Chimica Acta*, 94: 181–186.

[61]. Watling, R.J. (1978) Use of a slotted tube for determination of lead, zinc, cadmium, bismuth, cobalt, manganese and silver by atomic-absorption spectrometry. *Analytica Chimica Acta*, 97: 395–398.

[62]. Ataman, O.Y. (2008) Vapor generation and atom traps: Atomic absorption spectrometry at the ng/L level. *Spectrochimica Acta Part B: Atomic Spectroscopy*, 63: 825–834.

[63]. Burns, D.T., Chimpalee, N., and Harriott M. (1994) Applications of a slotted tube atom trap and flame atomic-absorption spectrometry-determination of tin in copper-based alloys after hydride generation. *Fresenius J. Anal. Chem,* 349: 530-532.

[64]. Burns, D.T., Chimpalee, N., and Harriott, M. (1995) Applications of a slotted tube atom trap and flame atomic absorption spectrometry: determination of bismuth in copper-based alloys with and without hydride generation. *Anal. Chim. Acta*, 311: 93-97.

[65]. Yaman, M. (1999) Determination of cadmium and lead in human urine by STAT-FAAS after enrichment on activated carbon. *Journal of Analytical Atomic Spectrometry*, 14: 275–278.

[66]. Lau, C., Held, A., and Stephens, R. (1976) Sensitivity enhancements to flame aas by use of a flame atom trap. *Canadian Journal of Spectroscopy*, 21: 100–104.

[67]. Lau, C.M., Ure, A.M., and West, T.S. (1983) The determination of lead and cadmium in soils by atom-trapping atomic-absorption spectrometry. *Analytica Chimica Acta*, 146: 171–179.

[68]. Khalighie, J., Ure, A.M., and West, T.S. (1981) Atom-trapping atomic-absorption spectrometry of arsenic, cadmium, lead, selenium and zinc in air-acetylene and air-propane flames. *Analytica Chimica Acta*, 131: 27–36.

[69]. Turner, A.D., and Roberts, D.J. (1996) Metal determinations with a novel slotted-tube watercooled atom trap. *Journal of Analytical Atomic Spectrometry*, 11: 231–234.

[70]. Matusiewicz, H., and Kopras,M. (1997) Methods for improving the sensitivity in atom trapping flame atomic absorption spectrometry: Analytical scheme for the direct determination of trace elements in beer. *Journal of Analytical Atomic Spectrometry*, 12: 1287–1291.

[71]. Sun, H.W., Yang, L.L., Zhang, D.Q., and Sun, J.M. (1997) Direct determination of cadmium at parts-per-billion level in waters by derivative atomic absorption spectrometry using atom trapping technique. *Talanta*, 44: 1979–1986.

[72]. Ertaş, N., Helles, R.S., Kumser, S. and Ataman, O.Y. (1993) Alternative Atomization Techniques in Atom Trapping Atomic Absorption Spectrometry. Federation of Analytical Chemistry and Spectroscopy Societies, FACSS XX, Annual Conference, October 17-22, , Detroit, Michigan, USA.

[73]. Huang, G., Qian, S., and Yang, H. (1995) Study of slotted quartz tube atom-trapping atomic absorption spectrometry. *Ziran Kexueban Hua Xue Fen*, 41: 707–712.

[74]. Ertas, N., Korkmaz, D.K., Kumser, S., and Ataman, O.Y. (2002) Novel traps and atomization techniques for flame AAS. *Journal of Analytical Atomic Spectrometry*, 17: 1415–1420.

[75]. Korkmaz, D., Kumser, S., Ertas, N., Mahmut, M., and Ataman, O.Y. (2002) Investigations on nature of re-volatilization from atom trap surfaces in flame AAS. *Journal of Analytical Atomic Spectrometry*, 17: 1610–1614.

[76]. Korkmaz, D., Mahmut, M., Helles, R., Ertas, N., and Ataman, O.Y. (2003) Interference studies in slotted silica tube trap technique. *Journal of Analytical Atomic Spectrometry*, 18: 99–104.

[77]. Ataman O. Y. (2007) Economical alternatives for high sensitivity in atomic spectrometry laboratory. *Pak. J. Anal. Environ. Chem.* 8: 64-68.

[78]. Ataman, O.Y. (2008) Vapor generation and atom traps: Atomic absorption spectrometry at the ng/L level. *Spectrochimica Acta Part B: Atomic Spectroscopy*, 63: 825–834.

[79]. Dědina, J., and Tsalev, D. (1995) *Hydride Generation Atomic Absorption Spectrometry*. John Wiley & Sons, New York.

[80]. Dědina, J. (1988) Evaluation of hydride generation and atomization for AAS, *Progress in Analytical Spectroscopy*, 11: 251–360.

[81]. Sturgeon, R.E., and Mester, Z. (2002) Analytical applications of volatile metal derivatives. *Applied Spectroscopy*, 56: 202A–213A.

[82]. Guo, X.M., Sturgeon, R.E.,Mester, Z., and Gardner, G.J. (2004) Vapor generation by UV irradiation for sample introduction with atomic spectrometry. *Analytical Chemistry*, 76: 2401–2405.

[83]. Pavageau, M.-P., Krupp, E., Diego, A.d., Pecheyran, C., Donard, O.F.X., Mester, Z., and Sturgeon, R.E. (2004) *Sample preparation for trace element analysis*. Elsevier, Amsterdam.

[84]. Feng, Y.L., Lam, J.W., and Sturgeon, R.E. (2004) A novel approach to the estimation of aqueous solubility of some noble metal vapor species generated by reaction with tetrahydroborate (III). *Spectrochimica Acta Part B-Atomic Spectroscopy*, 59: 667–675.

[85]. Vercauteren, J., Peres, C., Devos, C., Sandra, P., Vanhaecke, F., and Moens, L. (2001) Stir bar sorptive extraction for the determination of ppq-level traces of

organotin compounds in environmental samples with thermal desorption-capillary gas chromatography-ICP mass spectrometry. *Anal. Chem.,* 73: 1509-1514.

[86]. Jitaru, P., Infante, H.G., and Adams, F.C. (2004) Simultaneous multi-element speciation analysis of organometallic compounds by solid-phase microextraction and multicapillary gas chromatography hyphenated to inductively coupled plasma-time-of-flight-mass spectrometry. *J. Anal. At. Spectrom.,* 19: 867-875.

[87]. Colombini, V., Bancon-Montigny C., Yang, L., Maxwell, P., Sturgeon, R.E., and Mester, Z., (2004) Headspace single-drop microextraction for the detection of organotin compounds. *Talanta,* 63: 555-560.

[88]. Chamsaz, M., Arbab-Zavar, M.H., and Nazraj, S. (2003) Determination of arsenic by electrothermal atomic absorption spectrometry using headspace liquid phase microextraction after in situ hydride generation. *J. Anal. At. Spectrom*., 18: 1279-1282.

[89]. D'Ulivo, A. (2004) Chemical vapor generation by tetrahydroborate(III) and other borane complexes in aqueous media: A critical discussion of fundamental processes and mechanisms involved in reagent decomposition and hydride formation. *Spectrochim. Acta Part B,* 59: 793-825.

[90]. Feng, Y.L., Sturgeon, R.E., and Lam, J.W. (2003) Chemical vapor generation characteristics of transition and noble metals reacting with tetrahydroborate (III). *J. Anal. At. Spectrom.,* 18: 1435-1442.

[91]. Pohl, P. (2004) Hydride Generation - Recent Advances in Atomic Emission Spectrometry. *Trends Anal. Chem.* 23: 87-101.

[92]. Wang, Q.Q., Liang, J.,Qiu, J.H., andHuang, B.L. (2004) Online pre-reduction of selenium((VI)) with a newly designed UV/TiO2 photocatalysis reduction device. *Journal of Analytical Atomic Spectrometry*, 19: 715–716.

[93]. Panichev, N., and Sturgeon, R.E. (1998) Atomic absorption by free atoms in solution following chemical reduction from the ionic state. Anal. Chem., 70: 670-1676.

[94]. Moor, C., Lam, J.W.H., and Sturgeon, R.E. (2000) A Novel Sample Introduction System for Selenium in Biological Samples. ,*J. Anal. At. Spectrom*., 15: 143-149.

[95]. Glavee, G.N., Klabunde, K.J., Sorensen, C.M., and Hadjipanayis, G.C. (1993) Sodium-borohydride reduction of cobalt ions in nonaqueous media-formation of ultrafine particles (nanoscale) of cobalt metal. Inorg. Chem., 32: 474-477.

[96]. Glavee, G.N., Klabunde, K.J., Sorensen, C.M., and Hadjipanayis G.C. (1995) Chemistry of Borohydride Reduction of Iron(II) and Iron(III) Ions in Aqueous and Nonaqueous Media. Formation of Nanoscale Fe, FeB, and Fe2B Powders. Inorg. Chem., 34: 28-35.

[97]. Feng, Y.L., Lam, J.W., and Sturgeon, R.E. (2001) Expanding the scope of chemical vapor generation for noble and transition metals. *Analyst*, 126: 1833–1837.

[98]. Luna, A.S., Sturgeon, R.E., and de Campos, R.C. (2000) Chemical vapor generation: Atomic absorption by Ag, Au, Cu, and Zn following reduction of aquo ions with sodium tetrahydroborate(III). *Analytical Chemistry*, 72: 3523–3531.

[99]. Matoušek, T., and Sturgeon, R.E. (2003) Surfactant Assisted Chemical Vapour Generation of Silver for AAS and ICP-OES: a Mechanistic Study. *J. Anal. At. Spectrom.*, 18: 487-494.

[100]. Chu, R.C., Baumgarn, Pa, and Barron, G.P. (1972) Arsenic determination at sub-microgram levels by arsine evolution and flameless atomic-absorption spectrophotometric technique. *Analytical Chemistry*, 44: 1476–1479

[101]. Thompson, K.C., and Thomerso, Dr (1974) Atomic-absorption studies on determination of antimony, arsenic, bismuth, germanium, lead, selenium, tellurium and tin by utilizing generation of covalent hydrides. *Analyst*, 99: 595–601.

[102]. D'Ulivo, A., and Dědina, J. (2002) The relation of double peaks, observed in quartz hydride atomizers, to the fate of free analyte atoms in the determination of arsenic and selenium by atomic absorption spectrometry. *Spectrochimica Acta Part B-Atomic Spectroscopy*, 57: 2069–2079.

[103]. Karadjova, I.B., Lampugnani, L., Dědina, J., D'Ulivo, A., Onor, M., and Tsalev, D.L. (2006) Organic solvents as interferents in arsenic determination by hydride generation atomic absorption spectrometry with flame atomization. *Spectrochimica Acta Part B-Atomic Spectroscopy*, 61: 525–531.

[104]. D'Ulivo, A., Dědina, J., Lampugnani, L., and Selecka, A. (2005) Mechanism of atomization interference by oxygen at trace level in miniature flame hydride atomizers. *Spectrochimica Acta Part B-Atomic Spectroscopy*, 60: 1270–1279.

[105]. Dědina, J., D'Ulivo, A., Lampugnani, L., Matoušek, T., and Zamboni, R. (1998) Selenium hydride atomization, fate of free atoms and spectroscopic temperature in miniature diffusion flame atomizer studied by atomic absorption spectrometry. *Spectrochimica Acta Part B-Atomic Spectroscopy*, 53: 1777–1790.

[106]. Dědina, J. (2007) Atomization of volatile compounds for atomic absorption and atomic fluorescence spectrometry: On the way towards the ideal atomizer. *Spectrochimica Acta Part B-Atomic Spectroscopy*, 62: 846–872.

[107]. Matoušek, T., Dědina, J., and Selecká, A. (2002) Multiple microflame quartz tube atomizer-further development towards the ideal hydride atomizer for atomic absorption spectrometry. *Spectrochim. Acta Part B,* 57: 451-462.

[108]. Figueiredo, E.C., Dědina, J., and Arruda, M.A.Z. (2007) Metal furnace heated by flame as a hydride atomizer for atomic absorption spectrometry: Sb determination in environmental and pharmaceutical samples. *Talanta*, 73: 621–628.

[109]. Gaspar, A., and Berndt, H. (2000) Thermospray flame furnace atomic absorption spectrometry (TS-FF-AAS)—a simple method for trace element determination with microsamples in the mu g/1 concentration range. *Spectrochimica Acta Part B-Atomic Spectroscopy*, 55: 587–597.

[110]. Drasch, G., Meyer, L.V., and Kauert, G. (1980) Application of the furnace atomic-absorption method for the detection of arsenic in biological samples by means of the hydride technique. *Fresenius Zeitschrift Fur Analytische Chemie*, 304: 141–142.

[111]. Freschi, C.D., Freschi, G.P.G., Neto, J.A.G., Nobrega, J.A., and Oliveira, P.V. (2005) Arsenic as internal standard to correct for interferences in the determination of antimony by hydride generation in situ trapping graphite furnace atomic absorption spectrometry. *Spectrochimica Acta Part B-Atomic Spectroscopy*, 60: 759–763.

[112]. Haug, H.O. (1996) Study on stable coatings for determination of lead by flow-injection hydride generation and in situ concentration in graphite furnace atomic absorption spectrometry. *Spectrochimica Acta Part B-Atomic Spectroscopy*, 51: 1425–1433.

[113]. Haug, H.O., and Liao, Y.P. (1995) Automated determination of tin by hydride generation using in situ trapping on stable coatings in graphite furnace atomic absorption spectrometry. *Spectrochimica Acta Part B-Atomic Spectroscopy*, 50: 1311–1324.

[114]. Yang, L.L., and Zhang, D.Q. (2003) In situ preconcentration and determination of trace arsenic in botanical samples by hydride generation-graphite furnace atomic absorption spectrometry with Pd-Zr as chemical modifier. *Analytica Chimica Acta*, 491: 91–97.

[115]. An, Y.,Willie, S.N., and Sturgeon, R.E. (1992) Flow-injection hydride generation determination of arsenic with insitu concentration in a graphite-furnace. *Spectrochimica Acta Part B-Atomic Spectroscopy*, 4: 1403–1410.

[116]. Lee, D.S. (1982) Determination of bismuth in environmental-samples by flameless atomicabsorption spectrometry with hydride generation. *Analytical Chemistry*, 54: 1682–1686.

[117]. Krivan, V., and Petrick, K. (1990) Hydride generation aas performed at 1800–2300-degrees-c atomization temperature using a graphite-furnace. *Fresenius Journal of Analytical Chemistry*, 336: 480–483.

[118]. Menemenlioglu, I., Korkmaz, D., and Ataman, O.Y. (2007) Determination of antimony by using a quartz atom trap and electrochemical hydride generation atomic absorption spectrometry. *Spectrochimica Acta Part B-Atomic Spectroscopy*, 62: 40–47.

[119]. Kratzer, J., and Dědina, J. (2005) In situ trapping of stibine in externally heated quartz tube atomizers for atomic absorption spectrometry. *Spectrochimica Acta Part B-Atomic Spectroscopy*, 60: 859–864.

[120]. Kratzer, J., and Dědina, J. (2008) Stibine and bismuthine trapping in quartz tube atomizers for atomic absorption spectrometry—Method optimization and analytical applications. *Spectrochimica Acta Part B-Atomic Spectroscopy*, 63: 843–849.

[121]. Cankur, O., Ertas, N., and Ataman, O.Y. (2002) Determination of bismuth using on-line preconcentration by trapping on resistively heated W coil and hydride generation atomic absorption spectrometry. *Journal of Analytical Atomic Spectrometry*, 17: 603–609.

[122]. Barbosa, F., de Souza, S.S., and Krug, F.J. (2002) In situ trapping of selenium hydride in rhodium-coated tungsten coil electrothermal atomic absorption spectrometry. *Journal of Analytical Atomic Spectrometry*, 17: 382–388.

[123]. M. Williams, E.H. Piepmeier, Commercial tungsten filament atomizer for analytical atomic spectrometry. *Anal. Chem.* 44 (1972) 1342-1344.

[124]. H. Berndt, G. Schaldach, Simple Low-cost Tungsten-coil Atomiser for Atomic Absorption Spectrometry. *J. Anal. At. Spectrom.* 3 (1988) 709-712.

[125]. Parsons, P.J., Qiao, H.C., Aldous, K.M., Mills, E., and Slavin, W. (1995) A low-cost tungsten filament atomizer for measuring lead in blood by atomic absorption spectrometry. *Spectrochim. Acta Part B,* 50: 1475-1480.

[126]. Dočekal, B., and Marek P. (2001) Investigation of *in situ* trapping of selenium and arsenic hydrides within a tungsten tube atomizer. *J. Anal. At. Spectrom.* 16: 831-837.

[127]. Dočekal, B., Güçer, Ş., and Selecká, A. (2004) Investigation of collection of arsenic and selenium hydrides on molibdenumfoil strip. *Spectrochim. Acta Part B*, 59: 487-495.

[128]. Krejči, P., Dočekal, B., and Hrušovská, Z. (2006) Trapping of hydride forming elements within miniature electrothermal devices. Part 3. Investigation of collection

of antimony and bismuth on a molybdenum-foil strip following hydride generation. *Spectrochim. Acta Part B* 61: 444-449.

[129]. Osama İsmail, M.S., "Determination of Cadmium by Cold Vapour Generation Atom Trapping Atomic Absorption Spectrometry", Middle East Technical University, Ankara, June 2000.

[130]. Korkmaz, D., Demir, C., Aydın, F., and Ataman, O.Y. (2005) Cold Vapour Generation and on-line Trapping of Cadmium Species on Quartz Surface Prior to Detection by Atomic Absorption Spectrometry. *J. Anal. At. Spectrom.* 20: 46-52.

[131]. Berzelius, J. J. (1818) *Annales de chimie et de physique* 7: 199-206.

[132]. Public Health Statement: Selenium" (PDF). Agency for Toxic Substances and Disease Registry. http://www.atsdr.cdc.gov/toxprofiles/tp92-c1.pdf, last accesed in 2009-01-05.

[133]. Tsalev, D. L. (1999) Hyphenated vapour generation atomic absorption spectrometric techniques. *J. Anal. At. Spectrom.* 14: 147–162

[134]. Tyson, J. F. Sundin, N.G., Hana, C.P., and McIntosh, S.A. (1997) Determination of selenium in urine by flow-injection hydride generation electrothermal atomic-absorption spectrometry with in-atomizer trapping. *Spectrochim. Acta Part B,* 52: 1773–1781.

[135]. Ertaş, G., and Ataman, O.Y. (2004) Electrothermal atomic absorption spectrometric determination of gold by vapour formation and in situ trapping in graphite furnace. *Appl. Spectrosc.* 58: 1243–1250.

[136]. Ajtony, Z., Szoboszlai, N., Bela, Z., Bolla, S., Szakál, P., and Bencs, L. (2005) Determination of total selenium content of cereals and bakery products by flow injection hydride generation graphite furnace atomic absorption spectrometry applying in-situ trapping on iridium-treated graphite platforms. *Mikrochim. Acta,* 150: 1–8.

[137]. Matusiewicz, H., and Kopras, M. (2003) *J. Anal. At. Spectrom.* 18: 1415–1425.

[138]. Williams, M., and Piepmeier, E.H. (1972) Commercial tungsten filament atomizer for analytical atomic spectrometry. *Anal. Chem.* 44: 1342–1344.

[139]. H. Berndt, G. Schaldach, Simple low-cost tungsten-coil atomizer for electrothermal atomic absorption spectrometry. J. Anal. At. Spectrom. 3 (1988) 709–712.

[140]. Parsons, P.J., Qiao, H.C., Aldous, K.M., Mills, E., and Slavin, W. (1995) A Low-cost Tungsten-filament atomic absorption spectrometry. *Spectrochim. Acta Part B,* 50: 1475–1480.

[141]. Hou, X., Yang, Z., and Jones, B.T. (2001) Determination of selenium by tungsten coil atomic absorption spectrometry using indium as a permanent chemical modifier. *Spectrochim. Acta Part B,* 56: 203–214.

[142]. Guo, X.-M., and Guo X.-W. (2001) Determination of ultra-trace amounts of selenium by continuous flow hydride generation AFS and AAS with collection on gold wire. *J. Anal. At. Spectrom.* 16: 1414–1418.

[143]. Kratzer, J., and Dědina, J. (2007) Arsine and selenium hydride trapping in a novel quartz device for atomic-absorption spectrometry. *Anal. Bioanal. Chem.* 388: 793–800.

[144]. Dočekal, (2004) B. Trapping of hydride forming elements within miniature electrothermal devices. Part 2. Investigation of collection of arsenic and selenium hydrides on a surface and in a cavity of a graphite rod. *Spectrochim. Acta Part B* 59: 497–503.

[145]. Matusiewicz, H., Krawczyk, M. (2006) On-line hyphenation of hydride generation with in situ trapping flame atomic absorption spectrometry for arsenic and selenium determination. *Anal. Sci.* 22: 249–253.

[146]. Mallan, L. (1971) “Suiting up for space: the evolution of the space suit” John Day Co., 216,.

[147]. Schmidbaur, H., Cronje, S., Djordjevic, B., and Schuster, O. (2005) Understanding gold chemistry through relativity . *Chem. Phys.* 311: 151–161.

[148]. Audi, G. (2003) The NUBASE evaluation of nuclear and decay properties. *Nuclear Phys. A* 729: 3–128.

[149]. Messori, L., and Marcon, G. (2004) "Gold Complexes in the treatment of Rheumatoid Arthritis". in Sigel, Astrid. Metal ions and their complexes in medication. CRC Press., 280.

[150]. The Demand for Gold by Industry". Gold bulletin. http://www.goldbulletin.org/assets/file/goldbulletin/downloads/Cooke_2_15.pdf, last accesed in 2009-06-06.

[151]. Shaw, C. F. (1999) Gold-based therapeutic agents. *Chemical Reviews*, 99: 2589–2600.

[152]. Shamsipur, M., and Ramezani, M. (2008) Selective determination of ultra trace amounts of gold by graphite furnace atomic absorption spectrometry after dispersive liquid-liquid microextraction. *Talanta,* 75: 294-.299.

[153]. Du, X. G., and Xu, S. K. (2001) Flow-injection chemical vapor-generating procedure for the determination of Au by atomic absorption spectrometry. *Fresenius' J. Anal. Chem.* 370: 1065–1070.

[154]. Xu S., and Sturgeon, R. E. (2005) Flow injection chemical vapor generation of Au using a mixed reductant. *Spectrochim. Acta, Part B,* 60: 101-107.

[155]. Ma, H.B., Fan, X.F., Zhou, H.Y., and Xu, S.K. (2003) Preliminary studies on flow-injection in situ trapping of volatile species of gold in graphite furnace and atomic absorption spectrometric determination. *Spectrochim. Acta Part B,* 58: 33-39.

[156]. Nichols, D. K. (1987) The Road to Trinity. Morrow' New York: Morrow. 42.

[157]. Oman, H. (1992) Aerospace and Electronic Systems. *Magazine,* 7: 51–53.

[158]. Edwards, H. W., and Petersen, R. P. (1936) *Phys. Rev.* 9: 871-888.

[159]. Wilson, Ray N. (2004) 'Reflecting Telescope Optics: Basic design theory and its historical development' Springer, 422.

[160]. Chopra, I. (2007) *The J. of antimicrobial chemotherapy,* 59: 587–90.

[161]. Pohl, P., and Zyrnicki, W. (2001) Study of chemical vapour generation of Au, Pd and Pt by inductively coupled plasma atomic emission spectrometry. *J. Anal. At. Spectrom*. 16: 1442-1445.

[162]. Overduin, S. D., and Brindle I. D. (2001) Determination of hydride-forming elements in high purity coppers by inductively coupled plasma atomic emission spectrometry. *J. Anal. At. Spectrom.* 16: 289-296.

[163]. Chanvaivit, S., and Brindle, I. D. (2000) Matrix independent determination of hydride-forming elements in steels by hydride generation-inductively coupled plasma atomic emission spectrometry. *J. Anal. At. Spectrom.* 15. 1015-1018.

[164]. Smichowski, P., and Marrero J. (1998) Comparative study to evaluate the effect of different acids on the determination of germanium by hydride generation inductively coupled plasma atomic emission spectrometry. *Anal. Chim. Acta*, 376: 283-291.

[165]. Hill, S. J., Chenery, S., Dawson, J. B., Evans, E. H., Fisher, A., Price, J. W., Smith, C. M. M., Sutton, K. L., and Tyson, J. F. (2000) Advances in atomic emission, absorption and fluorescence spectrometry, and related techniques. *J. Anal. At. Spectrom.* 15: 763-805.

[166]. Evans, E. H., Chenery, S., Fisher, A., Marshall, J., and Sutton, K. (1999) Atomic emission spectrometry. *J. Anal. At. Spectrom.* 14: 977-1004.

[167]. Matoušek, T., Dědina, J., and Vobecký, M. (2002) Continuous flow chemical vapour generation of silver for atomic absorption spectrometry using tetrahydroborate(III) reduction - system performance and assessment of the efficiency using instrumental neutron activation analysis. *J. Anal. At. Spectrom.* 17: 52-56.

[168]. Matoušek, T., and Sturgeon, R.E. (2004) Chemical vapour generation of silver: reduced palladium as permanent reaction modifier for enhanced performance. *J. Anal. At. Spectrom.* 19: 1014-1016.

[169]. Reich, F., and Richter, T. (1863) *Journal für Praktische Chemie* 90: 172-179.

[170]. Venetskii, S. (1971) Kaleidoscope. *Metallurgist,* 15: 148-156.

[171]. Sutherland, J. K. (1971) *The Canadian Mineralogist,* 10: 781-789.

[172]. Bachmann, K. J. (1981) Properties, preparation, and device applications of Indium-phosphide. *Annual Review of Materials Science,* 11: 441-447.

[173]. Bhuiyan, G., Hashimoto, A., and Yamamoto, A. ( 2003) Indium nitride (InN): A review on growth, characterization, and properties. *J. of Appl. Phys.* 94: 2779-2808.

[174]. Powalla, M., and Dimmler, B. (2000) Scaling up issues of CIGS solar cells. *Thin Solid Films,* 361: 540-546.

[175]. Matusiewicz, H., and Krawczyk M. (2007) Hydride generation-in situ trapping-flame atomic absorption spectrometry hybridization for indium and thallium determination. *J. Braz. Chem. Soc.* 18: 304-311.

[176]. Busheina, I. S., and Headridge, J. B. (1982) Determination of indium by hydride generation and atomic absorption spectrometry. *Talanta,* 29: 519-526.

[177]. Yan, D., Yan, Z., Chen, G., and Li, A.-M. (1984) Determination of indium and thallium by hydride generation and atomic absorpption spectrometry. *Talanta,* 31: 133-139.

[178]. Castillo, J.R., Mir, J.M., and Gomez, M.T. (1988) Some observations on the determination of indium by atomic absorption spectrometry using the volatile covalent hydride technique. *Microchem. J.* 38: 387-389.

[179]. Liao, Y., and Li, A. (1993) *J. Anal. At. Spectrom.* 8 633-637.

[180]. Cankur ,O. and Ataman, O.Y. (2007) Chemical vapor generation of Cd and on-line preconcentration on a resistively heated W-coil prior to determination by atomic

absorption spectrometry using an unheated quartz absorption cell. *J. Anal. At. Spectrom.* 22: 791–799.

[181]. Kula, I., Arslan, Y., Bakirdere, S., and Ataman, O.Y. (2008) A novel analytical system involving hydride generation and gold-coated W-coil trapping atomic absorption spectrometry for selenium determination at ng l(-1) level. *Spectrochimica Acta Part B-Atomic Spectroscopy*, 63: 856–860.

[182]. Titretir, S., Kendüzler, E., Arslan, Y., Bakırdere, S., and Ataman, O.Y. (2008) Determination of antimony by using tungsten trap atomic absorption spectrometry. *Spectrochim. Acta Part B* 63: 875-879.

[183]. Musil, S., Kratzer, J., Vobecký, M., Benada, O., and Matoušek, T. (2010) Silver chemical vapor generation for atomic absorption spectrometry: minimization of transport losses, interferences and application to water analysis. *J.Anal.At.Spectrom.* 25: 1618-1626.

[184]. Musil, S., Kratzer, J., Vobecký, M., Hovorka, J., Benada, O., and Matoušek, T. (2009) Chemical vapor generation of silver for atomic absorption spectrometry with the multiatomizer: Radiotracer efficiency study and characterization of silver species. *Spectrochim.Acta Part B,* 64: 1240-1247.

[185]. Matoušek, T., and Sturgeon, R.E. Surfactant assisted chemical vapour generation of silver for AAS and ICP-OES: a mechanistic study. *J.Anal.At.Spectrom.* 18: 487-494.

[186]. Dědina, J. (2010) in *Encyclopedia of Analytical Chemistry*, eds. R.A.Meyers and N.H.Bings, John Wiley & Sons, Ltd.

[187]. Benada, O., and Pokorný, V. (1990) Modification of the polaron sputter-coater unit for glow-discharge activation of carbon support films. *Journal of Electron Microscopy Technique,* 16: 235-239.

[188]. de Souza, S.S., Santos Jr, D., Krug, F.J., Barbosa, Jr F. (2007) Exploiting in situ hydride trapping in tungsten coil atomizer for Se and As determination in biological and water samples. *Talanta,* 73: 451-457.

[189]. Hernandez, P.C., Tyson, J.F., Uden, P.C., and Yates, D. (2007) Determination of selenium by flow injection hydride generation inductively coupled plasma optical emission spectrometry. J. Anal. At. Spectrom. 22: 298–304.

[190]. Schaumlöffel, D., Bierla, K., and Lobinski, R. (2007) Accurate determination of selenium in blood serum by isotope dilution analysis using inductively coupled plasma collision cell mass spectrometry with xenon as collision gas. J. Anal. At. Spectrom. 22: 318-321.

[191]. Li, Z.X. (2006) Studies on the determination of trace amounts of gold by chemical vapour generation non-dispersive atomic fluorescence spectrometry. *J.Anal.At.Spectrom.* 21: 435-438.

[192]. Matoušek, T., and Dědina, J. (2000) Fate of free selenium atoms in externally heated quartz tube atomizers for hydride generation atomic absorption spectrometry and their reatomization at tube ends studied by means of the determination of longitudinal free atom distribution. *Spectrochim.Acta Part B*, 55: 545-557.

[193]. Dědina, J., and Welz, B. (1993) Quartz tube atomizers for hydride generation atomic absorption spectrometry-fate of free arsenic atoms. *Spectrochim.Acta Part B* 48: 301-314.

[194]. Šíma, J., Rychlovský, P., and Dědina, J. (2004) The efficiency of the electrochemical generation of volatile hydrides studied by radiometry and atomic absorption spectrometry. *Spectrochim.Acta Part B,* 59: 125-133.

[195]. Dědina, J. (1982) Interference of volatile hydride forming elements in selenium determination by atomic absorption spectrometry with hydride generation. *Anal.Chem.* 54: 2097-2102.

[196]. Kratzer, J., Vobecký, M., and Dědina, J. (2009) Stibine and bismuthine trapping in quartz tube atomizers for atomic absorption spectrometry. Part 2: a radiotracer study. *J.Anal.At.Spectrom.* 24: 1222-1228.

[197]. Dočekal B., Dědina J., and Krivan, V. (1997) Radiotracer investigation of hydride trapping efficiency within a graphite furnace. *Spectrochim.Acta Part B*, 52: 787-794.

## CURRICULUM VITAE


**Personal Information**

- Date of Birth:12.11.1980
- Place of Birth: ANKARA
- Address : METU Chemistry Department Analytic Chemistry Laboratory, Ankara
- Phone : 90 312 21032 37
- e-mail :yarslan@metu.edu.tr


**Work**

- [2002-2003] as Student Assistant in Gazi University, Department of Chemistry, Ankara
- [2004-] as Research Assistant in Middle East Technical University, Department of Chemistry, Ankara

**Education**

- [2005-] PhD Middle East Technical University, Chemistry Department, Ankara
- [2002- 2005] MS Gazi University, Science-Art Faculty,Ankara
- [1998-2002] BS Gazi University, Science-Art Faculty, Ankara

**Publications:**

**1 Arslan Y.**, Ünal H.I., Yılmaz H., Sarı B., *Electrorheological properties of Kaolinite, Polyindole, and Polyindole/Kaolinite Composite Suspensions*, **Journal of Applied PloymerScience,2007,104,3484-3493.**

**2** Pitcher M. W., **Arslan Y.,** Edinç P., Kartal M., Masjedi M., Metin Ö., Şen F., Türkarslan Ö. and Yiğitsoy B., *Recent Advances in the Synthesis and Applications of Inorganic Polymers,* **Phosphorus, Sulfur and Silicon, 2007, 182, 2861-2880.**

**3** Kula İ., **Arslan Y.,** Bakirdere S., Ataman OY., *A Novel Analytical System for Determination of Ultra-Trace Amounts of Selenium by Hydride Generation and Gold Coated Tungsten Coil Trap Atomic Absorption Spectrometry*, **Spectrochimica Acta Part-B,2008,63,856-860.**

**4** Titretir S., Kendüzler E., **Arslan Y.,** Kula İ., Bakirdere S., Ataman OY., *Determination of Antimony by Using Tungsten Trap Atomic Absorption Spectrometry,* **Spectrochimica Acta Part-B, 2008, 63, 875-879.**

**5** Uğurlu M., Kula I., Karaoğlu M. H., **Arslan Y**., *Removal of Ni(II) ions from aqueous solutions using activated-carbon prepared from olive Stone by $ZnCl_2$ activation,* **Environmental Progress&Sustainable Energy, 2009, 28, 547-557.**

**6** Kula I, **Arslan Y.,** Bakırdere S., Titretir S., Kendüzler E., Ataman O. Y., *Determination and Interference studies of bismuth by tungsten trap hydride generation atomic absorption spectrometry,* **Talanta, 2009, 80, 127-132.**

**7** Bakırdere S., Aydın F., Bakırdere E.G., Titretir S., Akdeniz İ., Aydın I., Yıldırım E., **Arslan Y.,** *From mg/kg top g/kg levels: A story of Trace Element Determination: A Review,* **Applied Spectroscopy Review, 2011, 46, 38-66.**

**8 Arslan Y.,** Yıldırım E., Gholami M., Bakırdere S.*, A New Perspective for Lower Detection Limits in Speciation Analysis: High Performance Liquid Chromatography-Chemical Vapour Generation Coupling: A Review,* **Trends in Analytical Chemistry, 2011, 30, 569-585.**

**9 Arslan Y.,** Matoušek T., Kratzer J., Musil S., Benada O., Vobecký M., Ataman O. Y., Dědina J., *Gold Volatile Compound Generation: Optimization, Efficiency and Characterization of the Generated Form,* **Journal of Analytical Atomic Spectrometry, 2011, 26, 828-837.**

**10** Muezzinoglu T., Korkmaz M., Neşe N., Bakırdere S., **Arslan Y.,** Ataman O.Y., *Prevalence of Prostate cancer in High Boron-Exposed population: A Community-Based Study,* **Biological Trace Element Research, Accepted (2011).**

**11** Kula İ., Solak M.H., Uğurlu M., Işıloğlu M., **Arslan Y.,** *Determination of Mercury, Cadmium, Lead, Zinc, Selenium and Iron by ICP-OES in Mushroom Samples From Around Thermal Power Plant in Muğla, Turkey,* **Bulletion of Environmental Contamination and Toxicology, Under Review (2011).**

**12 Arslan Y.,** Kendüzler E., Ataman O.Y., *Indium Determination using Slotted Quartz Tube-Atom Trap-*Flame Atomic Absorption Spectrometry and Interference Studies,* **Talanta, Under Review (2011)**

**International Conference Papers**

**1** Titretir S., Kendüzler E., **Arslan Y.,** Kula İ., Bakirdere S., Ataman OY., Determination of Antimony by Using Tungsten Trap Atomic Absorption Spectrometry, Colloquium Spectroscopicum Internationale XXXV, 23-27 September 2007, Xiamen-China.

**2** Kula İ., **Arslan Y.,** Bakirdere S., Ataman OY., A Novel Analytical System for Determination of Ultra-Trace Amounts of Selenium by Hydride Generation and Gold Coated Tungsten Coil Trap Atomic Absorption Spectrometry, Colloquium Spectroscopicum Internationale XXXV, 23-27 September 2007, Xiamen-China.

**3** Kula İ., **Arslan Y.,** Titretir S., Bakirdere S., Titretir S., Ataman OY., Interference Studies for Bismuth Determination by Tungsten Trap Atomic Absorption Spectrometry, Colloquium Spectroscopicum Internationale XXXV, 23-27 September 2007, Xiamen-China.

**4** Titretir S., Bakirdere S., **Arslan Y.,** Aydın F ., Ataman OY., Interference Studies for Pb Determination by Tungsten Trap Atomic Absorption Spectrometry, $5^{th}$ Aegean Analytical Chemistry Days, 5-8 October 2006, Thessaloniki-Greece.

**5** Kula İ., Yıldız D., Şahin N., Uğurlu M., **Arslan Y.,** Determination of Cd and Zn by Flame Atomic Absorption Spectrophotometry after Preconcentration by Streptmycs Albs immbilized on Sepiolite, $6^{th}$ Aegean Analytical Chemistry Days, 9-12 October 2008, Denizli-Tukey.

**6** Gholami M., **Arslan Y.,** Bakırdere S., Ataman O.Y., Determination of Gold Concentration in ng $mL^{-1}$ Levels by Hydride Generation Atomic Absorption

Spectrometry Using a Novel Gas Liquid Separator and W-coil Trap, 6th Aegean Analytical Chemistry Days, 9-12 October 2008, Denizli-Tukey.

**7** Tekbaş Z., Bakırdere S., Alp T.N., **Arslan Y**., Şenol F., Ataman O.Y., Development of a Sensitive Analytical Method for Antimony Determination using a Ta-Coated SQT and FAAS, 6th Aegean Analytical Chemistry Days, 9-12 October 2008, Denizli-Tukey.

**8** Matoušek T., Musil S., Kratzer J., **Arslan Y.,** Hovorka J., benada O., Vobecký M., Generation of Volatile Species of Transition and Noble Metals by aqueous Tetrahaydroborate, Colloquium Spectroscopicum Internationale XXXVI, 30 August-3 September 2009, Budapest-Hungary.

**9 Arslan Y.,** Matoušek T., Kratzer J., Musil S., ataman O. Y., Determination of Gold by chemical Hydride Generation atomic Absorption Spectrometry, Colloquium Spectroscopicum Internationale XXXVI, 30 August-3 September 2009, Budapest-Hungary

**10** Gholami M., **Arslan Y.,** Ataman O. Y., Determination of Silver at ng $mL^{-1}$ levels by Preconcentration on a aW-coil Trap and Hydride generation Atomic Absorption Spectrometry, Colloquium Spectroscopicum Internationale XXXVI, 30 August-3 September 2009, Budapest-Hungary.

**11** Yıldırım E., **Arslan Y.,** Bakırdere S., Akay P., Ataman O. Y., Determination of Zinc by Vapour Generation Atomic Absorption Spectrometry, 6 th International Conference on Instrumental Method of Analysis Modern-Trends and Applications (IMA 2009), Athens, Greece.

**12** Akay P., **Arslan Y.,** Bakırdere S., Yıldırım E., Ataman O. Y., Inorganic Antimony Speciation Using W-coil Atom Trap and Hydride Generation Atomic Absorption Spectrometry, 6 th International Conference on Instrumental Method of Analysis Modern-Trends and Applications (IMA 2009), Athens, Greece.

**13** Müezzinoğlu T., Korkmaz M., Neşe N., Bakırdere S., **Arslan Y.,** Ataman O. Y., Lekili M., The Prevalence of Prostate Cancer in High Boron-Exposed Population: Community Based Study. "9$^{th}$ International Prostate Forum 2009", 2009, p.80.

**14** Musil S., Kratzer J., **Arslan Y.,** Vobecký M., Benada O., Matoušek T., Ataman O. Y., Dědina J. **,** Chemical vapor generation of gold for AAS: $^{198,199}$Au radiotracer efficiency study and characterization of gold species, European symposium on Atomic Spectrometry, 5-8 September 2010, Wroclaw, Poland.

**15** Yıldırım E., Akay P., **Arslan Y.,** Bakırdere S., Ataman O.Y., Tellurium Speciation Using Hydride Generation Atomic Absorption Spectrometry and in-situ Graphite Cuvette Trapping, 7$^{th}$ Aegean Analytical Chemistry Days AACD 2010, 30 September-03 October 2010, Lesvos, Greece.

**16 Arslan Y.,** Kendüzler E., Ataman O.Y., A Sensitive Analytical Method For Indium Determination Using SQT-AT-FAAS and Interference Studies, 30 September-03 October 2010, Lesvos, Greece.

**17** Kula İ., Halil Solak M., Uğurlu M., Işıloğlu M., Arslan Y., Determination of Cadmium, Iron, Lead, Selenium, Zinc and Mercury by ICP-OES in Mushroom Samples from Around Thermal Power Plant in Muğla, Turkey, 30 September-03 October 2010, Lesvos, Greece.

**18** Musil S., **Arslan Y.,** Kratzer J., Vobecký M., Benada O., Matoušek T., Rychlovský P., Ataman O. Y., Dědina J., Gold chemical vapor generation by tetrahydroborate reduction for AAS: radiotracer efficiency study and characterization of gold species, 23-24 September 2010, 6th International Student Conference in Prague,CzechRepublic.

**National Conference Papers**

**1** Titretir S., Bakırdere S., **Arslan Y.,** Aydın F., Ataman OY., Tungsten Sarmal Tuzaklı AAS ile Sigara İçen İnsanların Saçında Kurşun Tayini, XX. Ulusal Kimya Kongresi, 4-8 Eylül 2006, Kayseri.

**2** Eroğlu Ş., Bakırdere S., **Arslan Y.,** Kula İ., Titretir S., Kendüzler E., Ataman OY., Determination of Lead in Anatolian Spices using W-Trap Hydride Generation Atomic Absorption Spectrometry, X. Ulusal Spekstroskopi Kongresi, 04-07 Temmuz 2007, Urla-İzmir.

**3** Titretir S., Kendüzler E., **Arslan Y.,** Kula İ., Bakırdere S., Ataman OY., Meyvesuyu Örneklerinde W-Sarmal Atom Tuzaklı Hidrür Oluşturmalı Atomik Absorpsiyon Spektrometri ile Kurşun Tayini, 21. Ulusal Kimya Kongresi, 23-27 Ağustos 2007, Malatya.

**4** Korkmaz M., Müzezzinoğlu T., Lekilli M., Neşe N., Bakırdere S., **Arslan Y.,** Ataman OY., Bor Mineralinin Prostat Kanserine Etkisinin Belirlenmesi: Topluma Dayalı Çalışma, X. Ulusal Tıbbi Biyoloji ve Genetik Kongresi, 6-9 Eylül 2007, Antalya.

**5** Korkmaz M., Müezzinoğlu T., Neşe N., Bakırdere S., **Arslan Y.,** Ataman O. Y., Lekilli M., "Bor Mineralinin Prostat kanserine Etkisinin Belirlenmesi: Topluma dayalı

çalışma (En İyi Klinik Çalışma Ödülü)", 8. Ankara Üroonkoloji Kursu, Sheraton Otel & Convention Center, Ankara, 28 Kasım-2 Aralık 2007.

**6** Titretir S., Bakırdere S., **Arslan Y.,** Ataman OY., Hidrür Oluşturmalı ve Tungsten Sarmal Tuzaklı Sistemde Antimon Tayini, III. Ulusal Analitik Kimya Kongresi, 05-07 Temmuz 2006, Çanakkale.

**7 Arslan Y**., Yılmaz H., Ünal H.İ., Kaolin, Poliindol ve Poliindol/Kaolin Kompozitinin Sentezi, Karakterizasyonu ve Elektroreolojik Özelliklerinin İncelenmesi, XIX. Ulusal Kimya Kongresi, 30 Eylül-4 Ekim 2005, Kuşadası.

**8** Gholami M., **Arslan Y.,** Ataman O.Y., Determination of Gold by chemical Vapour Generation AAS using a Novel Gas-Liquid Separator, XXII. Ulusal Kimya Kongresi 6-10 Ekim 2008, Mağusa, Kıbrıs.

**9** Karakuş M., Kaya E., **Arslan Y.,** Ataman O. Y., Su Örneklerinde İnorganik Arsenik Türlendirmesi, XI. Ulusal Spekstroskopi Kongresi, 24-27 Haziran 2009, Gazi Universitesi-Ankara.

**10** Kaya E., Karakus M., **Arslan Y.,** Ataman O. Y., Balık Orneklerinde Toplam Arsenik Tayini, XI. Ulusal Spekstroskopi Kongresi, 24-27 Haziran 2009, Gazi Universitesi-Ankara.

**11** Demirtaş İ., Bakırdere S., **Arslan Y.,** Ataman O.Y., Tantalum Kaplanmış Yarıklı Kuvars Tüp Atom Tuzağı-Alevli AAS ile Kurşun Tayini, XI. Ulusal Spekstroskopi Kongresi, 24-27 Haziran 2009, Gazi Universitesi-Ankara.

**12 Arslan Y.,** Kendüzler E., Kula İ., Ataman O. Y., Yarıklı Kuvars Boru-AAS ile İndiyum Tayini, XI. Ulusal Spekstroskopi Kongresi, 24-27 Haziran 2009, Gazi Universitesi-Ankara.

**13** Ataman S., Karaman G., Bora S., Akay P., **Arslan Y.,** Bakırdere S., Ataman O. Y., İdrar Orneklerinde ICP-OES ile Bor Tayini, XI. Ulusal Spekstroskopi Kongresi, 24-27 Haziran 2009, Gazi Universitesi-Ankara.

**14 Arslan Y.,** Matoušek T., Ataman O.Y., Dědina J., Determination of Gold by Volatile Compound Generation Atomic Absorption Spectrometry (VCG-AAS) with Different Atomizers and in-situ Trapping of the Volatile Au Species in Graphite Tubes, 5. Ulusal Analitik Kimya Kongresi, 21-25 Haziran 2010, Atatürk Üniversitesi-Erzurum.

**15** Aydın M., Özdemir E., Özcan Ş., Bora S., **Arslan Y.,** Bakırdere S., Ataman O.Y., Semen Örneklerinde ICP-MS ile Bor Tayini, 5. Ulusal Analitik Kimya Kongresi, 21-25 Haziran 2010, Atatürk Üniversitesi-Erzurum.

**16** Yıldırım E., Bora S., **Arslan Y.,** Bakırdere S., Ataman O.Y., Hava Filtresi Örneklerinde ICP-OES ile Bor Tayini, 5. Ulusal Analitik Kimya Kongresi, 21-25 Haziran 2010, Atatürk Üniversitesi-Erzurum.

**Grands**

**1 Perkin Elmer Excellent Poster Award,** Interference Studies for Bismuth Determination by Tungsten Trap Atomic Absorption Spectrometry, Colloquium Spectroscopicum Internationale XXXV, 23-27 September 2007, Xiamen-China.

**2 Klinik Üroonkoloji Alanında Birincilik Ödülü,** Bor Mineralinin Prostat Kanserine Etkisinin Belirlenmesi: Topluma Dayalı Çalışma, 8. Ankara Üroonkoloji Kursu, Sheraton Otel & Convention Center, Ankara, 28 Kasım-2 Aralık 2007.

**3 En İyi Poster Dalında 3. lük Ödülü**, Determination of Lead in Anatolian Spices using W-Trap Hydride Generation Atomic Absorption Spectrometry, X. Ulusal Spekstroskopi Kongresi, 04-07 Temmuz 2007, Urla-İzmir.

**4 JAAS Excellent Poster Award,** Determination of Gold by Volatile Compound Generation Atomic Absorption Spectrometry, Colloquium Spectroscopicum Internationale XXXVI, 30 August-3 September 2009, Budapest, Hungary.

**Projects**

**1 Bor Mineralinin İnsanda Erkek Fertilitesi ve Prostat Kanserine Etkisinin Belirlenmesi**, BOREN, Proje No: AR-GE/6, Mayıs 2007. (Completed).

**2 Elektrokimyasal Hidrür Oluşturmalı Atomik Absorpsiyon Spektrometri ile Bizmut Tayini için Duyarlı Yöntem Geliştirilmesi,** TUBİTAK, Proje No: 106T089, Temmuz 2008. (Completed).

**3 Kolayca Hidrür Bileşiği Oluşturmayan Bazı Elementlerin Tayini İçin Buhar Oluşturmalı ve Atom Tuzaklı AAS Kullanarak yeni Yöntemler,** TUBİTAK, Proje No: 109T239, Aralık 2009-Aralık 2011.